

Stony Brook University



OFFICIAL COPY

The official electronic file of this thesis or dissertation is maintained by the University Libraries on behalf of The Graduate School at Stony Brook University.

© All Rights Reserved by Author.

**The Functional Analysis of Four Connexin50 Variants to Determine the
Physiological Relevance of Connexin50 Protein Domains**

A Dissertation Presented

by

Adam Michael DeRosa

to

The Graduate School

in Partial Fulfillment of the

Requirements

for the Degree of

Doctor of Philosophy

in

Genetics

Stony Brook University

December 2007

Stony Brook University

The Graduate School

Adam Michael DeRosa

We, the dissertation committee for the above candidate for the Doctor of Philosophy Degree in Genetics hereby recommend acceptance of this dissertation.

Thomas W. White, Advisor

Associate Professor, Physiology and Biophysics

Martha Furie, Chairperson

Professor, Pathology

Richard T. Mathias

Professor, Physiology and Biophysics

Michael Hadjiargyrou

Associate Professor, Biomedical Engineering

Xiaohua Gong

Associate Professor, School of Optometry
University of California at Berkeley

This dissertation is accepted by the Graduate School

Lawrence Martin

Dean of the Graduate School

Abstract of the Dissertation

**The Functional Analysis of Four Connexin50 Variants to Determine the
Physiological Relevance of Connexin50 Protein Domains**

by

Adam Michael DeRosa

Doctor of Philosophy

in

Genetics

Stony Brook University

2007

In the lens, gap junctions link the cytosols of neighboring cells to form the functional syncytium essential for proper organ development and the maintenance of fiber cell homeostasis. Gap junctions are aggregates of intercellular channels made from transmembrane proteins called connexins. There are three connexins (Cx) present in the lens: Cx43, Cx46, and Cx50. Genetic alterations in Cx46 and Cx50 have directly linked these genes to the formation of cataracts in both mice and humans. Connexins contain four transmembrane domains, linked by a cytoplasmic loop, two extracellular loops, and cytosolic amino and carboxyl terminals. Mutations in different Cx50 domains may have diverse effects on channel function, and the inherent changes may play a role in cataract development in the mammalian lens. This dissertation examines the functional consequences of three cataract causing Cx50 mutants: Cx50-G22R (N-terminal), Cx50-

S50P (extracellular loop 1), and Cx50-R205G (extracellular loop 2). It also analyzes a C-terminally truncated Cx50 protein, which mimics a developmentally regulated post-translational processing event.

The cataract-inducing Cx50 mutations all exhibited loss of function, as expression of these subunits alone failed to induce electrical coupling *in vitro*. Truncated Cx50 formed functional channels with significantly reduced coupling. Immunofluorescent microscopy revealed that while Cx50-G22R, Cx50-R205G, and truncated Cx50 subunits localized to the plasma membrane, Cx50-S50P subunits formed junctional plaques only when co-expressed with wild-type Cx46. Mixed expression of any of the mutant proteins with wild-type Cx46 facilitated the formation of gap junction channels with unique gating properties. Conversely, co-expression of wild-type Cx50 and G22R, S50P, or truncated Cx50 subunits induced minor alterations in channel function. In contrast, the mixing of wild-type Cx50 and Cx50-R205G abolished coupling, a finding consistent with dominant negative inhibition. These findings suggest that each of the cataract-associated Cx50 mutations uniquely interacted with the wild-type fiber connexins to form gap junctions with altered functional properties, a phenomenon that may help to explain the differences in lens pathologies observed *in vivo*. C-terminal truncation of Cx50 resulted in a decrease in conductance independent of alterations in gating, a finding consistent with the regulated reduction in coupling observed during lens fiber differentiation.

Table of contents

List of Figures.....	viii
List of Tables.....	xi
List of Abbreviations.....	xii
Acknowledgements.....	xvii
I. Introduction.....	1
II. Hypotheses and Specific Aims.....	30
III. Materials and Methods.....	35
IV. The physiological role of Cx50-G22R in lens development and homeostasis.....	42
Abstract.....	43
Results.....	45
Discussion.....	52
Figures and Tables.....	56

V. The cataract inducing Cx50-S50P mutation dominantly alters wild-type lens connexin channel gating.....	72
Abstract.....	73
Results.....	74
Discussion.....	83
Figures and Tables.....	88
VI. The loss-of-function Cx50-R205G mutation dominantly alters wild-type lens connexin function.....	107
Abstract.....	108
Results.....	109
Discussion.....	114
Figures and Tables.....	116
VII. Functional characterization of a naturally occurring Cx50 truncation.....	126
Abstract.....	127
Results.....	128
Discussion.....	134

Figures and Tables.....	138
VIII. Concluding Remarks.....	156
Summary of alysis.....	157
IX. References.....	163

List of Figures

I-1. Peptide map of murine Cx50 protein.....	20
I-2. Structure and diversity of gap junction channels.....	22
I-3. A diagram of a vertebrate lens cross section.....	24
I-4. A diagram of the lens circulation model.....	26
I-5. Cataracts form in connexin knockout lenses.....	28
IV-1. Knocked-in Cx46 suppresses the severe cataract of the Cx50-G22R mutation.....	57
IV-2. Histology reveals normal fiber morphology in the Cx50 ^(G22R/Cx46) Cx46 ^(-/-)	59
IV-3. Cx50-G22R does not affect embryonic lens development.....	61
IV-4. Immunohistochemical staining of lens sections.....	63
IV-5. Western blot data show that the Cx50-G22R protein level is increased in the Cx50 ^(G22R/Cx46) Cx46 ^(-/-) lens.....	65
IV-6. Western blot analysis of <i>Xenopus</i> oocytes.....	67
IV-7. Voltage-gating properties of homotypic and mixed channels.....	69
IV-8. Mutant Cx50-G22R localized to the plasma membrane.....	71

V-1. Cx50-S50P fails to form functional intercellular channels.....	88
V-2. Voltage gating properties of homotypic wild-type Cx50 channels and channels co-expressing Cx50-S50P and wild-type Cx50 subunits.....	90
V-3. Voltage gating properties of homotypic and heteromeric Cx46 channels.....	92
V-4. Comparison of steady state conductance properties.....	94
V-5. Gating analysis of heterotypic wild-type and coinjected channels.....	96
V-6. S50P requires Cx46 to form functional hemichannels in <i>Xenopus</i> oocytes.....	98
V-7. Immunofluorescent imaging of Cx50-S50P <i>in vitro</i> and <i>in vivo</i>	100
V-8. Description of embryonic and adult lens phenotypes produced by mixing Cx50-S50P and wild-type lens fiber connexins.....	102
VI-1. Homozygous mutant lenses develop microphthalmia and cataract.....	117
VI-2. Functional expression of wild-type lens fiber connexins and mutant Cx50-R205G subunits in <i>Xenopus</i> oocytes.....	119
VI-3. Voltage-gating properties of homotypic Cx46, and heteromeric wild-type Cx46 and Cx50-R205G channels.....	121
VI-4. Immunofluorescent imaging of wild-type and Cx50-R205G proteins in transfected HeLa cells.....	123

VII-1. Western blot analysis of <i>Xenopus</i> oocyte extracts indicates similar expression of full-length (Cx50) and truncated (Cx50tr290) proteins.....	139
VII-2. Truncated Cx50 forms functional intercellular channels.....	141
VII-3. Voltage-gating properties of full-length, truncated, and heterotypic Cx50 channels.....	143
VII-4. Immunofluorescent imaging of Cx50 in transfected HeLa cells.....	145
VII-5. Cx50tr290 subunits form functional intercellular channels with reduced coupling in N2A cell pairs.....	147
VII-6. Voltage dependence and gating kinetics of truncated Cx50 channels in transfected cells.....	149
VII-7. Cx50tr290 and full-length Cx50 have identical single channel properties.....	151
VII-8. pH gating sensitivity of full-length and truncated Cx50 channels.....	153

List of Tables

Table I-1. Summary of all reported Cx50 mutations.....	30
Table V-1. Boltzmann parameters for wild-type and mixed channels containing Cx50-S50P.....	104
Table V-2. Quantitative analysis of gap junctional plaque formation in transiently transfected HeLa cells.....	106
Table VI-1. Boltzmann parameters for wild-type and mutant channels containing Cx50-R205G.....	125
Table VII-1. Boltzmann parameters for full-length and truncated Cx50 channels.....	155

List of Abbreviations

<i>Aey5</i>	Connexin50 V64A
ARVO	Association for research in vision and ophthalmology
ATP	Adenosine triphosphate
BSA	Bovine serum albumin
Ca ²⁺	Calcium
CaCl ₂	Calcium chloride
cAMP	Cyclic adenosine monophosphate
cDNA	Complementary deoxyribonucleic acid
cGMP	Cyclic guanine monophosphate
cRNA	Complementary ribonucleic acid
C-terminal	Carboxy terminus
Cx38	Connexin38
Cx43	Connexin43
Cx46	Connexin46
Cx50	Connexin50
CZP	Cataract zonular pulverulent
DAPI	4', 6-diamidino-2-phenylindole
DF	Differentiated fiber cells
DTT	Dithiothreitol
E1	Extracellular loop 1
E2	Extracellular loop 2
E48K	Connexin50 E48K

EDTA	Ethylenediaminetetraacetic acid
EGFP	Enhanced green fluorescent protein
EGTA	Ethylene glycol tetraacetic acid
ENU	Ethyl nitrosourea
F1	First generation
F32L	Connexin46 F32L
F-actin	Filamentous actin
FITC	Fluorescein isothiocyanate
FURA2	Acetoxymethyl 2-[5-[bis[(acetoxymethoxy-oxo-methyl)methyl]amino]-4-[2-[2-[bis[(acetoxymethoxy-oxo-methyl)methyl]amino]-5-methyl-phenoxy]ethoxy]benzofuran-2-yl]oxazole-5-carboxylate
G22R	Connexin50 G22R
Ga	Gauge
G_j	Junctional conductance
G_{jss}	Steady state junctional conductance
H ₂ O	Dihydrogen Oxide
HCl	Hydrochloric acid
HeLa	Immortalized human epithelial cell line
HEPES	4-(2-Hydroxyethyl)piperazine-1-ethanesulfonic acid
I247M	Connexin50 I247M
IACUC	Institutional Animal Care and Use Committee
IgG	Immunoglobulin G
I_j	Junctional current
I_{jss}	Steady state junctional current

I_m	Membrane current
IP_3	Inositol triphosphate
K^+	Potassium
KCl	Potassium chloride
kDa	Kilodalton
Lop10	Lens opacity 10
Lp82	Lens calpain protease
MB	Modified Barth's Medium
MF	Mature fiber cells
$MgCl_2$	Magnesium chloride
MIP	Major Intrinsic Peptide
mm	Millimeter
mM	Millimolar
MS-222	Tricaine methanesulfonate
mV	Millivolt
$M\Omega$	Megaohm
N188T	Connexin46 N188T
N63S	Connexin46 N63S
nA	Nanoamperes
Na^+	Sodium
Na_2CO_3	Sodium bicarbonate
NaN_3	Sodium azide
NaOH	Sodium hydroxide

nM	Nanomolar
No2	Connexin50 D47A
ODDD	Oculodentodigital dysplasia
OsO ₄	Osmium tetroxide
P187L	Connexin46 P187L
P59L	Connexin46 P59L
P88S	Connexin50 P88S
PBS	Phosphate buffered saline
PCR	Polymerase chain reaction
pS	Picosiemens
PVDF	Polyvinylidene fluoride
R205G	Connexin50 R205G
R23T	Connexin50 R23T
RNA	Ribonucleic acid
RT-PCR	Reverse transcription polymerase chain reaction
S380FS	Connexin46 S380FS
S50P, <i>LI</i>	Connexin50 S50P
SDS-PAGE	Sodium dodecyl sulfate polyacrylamide gel electrophoresis
Tr290	Truncated Connexin50
Tx-100	Triton X-100
V _j	Junctional voltage
V _m	Membrane voltage
β	Beta crystallin protein

γ	Gamma crystallin protein
γ_j	Unitary conductance
μg	Microgram
μM	Micromolar
τ	Channel closure rate

Acknowledgements

Graduate school has provided a great opportunity to meet many interesting and exceptional people; my only regret is that there is not enough paper to include them all here. To these friends, I would like to convey my most heartfelt and sincere gratitude for all they have done for me as I proceeded toward this day.

I will however, take a moment to acknowledge those closest to me during this time. My thesis advisor, Dr. Thomas White, for anyone who knows Tom, they will easily realize that he is a truly great scientist, but after four years in his laboratory I am *honored* to say that he is an even more exceptional person and friend. My only hope is that everyone has a mentor like Tom.

To those people in the White laboratory: Gulistan, Dwan, Teresa, and Helen... I must thank you all for helping me reach this point in my journey. I would especially like to thank Caterina Sellitto, who has, without a doubt, made the lab a more comfortable place for me.

Finally, I have to acknowledge my family for all of their unwavering support. My parents, Sal and Mary Ann, who have provided so much for me that I can not even begin to list it all here. The amount of gratitude I owe to my parents is unfathomable and I can only hope that one day I will be able to repay them for everything they have given me.

Chapter I

Introduction

Gap junction organization and function

Gap junctions are dynamic intercellular channels that provide a vital pathway for transporting many of the ions and small molecules essential for the proper growth and development of various multicellular organisms (Bennett, 1994). All gap junctions modulate physiological processes by ionically coupling cells via the regulated exchange of ions (Ca^{2+} , Na^+ , K^+) between neighboring cells; however, biochemical coupling, or the sharing of larger metabolites and nutrients (cAMP, cGMP, IP_3) between cells, is dependent on the protein composition of these channels (Veenstra et al., 1994) (Goldberg et al., 1999) (Valiunas et al., 2002). The structural, and thus physiological, diversity of gap junctions depends on the specific connexin subunits contributing to channel formation. To date, the connexin gene family contains over 20 members, which are expressed in an overlapping, tissue-dependent pattern (Willecke et al., 2002) (Gerido and White, 2004). Gap junctions are formed when six connexin subunits oligomerize and are trafficked to the plasma membrane to form the connexons or hemichannels (single membrane channels) that align in the extracellular space between two adjacent cells to create full intercellular channels known as gap junctions (Evans and Martin, 2002). A connexin includes cytoplasmic amino and carboxyl termini; thought to mediate channel voltage gating (Bennett et al., 1993) (Purnick et al., 2000) (Peracchia et al., 2004) and pH sensitivity (Eckert, 2002) (Peracchia et al., 2004), respectively. Additionally, each connexin contains four transmembrane domains, linked by a single cytoplasmic loop and two extracellular loops, E1 and E2, thought to play a role in connexon docking and channel gating (Bukauskas et al., 1995) (Foote et al., 1998) (Figure I-1). Gap junctions will vary in complexity according to the connexin composition of each oligomer. Each

connexon or hemichannel can be of uniform (homomeric) or varying (heteromeric) connexin composition, and neighboring cells may contribute either heteromeric or homomeric connexons to form full intercellular channels known as heteromeric, heterotypic or homotypic gap junctions (Figure I-2). Recent studies have shown that mixing the connexin composition of gap junctions changes both the permeability and electrophysiological properties of these channels (Goldberg et al., 1999) (Valiunas et al., 2002) (Veenstra, 1996) (Cao et al., 1998) (Bevans et al., 1998) (Niessen et al., 2000), while mutation, removal, or genetic replacement of specific connexins can lead to distinct physiological defects and disease (Willecke et al., 2002) (Gerido and White, 2004) (White and Paul, 1999).

Gap junctions and disease

Communication between adjacent cells plays an important role in maintaining tissue homeostasis in many organisms. Thus, governing the response to environmental stimuli requires that multicellular organisms utilize a variety of intercellular communication mechanisms, such as hormone signaling, cell-cell adhesion, or receptor-mediated signaling cascades. Despite the obvious abundance in communication options that each cell type or tissue contains, disruption or loss of any individual pathway can result in distinct pathologies and disease. For example, recent studies have implicated connexins in a variety of human diseases, including deafness, skin disease, neuropathy, and cataract (Anand and Hackam, 2005) (White and Bruzzone, 2000b) (Bergoffen et al., 1993) (Kelsell et al., 1997) (Gong et al., 2007). Recent evidence has linked two distinct principles with connexin-related disease. First is the lack of functional redundancy displayed in tissues expressing multiple connexins. For instance, many tissues express a

multitude of connexins, yet mutations in any one connexin can lead to disease without altering the expression or function of other connexins. Additionally, the degree to which a mutated connexin can interact with wild-type connexin isoforms is variable, a phenomenon that presents yet another factor to consider when examining the effects of connexin mutations on genetic disease. This dissertation will focus on only one connexin gene, connexin50, and analyze its role in cataract development in the mammalian lens by examining its ability to interact with other connexin isoforms expressed in the lens.

Gap junction mediated transport in the lens

The lens is an avascular spherical organ suspended between the aqueous and vitreous humors of the eye. The anterior surface consists of a single layer of epithelial cells, while the remaining organ mass is made of highly differentiated fiber cells (Figure I-3). The lens first forms as a hollow ball of epithelial cells that invaginates from the surface ectoderm. The posterior cells then elongate toward the anterior surface, producing a solid sphere. Thereafter, the aforementioned epithelial cells proliferate, migrate to the equator and elongate until they stretch from the anterior to posterior poles, forming new lens fibers (Menko, 2002). Morphological differentiation of fiber cells is accompanied by changes in protein synthesis, including the upregulation of a distinct set of lens membrane channels and a family of cytoplasmic proteins known as the crystallins (Piatigorsky, 1981) (Donaldson et al., 2001). Differentiated fiber cells undergo further development as they are transformed into the mature fibers found deeper in the core of the lens. These changes include the proteolytic cleavage of the C-terminus of several membrane proteins including the connexins (Lin et al., 1997) (Kistler et al., 1990). While the precise relevance of this endogenous truncation remains elusive, C-terminus cleavage

coincides with gap junctional plaque reorganization, changes in the pH gating sensitivity of the channels, and the stabilization of these trans-membrane proteins (Mathias et al., 1991) (Gruijters et al., 1987) (Zampighi et al., 1992). The first lens fiber cells enter the final stages of differentiation on day 12 of mouse embryonic development (Bassnett, 2002). However, the processes of fiber differentiation persist as the lens continues to accumulate new cells throughout the life of the organism.

One function of the lens is accommodation, a process allowing the eye to focus on images at different focal distances. To provide accommodation, the lens requires several unique physiological properties. First, high levels of crystallin synthesis must occur to increase the refractive index of the fiber cell cytoplasm. Second, it must be devoid of light-scattering elements like cytoplasmic organelles, which are degraded during the final stages of fiber differentiation. Finally, the extracellular spaces between fiber cells must be very thin, even narrower than the wavelength of visible light, to maintain a continuous high refractive index throughout the organ. Once fiber cells become crystalline-enriched and depleted of all light-scattering organelles, they gain the capacity to provide the lens with the clarity and high refractive index necessary to properly focus light onto the retina (Piatigorsky, 1981) (Bassnett, 2002) (Goodenough, 1992).

The extensive specialization of fibers required to provide transparency presents unique challenges for these cells. The mature fiber cells contain no cytosolic organelles, thereby lacking the mitochondria essential for ATP production, the endoplasmic reticulum critical for protein synthesis, and nuclei. Additionally, the lens does not have blood vessels for removing harmful cellular waste, necessitating a distinctive mode of intercellular transport for exchanging metabolites and ions with the surface epithelium.

To address these transport challenges, the lens has developed a unique circulatory system, driven by a standing flow of ionic current generated via differences in electromotive membrane potentials between surface and core fiber cells (Mathias et al., 1997).

It is believed that current enters the lens traveling inward at the anterior and posterior poles and outward at the equator where it exits the lens (Mathias et al., 1997). Na^+ , the primary ionic courier, enters the extracellular spaces (from the aqueous and vitreous humors) at the lens surface and flows inward crossing into the fiber cells in a gradient dependent manner. Once internalized, sodium flow reverses direction and is transported back to the lens surface via gap junctions (Figure I-4). As the intercellular current nears the surface epithelium, it is directed toward the lens equator where gap junctional coupling and Na/K-ATP-ase activity are concentrated (Mathias et al., 1997) (Gao et al., 2000) (Candia and Zamudio, 2002) (Tamiya et al., 2003). Similarly, fluid flow through the lens is believed to follow the same circulation pattern as Na^+ and Ca^{2+} , facilitating the transport of various metabolites and cellular waste throughout the lens (Donaldson et al., 2001).

Gap junctions play a critical role in the postnatal growth and differentiation of the lens. They are also a vital component of the circulating current that ensures lens homeostasis and prevents crystallin precipitation and cataract. While these roles have previously been postulated for the intercellular communication provided by lens gap junctions (Goodenough, 1992), the need for three different connexin subunits, namely Cx43, Cx46 and Cx50, has only recently been elucidated.

Lens specific connexin expression

The vertebrate lens is a functional syncytium connected by gap junctions. The mammalian lens expresses a unique assortment of connexins: connexin 43 (Cx43, GJA1), connexin46 (Cx46, GJA3), and Connexin50 (Cx50, GJA8), which form the intercellular channels of the lens (Gerido and White, 2004) (White and Bruzzone, 2000a). These channels mediate a substantial portion of the intercellular transport of essential ions and molecules between the metabolically active epithelium and the quiescent fiber cell core (Mathias et al., 1997) (Jacobs et al., 2001). Cx43, expressed primarily in the epithelium, is absent from lens fibers, while Cx46 exhibits the opposite expression pattern, being found exclusively in lens fiber cells (Paul et al., 1991) (Gong et al., 1997). Conversely, Cx50 is present in both the epithelium and differentiated fibers (White et al., 1992) (Rong et al., 2002). This overlapping, yet distinct, pattern of connexin expression contributes to a variation in junctional communication based on the connexin composition of specific channels.

While the precise physiological contribution of each connexin is not fully understood *in vivo*, the unique gating properties of all lens connexins have been well characterized *in vitro* through channel electrophysiology using exogenous expression systems, such as the mammalian cell or paired *Xenopus* oocyte systems. All three homotypic gap junctions are sensitive to voltage gating, albeit to different extents. Variations in voltage dependence are channel-specific, with Cx43 being the least responsive to gating by voltage, and Cx50 channels being the most sensitive to voltage gating (Ebihara and Steiner, 1993) (White et al., 1994b). The three connexins also exhibit differences in single channel conductance (γ_j): Cx43 generates two distinct conductances

of 60 and 90 pS, a difference modulated by protein phosphorylation (Fishman et al., 1991) (Moreno et al., 1994); Cx46 exhibits a moderate γ_j of ~140 pS (Hopperstad et al., 2000); and single homotypic Cx50 channels induce ~220 pS of unitary conductance (Srinivas et al., 1999).

Due to the overlapping expression pattern of Cx50, neighboring cells can contribute hemichannels of assorted connexin composition. The ability of Cx46 and Cx50 to form heterotypic channels *in vivo* has been well documented (White et al., 1994a) (Konig and Zampighi, 1995) (Jiang and Goodenough, 1996), while the capability of Cx43 and either Cx46 or Cx50 to form mixed channels is yet to be determined. Mammalian and amphibian expression systems have also been used to analyze the formation and functional properties of junctions containing two connexons with distinct connexin subunits (heterotypic) and of junctions that contain multiple connexin types in each connexon (heteromeric). Heterotypic channels containing Cx50 and Cx46 homomeric connexons exhibit a γ_j of ~165pS, an intermediate value when compared to those of either homotypic channel (Hopperstad et al., 2000). The unitary conductance of heteromeric channels is variable, staying above the γ_j of Cx46, yet never exceeding that of Cx50 homotypic channels (Hopperstad et al., 2000) (Srinivas et al., 2005). These intrinsic differences in channel gating properties appear to play an essential role in lens physiology, a hypothesis further supported by genetic manipulation of mammalian lens connexins.

Genetic manipulation of lens connexins

The involvement of Cx43, Cx46 and Cx50 in lens development and function has been elucidated through the use of transgenic mice. While the genetic knockout of Cx43

results in neonatal lethality (Reaume et al., 1995) (White et al., 2001), the physiological role of Cx46 and Cx50 in the lens has been well documented (Gong et al., 1997) (Rong et al., 2002) (White et al., 1998).

Connexin 43 is expressed in various tissues throughout the body, such as the heart, brain, and adrenal gland (Gerido and White, 2004); thus, genetic knockout of Cx43 leads to cardiac malformation and neonatal death (Reaume et al., 1995). The examination of Cx43's involvement in lens development has been limited to prenatal studies using Cx43 knockout mice. Interestingly, murine Cx43 knockout animals isolated at embryonic day 18 exhibit phenotypically normal lenses (White et al., 2001), demonstrating that Cx43 is not essential for proper lens fiber cell development. However, these embryonic knockout lenses display a reduction in cell-cell communication, a finding that may implicate a possible role for Cx43 in postnatal lens development (White et al., 2001).

Conversely, deletion of Connexin50 produces viable offspring with distinct lens phenotypes that can be studied throughout development (White et al., 1998). Genetic knockout of Cx50 generates lenses with a mild nuclear cataract and a significant decrease in organ size (Figure I-5A). Additionally, these lenses exhibit delayed fiber cell maturation, which is a result of slowed denucleation during the DF-MF transition (Rong et al., 2002). Interestingly, conductance measurements taken from Cx50 knockout lenses exhibit a 50% decrease in differentiated fiber cell coupling, yet coupling remains largely unchanged in the mature fibers (Baldo et al., 2001). Furthermore, the decrease in organ growth results from a decreased number of lens fiber cells, not altered cell size, a phenomenon caused by diminished epithelial cell mitosis and proliferation (White, 2002) (Sellitto et al., 2004). These findings maintain that Cx50 plays an essential role in proper

lens growth through its ability to recruit epithelial cells into the cell cycle, as well as suggest a prevalent role for Cx50 in the coupling of primary lens fibers.

Similarly, Cx46 deletion produces viable offspring with identifiable lens defects. Murine Cx46 knockout lenses develop a distinct nuclear cataract during postnatal week 3, found to be the result of aberrant crystallin precipitation in lens fibers (Gong et al., 1997). Interestingly, Cx46 knockout lenses (Figure I-5B) exhibit no growth defect, as these lenses are comparable in size to wild-type lenses (Figure I-5D), inferring that Cx46 is primarily responsible for mediating lens clarity, but not growth. To further determine the precise physiological relevance of Cx46 in lens development, genetic replacement (knock-in) of Cx50 with Cx46 has been carried out in transgenic mice (White, 2002). When the Cx50 gene locus is replaced with the Cx46 coding region (Cx50^(Cx46/Cx46) Cx46^(+/+)), mice develop clear lenses devoid of the nuclear cataract associated with Cx46 knockout (Figure I-5E). These lenses, however, show a substantial growth defect similar to that found in Cx50 knockout mice (Rong et al., 2002) (White et al., 1998) (White, 2002). Taken together, these data indicate that Cx46 plays a unique and essential role in maintaining lens clarity, but is independent of lens growth.

Heterozygous Cx46 knock-in lenses provide further insight into the importance of lens connexin diversity. Interestingly, the presence of Cx46 in the epithelium leads to the production of a distinct cataract phenotype, creating lenses with a unique lamellar opacity located just below the anterior epithelium (Figure I-5F). Additionally, these heterozygous knock-in lenses exhibit normal growth rates when compared to wild-type lenses, indicating that the novel mixing of fiber connexins in the epithelium creates a dominant cataract distinct from that of the Cx46 knockout lens.

Additional support for the crucial function of connexins in proper lens growth and homeostasis comes from the creation of double knockout mice lacking both copies of Cx46 and Cx50 (Cx50^(-/-) Cx46^(-/-)) (Dunia et al., 2006) (Xia et al., 2006a). Double knockout lenses exhibit malformed inner fibers and a dense nuclear cataract, an opacity considerably more severe than that of either knockout animal (Figure I-5C). Recent studies reveal that the distinct double knockout phenotype is the result of mature fiber cell swelling (Dunia et al., 2006) (Xia et al., 2006a). This phenomenon leads to additional downstream physiological changes, such as altered γ -crystallin production and a deficiency in the ability of mature fiber cells to properly transport fluid and essential small molecules throughout the lens core. Taken together, these findings suggest that gap junctional communication in the lens is essential for maintaining lens fiber cell homeostasis, and thus a loss of gap junction mediated transport in the lens leads to cataract.

Cx46 prevents cataract

The research described above has identified a critical role for Cx46 in maintaining lens clarity, particularly in the highly specialized mature fiber cells that depend on Cx46-mediated gap junctional coupling for communication with the metabolically active surface epithelium. Furthermore, calcium-dependent proteolytic activity of Lp82 has been identified as an important trigger of cataractogenesis in Cx46 knockout mice (Baruch et al., 2001). The nature of the connection between Cx46, gap junctional coupling, calcium, and lens cataract development has recently been identified by integrating data from the numerous studies described above with a novel method of calcium measurement in the intact lens (Gao et al., 2004).

Because Cx46 is presumed to be the only connexin providing gap junctional coupling in the mature fiber cells (Baldo et al., 2001) (Martinez-Wittinghan et al., 2004), it forms a critical component of the lens internal circulation system (Mathias et al., 1997) (Donaldson et al., 2001). This model predicts a circulation of Ca^{2+} in the lens, where the Cx46 containing gap junctions coupling the interior fiber cells to the surface cells would be an essential component of calcium homeostasis.

This hypothesis has been tested by studying calcium homeostasis in wild-type, Cx46 knockout, and Cx46 knock-in lenses, which exhibit different degrees of gap junctional coupling in their mature fibers. Intracellular Ca^{2+} is measured by injecting FURA2 into fiber cells and mapping the gradient of calcium concentration from center to surface in each type of lens (Gao et al., 2004). In wild-type lenses, the Ca^{2+} concentration varies smoothly from 700 nM in the center to 300 nM at the surface. In the knock-in lenses, calcium varies from about 500 nM at the center to 300 nM at the surface. As described above, knock-in lenses have about twice the coupling conductance in their mature fibers compared to wild-type lenses, due to the additional copies of Cx46 being expressed from the Cx50 gene locus. When the coupling conductance doubles, the Ca^{2+} concentration gradient halves, suggesting that Cx46 gap junctions represent the limiting factor in the Ca^{2+} efflux pathway. Data from Cx46 knockout lenses further support this idea. Their mature fiber coupling conductance is zero, hence the efflux path is blocked and calcium accumulates to a concentration of $\sim 2 \mu\text{M}$ in the mature fibers. As reviewed above, this accumulation of Ca^{2+} in Cx46 knockout lenses correlates with a dense central cataract, triggered by activation of the calcium-dependent protease, Lp82 (Gong et al., 1997) (Baruch et al., 2001) (Gao et al., 2004). Taken together, these data provide a

mechanism to describe each step leading to cataract formation: knockout of Cx46 causes loss of coupling of mature fiber cells; the efflux path for calcium is therefore blocked; calcium accumulates in the central cells; Lp82 is activated; Lp82 cleaves γ -crystallin; the cleaved γ -crystallin stimulates crystallin aggregation and precipitation.

One caveat to this mechanistic model is that while the knock-in lenses have increased coupling in the central fibers, they also show significantly reduced coupling in the outer fibers. This suggests that the magnitude of coupling in the differentiating fibers is not critical to the circulation, provided that coupling remains concentrated toward the lens equator. In wild-type lenses, gap junctional conductance is maximal at the lens equator and minimal at the anterior and posterior poles (Baldo and Mathias, 1992). In the knock-in lenses, the radial variation in differentiating fiber conductance is preserved, with the equatorial differentiating fibers having a greater conductance than the posterior pole. Thus, as long as the strong bias of coupling toward the equator is preserved, the reduced magnitude of coupling in the differentiating fibers of knock-in lenses does not limit the circulating current.

Connexin mutations cause cataract

The crucial nature of gap junctional communication in the lens is further evidenced by recent reports indicating that mutations in various connexin genes can result in hereditary disease in humans and mice (Willecke et al., 2002) (Gerido and White, 2004) (Evans and Martin, 2002). Autosomal dominant cataracts, CZP1 and CZP3, have been associated with mutations in Cx50 and Cx46, respectively (Shiels et al., 1998) (Mackay et al., 1999), while genetic alterations within the Cx43 coding region lead to oculodentodigital dysplasia, ODDD (Paznekas et al., 2003). These mutations not only

demonstrate the importance of gap junctional communication to an organism, but also provide a valuable resource for determining the molecular mechanisms behind connexin-associated genetic disease.

Mutations within the Cx46 and Cx50 genes are common causes of inherited cataracts in humans and mice. The role of Cx50 in lens homeostasis and proper organ function has been further elucidated by the association of a variety of mutations in the Cx50 coding region with distinct lens pathologies (Table 1) (Runge et al., 1992) (Steele, Jr. et al., 1998) (Xu and Ebihara, 1999) (Graw et al., 2001) (Chang et al., 2002) (Xia et al., 2006b) (Xia et al., 2006c). The first example of a connexin mutation producing cataract in mice is revealed by the analysis of *No2* mice. *No2* mice exhibit a semi-dominant, bilateral, congenital, nuclear cataract with a 30% reduction in lens mass (Steele, Jr. et al., 1998). The *No2* phenotype directly correlates with a single nucleotide transversion from A to C within the Cx50 gene locus, resulting in the formation of a novel Hha1 restriction site and an aspartate to alanine substitution at amino acid 47, Cx50-D47A (in the first extracellular domain). The *No2* mutation has been further analyzed using the paired *Xenopus* oocyte assay to compare the electrical properties of gap junctions formed by Cx50-D47A mutant subunits alone or in conjunction with endogenous lens fiber connexins. These studies show that Cx50-D47A fails to form homotypic gap junctions, yet is able to form functional intercellular channels when co-expressed with wild-type Cx50 or Cx46 (Xu and Ebihara, 1999). Although the electrophysiological properties of these channels have not been well characterized, the formation of functional heteromeric channels containing wild-type and mutant Cx50 indicates that Cx50-D47A does not act as a dominant negative suppressor of Cx50 (Xu

and Ebihara, 1999). Taken together, these data provide the first evidence that a mutation in a lens connexin can result in congenital hereditary cataract.

A substitution of glycine to arginine at codon 22 in the Cx50 coding region (Cx50-G22R) causes autosomal semi-dominant cataracts in *Lop10* mutant mice (Runge et al., 1992) (Chang et al., 2002). Homozygous *Lop10* mice, Cx50^(G22R/G22R) Cx46^(+/+), develop microphthalmia and dense cataracts resulting from severely disrupted cortical fibers with vacuoles and posterior capsule rupture. Similarly, a recent study by the Gong laboratory shows that the homozygous mutant lens fails to produce normal gap junctions between lens fiber cells, and that mutant Cx50-G22R subunits reduce the amount of phosphorylated wild-type Cx46 subunits (Chang et al., 2002). Interestingly, double homozygous Cx50^(G22R/G22R) Cx46^(-/-) mutant mice develop severe cataracts with normal cortical fibers (Chang et al., 2002). These data imply that the interaction of mutant Cx50-G22R proteins with wild-type Cx46 subunits contributes to the severe phenotype in *Lop10* mutant mice, and that the presence of endogenous Cx46 modulates the lens phenotypes of Cx50-G22R mutant mice.

A similar study revealing a novel mutation in the first extracellular domain of Cx50, Cx50-S50P, identified as *LI*, displays ruptured, cataractous lenses resulting from a T to C missense mutation at position 148 in the Cx50 gene, causing a serine to proline substitution at codon 50, Cx50-S50P (first extracellular domain). Histological analysis of the *LI* lens shows disrupted primary fiber cell formation (Gong et al., 2007) (Xia et al., 2006c) and vacuole development in the secondary fibers, while investigation of heterozygous *LI* mice reveals perturbed elongation of primary fiber cells (Xia et al.,

2006c). These data, taken in conjunction with the finding that Cx50 knockout and homozygous *LI* mice show normal primary cell development, suggest that an interaction between mutant and wild-type Cx50 subunits is necessary to disrupt embryonic fiber cell elongation (Dunia et al., 2006) (Xia et al., 2006c). *LI* mice crossed with Cx46 knockout mice to create mice lacking endogenous Cx46, but containing either mutant Cx50 alone or both Cx50-S50P and wild-type Cx50 alleles, further elucidate the role of Cx50-S50P in cataractogenesis. Mice heterozygous for the Cx50-S50P mutation and lacking endogenous Cx46, Cx50^(S50P/+) Cx46^(-/-), develop a dense nuclear cataract with a transparent cortex, while lens histology reveals disrupted nuclear fibers with relatively normal cortical fibers (Xia et al., 2006c). This phenotype differs from the Cx50^(S50P/+) Cx46^(+/+) mice, indicating a defect in the ability of Cx50-S50P to interact with Cx46 in the mature lens fibers. Furthermore, the creation of transgenic mice containing only one copy of mutant Cx50, Cx50^(S50P/-) Cx46^(-/-), produces lenses with a large, dense nuclear cataract, similar to those exhibited by double knockout mice, Cx50^(-/-) Cx46^(-/-) (Xia et al., 2006c) (Gong et al., 2007). Taken together, these data reveal an essential role for gap junction-mediated intercellular communication between primary lens fibers during embryonic development, as the presence of Cx50-S50P subunits alone fails to induce fiber cell growth defects. These findings support the hypothesis that an interaction between endogenous lens connexins is required for proper organ growth, function, and development *in vivo*.

Recently, large scale ethylnitrosourea (ENU) mutagenesis of mice has been conducted, giving rise to an F₁ generation of mice displaying congenital cataract phenotypes. Genotypic analysis of these cataractous mice reveals many alterations

within the γ and β crystallin coding regions, as well as several unique Connexin50 mutations. One such mutation, initially known as *Aey5*, is the product of a T to C mutation at position 191 in the Cx50 coding region, resulting in a valine to alanine substitution at amino acid 64 (in the first extracellular loop) (Graw et al., 2001). This mutation, now known as Cx50-V64A, causes a unique lens pathology, specifically a nuclear and posterior opacity that progresses from postnatal day 12 through the second month of life. Additionally, histological lens sections show the formation of large vacuoles that evolve toward the degeneration of the secondary lens fibers. Furthermore, *Aey5* lenses exhibit a severe growth defect and nuclear remnants in their anterior secondary fibers, indicating an aberration in the denucleation process during fiber cell maturation (Graw et al., 2001).

A separate ENU mutagenesis screen provides similar mutant animals, such as mice possessing the Cx50-R205G allele, which develop a distinct cataract and ocular phenotype. Genome-wide linkage analysis shows the autosomal semi-dominant cataract phenotype exhibited *in vivo* to be the result of a missense C to G mutation in the Cx50 coding region, causing a single amino acid transition from arginine to glycine at codon 205 (R205G). Unlike G22R (in N-terminus) and S50P (in the first extracellular loop), this point mutation is located in the second extracellular loop of Cx50.

Throughout life, lens epithelial cells proliferate, migrate to the lens equator, and elongate by stretching from anterior to posterior poles, resulting in the formation of lens fibers (Menko, 2002). These cells then undergo a series of specialized differentiation processes, including proteolytic cleavage of the C termini of fiber cell connexins (Lin et al., 1997) (Kistler et al., 1990). Although the functional relevance of this endogenous

truncation remains unknown, cleavage coincides with junctional plaque reorganization and protein stabilization (Mathias et al., 1991) (Gruijters et al., 1987) (Zampighi et al., 1992).

Several lines of evidence indicate that the carboxyl terminus may play an important role in channel gating and permeability. Two calpain cleavage sites have been identified at amino acids 290 and 300 within the carboxyl terminus of Cx50 (Lin et al., 1997); however, conflicting results on the relationship between Cx50 truncation and pH gating have been published (Lin et al., 1998) (Xu et al., 2002) (Stergiopoulos et al., 1999) (Peracchia et al., 2004). Some reports have shown greatly reduced pH sensitivity after truncation of the C-terminus (Lin et al., 1998) (Xu et al., 2002), whereas other data have shown the persistence of pH gating after cleavage (Stergiopoulos et al., 1999). This dissertation uses the paired *Xenopus* oocyte system in conjunction with transfected mammalian cells to clarify the functional differences in voltage and pH gating between gap junctions composed of full-length Cx50 and its naturally occurring C-terminal truncation.

Figure I-1. Peptide map of murine Cx50 protein. This diagram displays the individual amino acids that comprise the full-length Cx50 peptide. The map clearly shows the cytoplasmic N-terminus, intracellular loop, and C-terminal domains within the cell. Extracellular loops 1 and 2 are seen in the extracellular space, while the four short transmembrane domains traverse the plasma membrane.

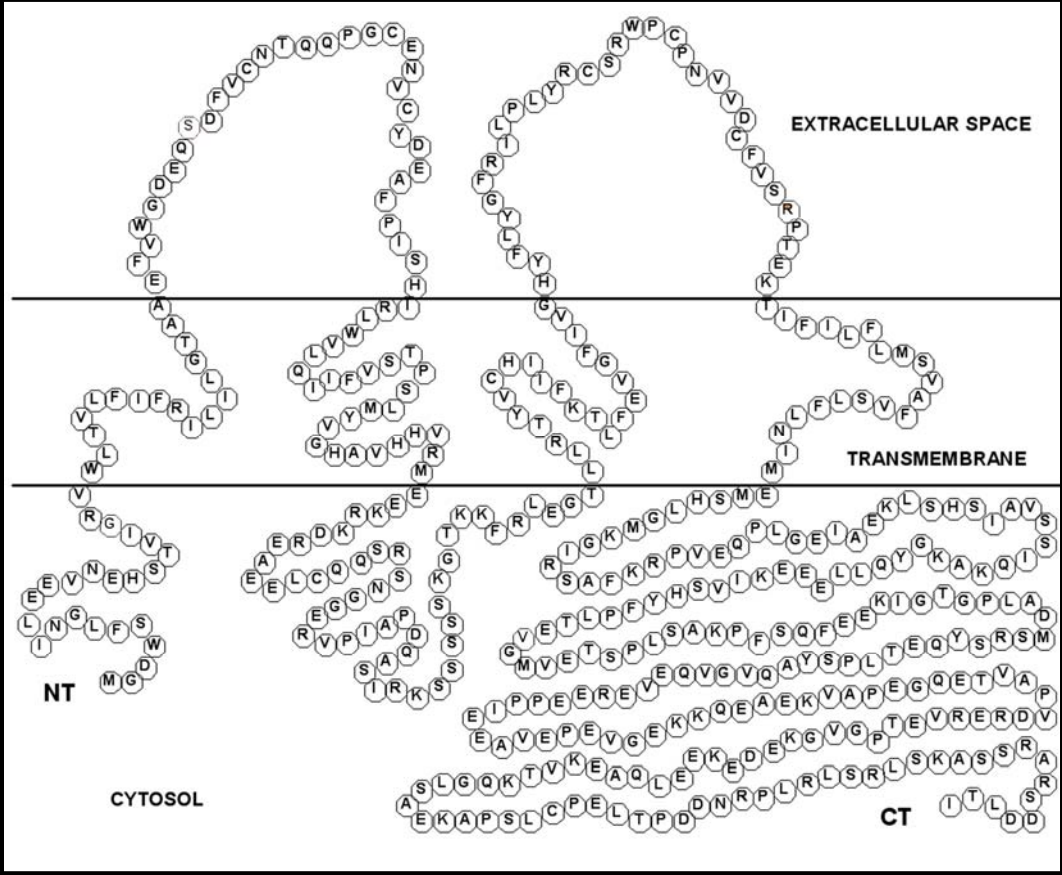


Figure I-2. Structure and diversity of gap junction channels. Connexin subunits determine the structural and functional diversity of gap junctions by forming homomeric or heteromeric connexons. The alignment of connexons in the extracellular spaces of adjacent cells forms various types of intercellular channels such as homotypic, heterotypic, or heteromeric gap junctions. (Evans and Martin, 2002)

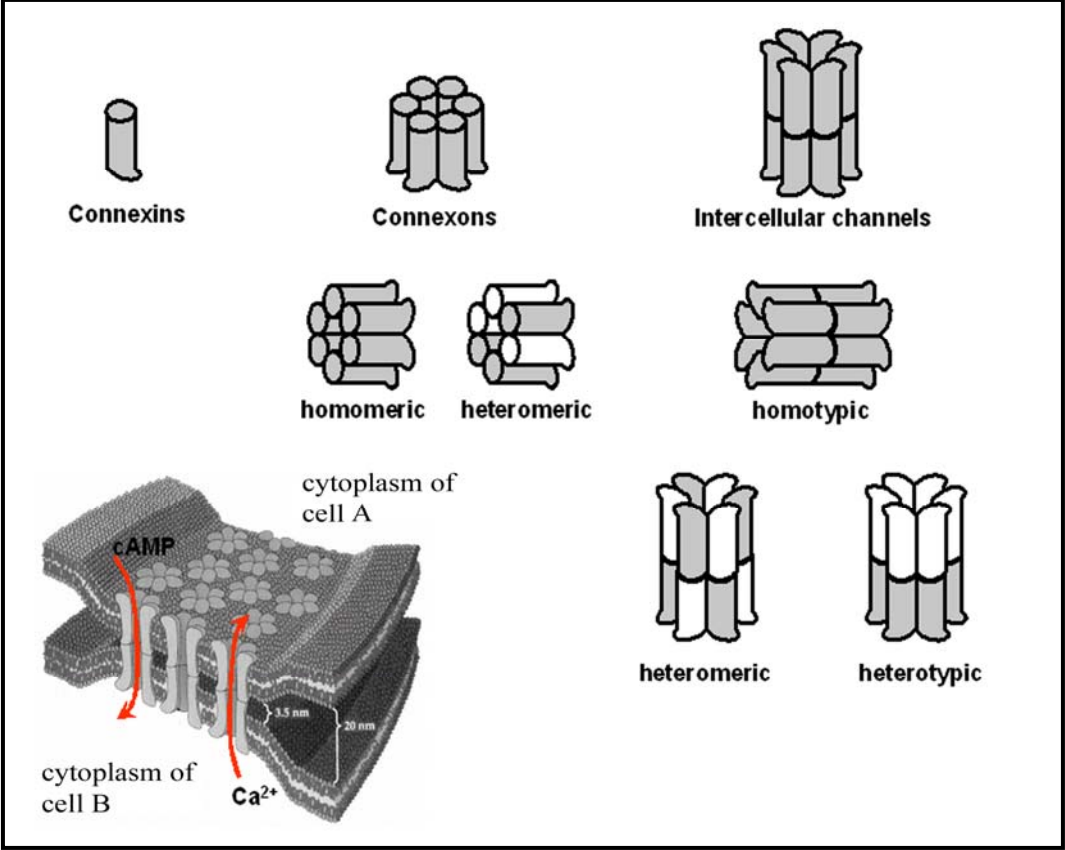


Figure I-3. Diagram of a vertebrate lens cross section cut through the anterior-posterior axis. The lens consists of three distinct cellular subsets. The metabolically active epithelium (light gray) is a single layer of cells spanning the anterior surface of the lens. Below the epithelium are the differentiating fibers (white). The inner core of the lens contains the highly specialized mature fiber cells that comprise the remaining 80% of organ mass (dark gray). (Taken from DeRosa et al. (2005) Intercellular communication in lens development and disease. In *Gap Junctions in Development and Disease*. E. Winterhager, Ed.)

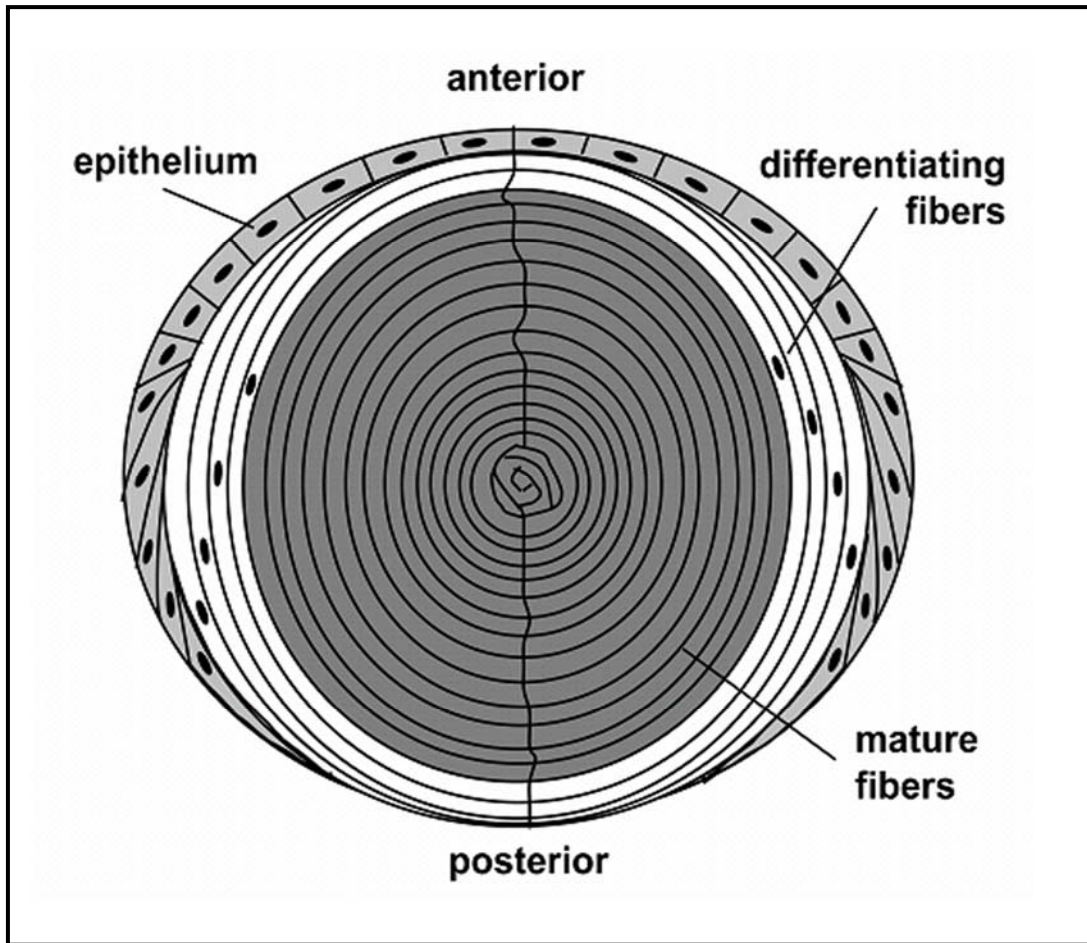


Figure I-4. Diagram of the lens circulation model. (A) In an intact lens, current flows in the pattern indicated by the arrows. (B) The major ion carrier of the circulating current appears to be sodium, which enters the lens along the extracellular spaces between cells, then moves down its electrochemical gradient into fiber cells, where it returns to the surface via gap junctions. The pattern of gap junction coupling in the differentiating fibers directs the intracellular current flow to the lens equator, where the epithelial cells transport it out of the lens using Na/K-ATPase activity. (Taken from DeRosa et al. (2005) Intercellular communication in lens development and disease. In *Gap Junctions in Development and Disease*. E. Winterhager, Ed.)

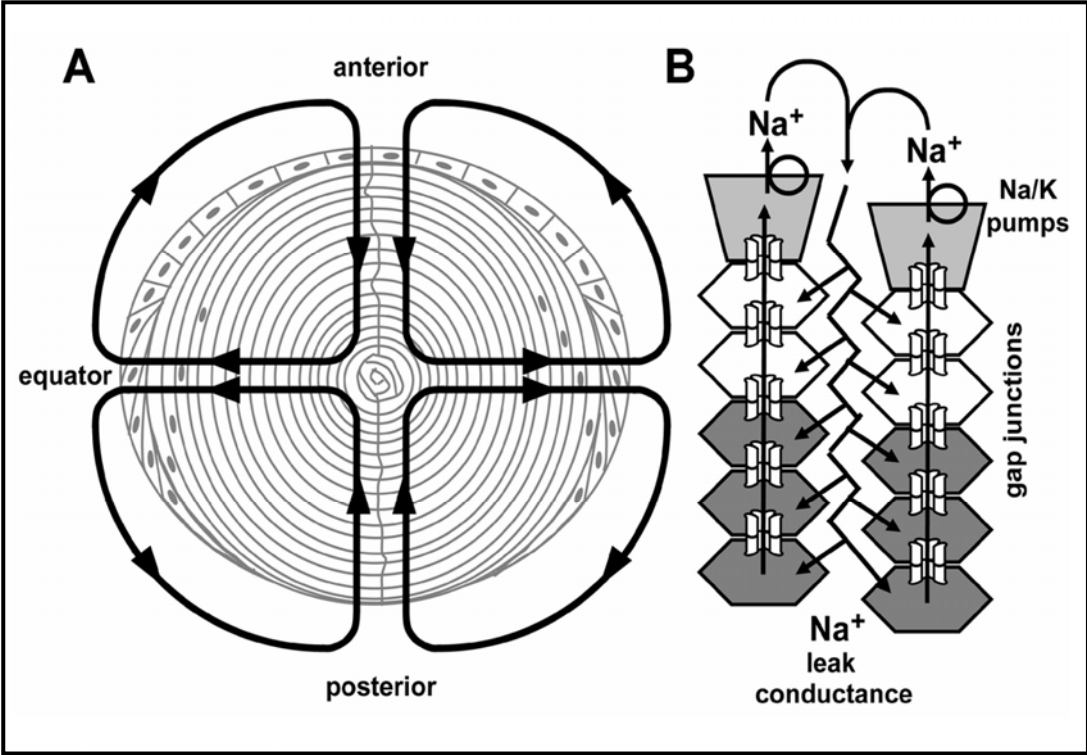


Figure I-5. Cataracts form in connexin knockout lenses. Views looking down on the equatorial edge of Cx50 knockout (A), Cx46 knockout (B), and a Cx46/Cx50 double knockout (C) are shown. Deletion of Cx50 produces a small lens with a mild cataract. Knockout of Cx46 results in a severe cataract, but normal lens size. Disruption of both connexin genes results in dense cataract and small size. Wild-type lenses (D) maintain transparency, as do knockover lenses (E), which are smaller than normal, but clear. Thus, Cx46 alone can maintain lens clarity when expressed from the Cx50 locus (compare E with A and B). Heterozygous knock-in lenses (F) develop dense cataracts in the central anterior region of the lens, in addition to an irregular diffraction under the epithelium. Therefore, incongruous mixing of Cx46 and Cx50 in heterozygous knock-ins causes cataract. (Taken from DeRosa et al. (2005) *Intercellular communication in lens development and disease*. E. Winterhager, Ed.)

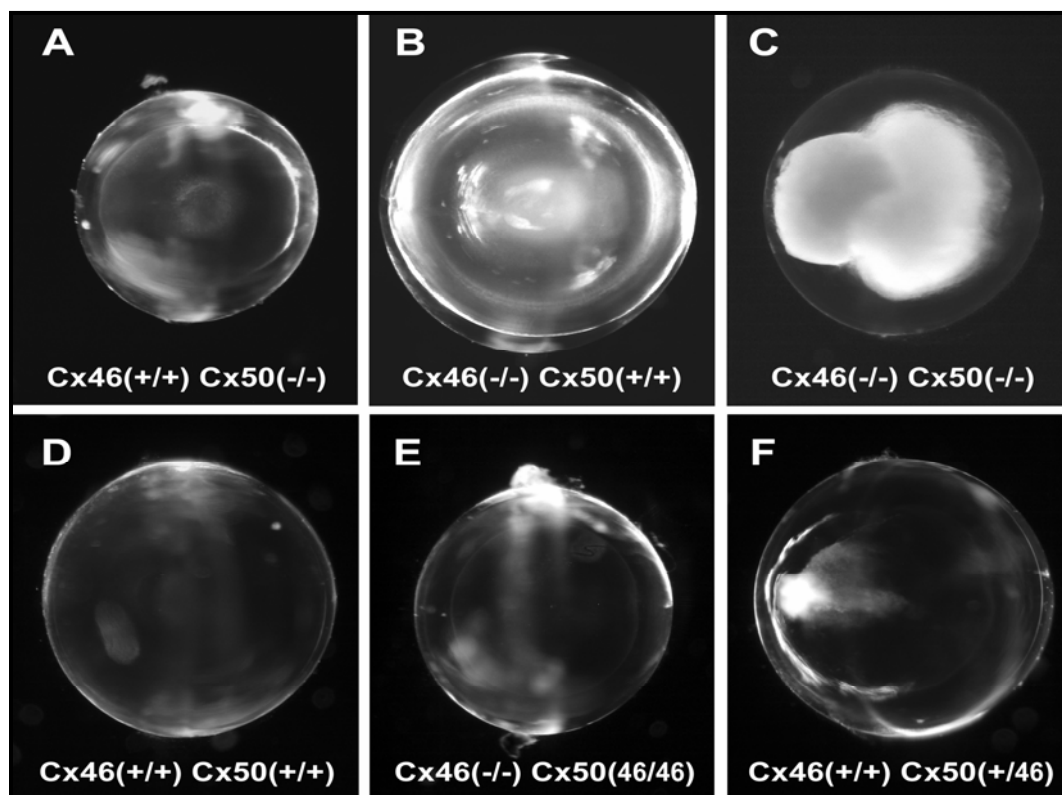


Table I-1. Summary of all reported Cx50 mutations and their mutant phenotypes

Cx50 Mutation (Domain)	Lens Phenotype	Reference
1. D47A (E1 Loop)	<ul style="list-style-type: none"> • Semi-dominant, congenital nuclear cataract • Smaller lenses 	<ul style="list-style-type: none"> • (Steele, Jr. et al., 1998) • (Xu and Ebihara, 1999)
2. G22R (N-Term.)	<ul style="list-style-type: none"> • Disrupted cortical fibers • Dense nuclear cataract • Posterior rupture • Smaller lenses 	<ul style="list-style-type: none"> • (Runge et al., 1992) • (Chang et al., 2002) • (Xia et al., 2006b)
3. S50P (E1 Loop)	<ul style="list-style-type: none"> • Dominant whole cataract • Disrupted fiber cell formation • Vacuole formation • Posterior rupture • Smaller lenses 	<ul style="list-style-type: none"> • (Xia et al., 2006c) • (DeRosa et al., 2007)
4. V64A (E1 Loop)	<ul style="list-style-type: none"> • Dense nuclear and posterior cataract • Malformed secondary fibers • Smaller lenses 	<ul style="list-style-type: none"> • (Graw et al., 2001)
5. R205G (E2 Loop)	<ul style="list-style-type: none"> • Dense nuclear cataract • Smaller lenses 	<ul style="list-style-type: none"> • Personal communication

Chapter II

Hypotheses and Specific Aims

Specific Aims

Cataract is one of the leading causes of blindness worldwide. Thus, it is important to find an appropriate model for studying the developmental processes that govern cataract formation. Transgenic mice lacking Cx46 and Cx50 demonstrate the importance of connexin expression and diversity in the lens. Additionally, mutations within the Cx46 and Cx50 gene loci cause cataracts in both humans and mice. The working hypothesis for this dissertation is that mutations in different Cx50 domains may have diverse effects on channel function, and these changes may play a role in cataract development in the mammalian lens. This hypothesis drives the universal aim of my dissertation, which is to analyze the functional consequences of four distinct Cx50 protein variants: three cataract-causing Cx50 mutants (an N-terminal mutant, Cx50-G22R; an extracellular loop one mutant, Cx50-S50P; an extracellular loop two mutant, Cx50-R205G), and a C-terminally truncated variant, Cx50tr290. The data herein provide new insights and further define the functional significance Cx50 in the lens.

Specific Aim 1: Characterize the effects of the Cx50-G22R mutation on gap junction channel function. Recent studies reveal that the N-terminus of many connexins, including Cx50, plays an important a role in the regulation of channel voltage gating (Peracchia and Peracchia, 2005) (Purnick et al., 2000) (Verselis et al., 1994) (Bruzzone et al., 2003).

Thus, I hypothesize that Cx50-G22R mutant subunits alter gap junction channel function through unique interactions with wild-type fiber connexins, resulting in the mutant phenotypes seen *in vivo*.

The experiments herein analyze the electrophysiological properties of gap junctions comprised of various combinations of wild-type lens fiber connexins and mutant Cx50-G22R subunits. Additionally, I examine the trafficking abilities of these mutant proteins *in vitro* and *in vivo*, and describe a possible physiological mechanism for the aberrant mutant phenotype caused by the G22R mutation.

Specific Aim 2: Analyze the functional characteristics of a cataract-inducing mutant protein, Cx50-S50P. Genetically engineered mice reveal that the combination of mutant Cx50-S50P and wild-type Cx50 subunits inhibits the elongation of primary fiber cells during embryonic development, while the combination of Cx50-S50P and wild-type Cx46 subunits disrupts the formation of secondary fiber cells in the postnatal lens (Xia et al., 2006c) (Gong et al., 2007).

I hypothesize that the mutant Cx50-S50P proteins dominantly alter wild-type Cx50 channel function, and that the co-expression of wild-type Cx46 and Cx50-S50P will form heteromeric gap junctions with unique functional properties.

This dissertation describes the physiological effects of the extracellular loop one mutant, Cx50-S50P, on lens development and function. I use single and dual-whole-cell voltage clamp techniques to determine the differences between gap junctions containing various combinations of wild-type and mutant connexin subunits. Additionally, I examine the localization properties of the S50P mutant protein alone, and in transfected HeLa cells expressing both Cx46 and Cx50-S50P subunits.

Specific Aim 3: Characterize the functional effects of the Cx50-R205G mutation.

Recent discovery of a novel cataract-causing mutation in the second extracellular domain of Cx50 reveals that homozygous Cx50-R205G mutant mice exhibit lenses with a dense nuclear opacity, a mild lamellar cataract, and severe microphthalmia.

I hypothesize that the Cx50-R205G mutation negatively affects wild-type channel function to generate the aberrant ocular phenotypes seen *in vivo*

This work details the ability of the Cx50-R205G mutant to alter intercellular channel function. My data compare the functional and localization abilities of the mutant Cx50-R205G protein to that of either wild-type lens fiber connexin, and characterize the electrophysiological consequences of this mutation *in vitro*.

Specific Aim 4: Identify the functional consequences of Cx50 truncation during fiber cell development. Cx50 undergoes proteolytic cleavage of its cytosolic C-terminus during the later stages of fiber cell differentiation. It has been previously reported that Cx50 mediated coupling is diminished in the mature fibers (Mathias et al., 1991) (Baldo and Mathias, 1992).

Thus, I hypothesize that the endogenous, calpain-mediated truncation of Cx50 proteins may inhibit coupling abilities, or alter their sensitivity to pH.

In this document, I characterize the electrical gating properties of the C-terminally truncated Cx50 variant, Cx50tr290, and its ability to functionally interact with full-length Cx50 subunits *in vitro*. Additionally, I examine the effects of C-terminal truncation on pH gating sensitivity in paired *Xenopus* oocytes.

Chapter III

Materials and Methods

Molecular Cloning

Mutant mouse Cx50-G22R, Cx50-S50P, and Cx50-R205G cDNAs were generated from total mRNAs of homozygous mutant lenses by RT-PCR using a pair of primers: (sense) 5' cgggatcctagtgagcaatgggcgac 3' and (anti-sense) 5' ggaattcgtcatatggtgagatcatc 3'. Mutant cDNA was subcloned into pCR-bluntII-TOPO vector (Invitrogen, Carlsbad, CA) and sequenced to confirm the single amino acid substitutions. Mutant cDNAs were further subcloned into the pCS2+ expression vector using the *EcoRI* restriction site. Murine Cx50tr290 and Human Cx50tr294 were prepared by inserting a stop codon (TGA) after amino acid 290 or 294 by PCR amplification. The PCR products were then subcloned into the pCS2+ and pIRES2-EGFP vectors (Clontech, Palo Alto, CA) between the *EcoRI-XhoI* restriction sites, and sequenced on both strands. Murine wild-type Cx50 (White et al., 1992) and Cx46 (White, 2002) were cloned between the *XhoI-XbaI* or the *XhoI-SpeI* sites of the pCS2+ expression vector, respectively.

***In vitro* transcription, oocyte microinjection, and pairing**

The aforementioned wild-type Cx50, Cx46, mutant Cx50, and truncated constructs were linearized using *NotI* and were transcribed (SP6 mMessage mMachine kit; Ambion, Austin, TX). Adult *Xenopus* females were anesthetized using MS-222, and ovaries were removed in a manner that fully conformed to the ARVO Statement for the Use of Animals in Ophthalmic and Vision Research. Stage V to VI oocytes were collected after ovarian lobes were defolliculated in a solution containing 50 mg/mL collagenase B and 50 mg/mL hyaluronidase in modified Barths (MB) medium without Ca²⁺. Cells were cultured in MB medium at room temperature. Cells were first injected

with 10 ng antisense *Xenopus* Cx38 oligonucleotide to eliminate endogenous intercellular channels. Twenty-four hours later, oocytes were reinjected with wild-type full-length Cx50 cRNA (20 ng/cell), wild-type Cx46 cRNA (5 ng/cell), Cx50tr290 cRNA (80 ng/cell), human Cx50tr294 cRNA (80 ng/cell), mutant Cx50 transcripts (5 ng/cell), or H₂O as a negative control. Vitelline envelopes were removed in a hypertonic solution (200 mM aspartic acid, 10 mM HEPES, 1 mM MgCl₂, 10 mM EGTA, and 20 mM KCl at pH 7.4), and oocytes were manually paired with the vegetal poles apposed in MB-containing Petri dishes.

Biochemical analysis of oocyte proteins

Oocytes were collected in 1 mL buffer containing 5 mM Tris pH 8.0, 5 mM EDTA, and protease inhibitors (White et al., 1992), and were lysed with a series of mechanical passages through needles of diminishing caliber (20, 22, and 26 gauge). Extracts were centrifuged at 1000g at 4°C for 5 minutes. The supernatant was then centrifuged at 100,000g at 4°C for 30 minutes. Membrane pellets were resuspended in SDS sample buffer (2 µL per oocyte), and samples were separated on 10% SDS gels and transferred to nitrocellulose membranes. Blots were blocked with 5% BSA in 1x PBS with 0.02% NaN₃ for 1 hour and subsequently probed with a rabbit anti-mouse Cx50 polyclonal primary antibody (White et al., 1992) or a rabbit anti-rat Cx46 polyclonal primary antibody (Paul et al., 1991). They were then incubated with an alkaline phosphatase-conjugated goat anti-rabbit IgG secondary antibody (Jackson Laboratories, Bar Harbor, ME). Band intensities were quantified (1D Image Analysis software; Eastman Kodak, Rochester, NY). Values from 3-4 independent experiments were

normalized to the mean value of band intensity of either the wild-type Cx50 or Cx46 sample.

Dual whole-cell voltage clamp

Gap junctional coupling between oocyte pairs was measured using dual whole-cell voltage clamp (Spray et al., 1981) (Bruzzone et al., 2003). Electrodes (1.2-mm diameter, omega dot; Glass Company of America, Millville, NJ) were pulled to a resistance of 1 to 2 M Ω with a vertical puller (Narishige, Tokyo, Japan) and filled with 3 M KCl, 10 mM EGTA, and 10 mM HEPES, pH 7.4. Voltage clamping of oocyte pairs was performed with two amplifiers (GeneClamp 500; Axon Instruments, Foster City, CA) controlled by a PC-compatible computer through interface (Axon Instruments). Software (pCLAMP 8.0; Axon Instruments) was used to program stimulus and data collection paradigms.

For measurements of junctional conductance (G_j), both cells of a pair were initially clamped at -40 mV, and alternating pulses of ± 20 mV were applied to one cell. Junctional current (I_j) was divided by the voltage to yield the conductance: $G_j = I_j / (V_1 - V_2)$. To analyze voltage gating, transjunctional potentials (V_j) of opposite polarity were generated by hyperpolarizing or depolarizing one cell in 20 mV steps (over a range of ± 120 mV). Steady state conductance was calculated at the end of the voltage pulse, normalized to the values determined at ± 20 mV, plotted against V_j , and fit to a Boltzmann relation of the form: $G_{jss} = (G_{jmax} - G_{jmin}) / (1 + \exp[A(V_j - V_0)]) + G_{jmin}$, where G_{jss} is the steady state junctional conductance, G_{jmax} (normalized to unity) is the maximum conductance, G_{jmin} is the residual conductance at large values of V_j , and V_0 is the transjunctional voltage at which $G_{jss} = (G_{jmax} - G_{jmin}) / 2$. The constant $A (= nq/kT)$

represents the voltage sensitivity in terms of gating charge as the equivalent number (n) of electron charges (q) moving through the membrane, k is the Boltzmann constant, and T is the absolute temperature.

To examine pH sensitivity, G_j measurements were taken in 30-second intervals by applying voltage steps of 10 mV (1-second duration) to one cell while the voltage in cell two was held constant at -40 mV. The oocyte chamber was perfused at a constant flow rate with MB medium containing Ca^{2+} and saturated with 100% CO_2 for a period of 5 minutes, followed by washout with normal MB solution for 12 minutes.

Electrophysiological recording of hemichannel currents

Macroscopic recordings of hemichannel currents were obtained from single *Xenopus* oocytes using a GeneClamp 500 amplifier controlled by a Digidata 1320 interface (Axon Instruments, Foster City, CA). pClamp 8.0 software (Axon Instruments) was used to program stimulus and data collection paradigms. To obtain hemichannel I-V curves, cells were initially clamped at -40 mV and subjected to 5 second depolarizing voltage steps ranging from -30 to $+60$ mV in 10 mV increments. Membrane currents were analyzed by recording hemichannel currents from cells injected with appropriate cRNA transcripts and incubated overnight in MB supplemented with 2 mM CaCl_2 .

Transient transfection and dual whole-cell patch-clamp electrophysiology

N2A cells were transiently transfected with Cx50 or Cx50tr290 cDNAs using the Lipofectamine 2000 (Gibco BRL) reagent and were plated at low density onto glass coverslips. Coverslips were transferred to the stage of a microscope (Diaphot; Nikon, Tokyo, Japan) and were bathed in a external solution containing 140 mM NaCl, 2 mM CsCl, 2 mM CaCl_2 , 1 mM MgCl_2 , 5 mM HEPES, 4 mM KCl, 5 mM dextrose, 2 mM

pyruvate, and 1 mM BaCl₂, pH 7.2. Each cell of a cell pair was voltage clamped with patch pipettes pulled on a micropipette puller (Flaming/Brown; Sutter P87; Sutter Instrument, Novato, CA) with patch-clamp amplifiers (Axopatch1D; Axon Instruments). Patch electrodes had resistances from 4 to 7 M Ω when filled with internal solution containing 130 mM CsCl, 10 mM EGTA, 0.5 mM CaCl₂, and 10 mM HEPES, pH 7.2. All current recordings were filtered at 0.2 to 0.5 kHz and were sampled at 2 to 5 kHz. Data were acquired (pCLAMP 8.0 software; Axon Instruments) and analyzed with that or another software (Origin 6.1; OriginLab Corp., Northampton, MA). Pairs were initially held at a common holding potential of 0 mV. To evaluate junctional coupling and macroscopic channel gating, depolarizing and hyperpolarizing pulses to various voltages were applied to one cell to establish a V_j gradient, and I_j was measured in the second cell (held at 0 mV). Single-channel currents were measured between weakly coupled cell pairs. All-point amplitude histograms were constructed, and data were fitted to Gaussian functions to determine the mean and variance of the baseline and open-channel current.

Transient transfection and immunocytochemical staining

HeLa cells were plated on 22 mm square coverslips and grown to 50% confluence, then transiently transfected with 2 μ g of connexin DNA subcloned into the pIRES2-EGFP (used for single transfections) or pCS2+ vector (used for co-transfection) using Lipofectamine 2000 (Gibco BRL, Gaithersburg, MD). After overnight incubation, cells were fixed with 1% paraformaldehyde in PBS and blocked with 5% BSA in PBS with 0.1% Triton X-100 and 0.02% NaN₃. HeLa cells expressing wild-type or mutant Cx50 alone were stained with a polyclonal rabbit anti-mouse Cx50 antibody at a 1:1000 dilution, followed by incubation with a Cy3-conjugated fluorescent goat anti-rabbit IgG

secondary antibody (Jackson ImmunoResearch Laboratories). Cells transfected with wild-type Cx46 cDNA were stained with a polyclonal rabbit anti-rat Cx46 antibody at a 1:1000 dilution, followed by incubation with a Cy3-conjugated fluorescent goat anti-rabbit IgG secondary antibody (Jackson ImmunoResearch Laboratories).

To examine the ability of Cx50-S50P to co-localize with wild-type Cx46 in gap junctional plaques, cells were co-transfected with both Cx50-S50P and wild-type Cx46 cDNAs, and stained with both a mouse anti-sheep Cx50 monoclonal primary antibody and a rabbit anti-rat Cx46 polyclonal primary antibody at a concentration of 1:1000. Next, a Cy2-conjugated goat anti-mouse IgG (Jackson Laboratories) secondary antibody was used to detect Cx50, and a Cy3-conjugated goat anti-rabbit IgG secondary antibody to detect Cx46 protein expression (Jackson Laboratories). Coverslips were mounted using media containing DAPI (Vectasheild, Vector Laboratories, Inc., Burlingame, CA) and subsequently viewed and photographed on an Olympus BX51 microscope using an Optronics MagnaFire digital camera. Gap junctional plaque formation was quantified by immunofluorescent microscopy. Images were photographed at either 60x or 100x and areas of cell-cell contact were examined for the presence of gap junctional plaques and counted.

Chapter IV

The physiological role of Cx50-G22R in lens development and homeostasis

Abstract

Mutations in Cx50 and Cx46 have been reported to cause cataracts in both humans and mice. To date, the mechanisms for how mutated Cx46 and Cx50 lead to a variety of cataracts are not well understood. Here, we tested the hypothesis that Cx50-G22R mutant subunits would alter channel formation and/or channel gating properties, contributing to the formation of the mutant lens phenotypes seen *in vivo*. It was previously found that Cx50^(G22R/-) Cx46^(-/-) mice developed severe cataracts with disrupted inner fibers and posterior rupture, while the Cx50^(G22R/Cx46) Cx46^(-/-) lens contained relatively normal inner fibers without lens posterior rupture. Additionally, recent research has indicated a role for connexin50 in embryonic lens development, as Cx50-heterozygous Cx50-S50P mutant lenses (Cx50^(S50P/+) Cx46^(-/-)) exhibited novel deficiencies in primary fiber cell elongation. Using the paired *Xenopus* oocyte system in conjunction with the dual whole-cell voltage clamp assay, we demonstrated that Cx50-G22R subunits alone failed to induce electrical coupling. However, the mixed expression of Cx50-G22R and wild-type Cx46 fiber connexins could form functional gap junction channels with reduced conductance and altered electrophysiological properties when compared to homotypic Cx46 channels. Conversely, co-expression of wild-type Cx50 and Cx50-G22R mutant subunits did not display any obvious changes in channel function when compared to homotypic wild-type Cx50 channels. Taken together, these findings suggest that endogenous wild-type Cx46 and Cx50-G22R mutant subunits interact to form functional heteromeric gap junction channels with unique gating characteristics, a phenomenon that may contribute to the aberrant ocular phenotypes seen *in vivo*. Similarly, our data implied that knock-in Cx46 subunits interact with mutant Cx50-G22R

subunits to form heteromeric channels that partially restore intercellular communication between lens fiber cells, providing a possible mechanism behind the partial rescue of the mutant lens phenotype.

Results

In the following chapter, I have included several figures that are the work of close collaborators and co-authors from the laboratory of Dr. Xiaohua Gong. These data have been incorporated to provide an appropriate context for my dissertation research. For an in-depth description of the methodology used to attain Figures IV-1-5, please refer to Xia et al. 2006 (Xia et al., 2006b). Figures IV-6, 7, 8 contain data derived from my experiments.

Knock-in Cx46 connexin prevents lens rupture and substantially reduces cataract caused by the Cx50-G22R mutation

To evaluate whether knock-in Cx46 could modulate the lens phenotypes caused by the Cx50-G22R mutation *in vivo*, we generated and characterized three different compound mutant mice: Cx50^(G22R/-) Cx46^(-/-), Cx50^(Cx46/-) Cx46^(-/-), and Cx50^(G22R/Cx46) Cx46^(-/-). These mice were produced by intercrossing the Cx50^(G22R/-) Cx46^(-/-) and Cx50^(Cx46/-) Cx46^(-/-) mice. Since these mice were in the Cx46^(-/-) background, we eliminated the contribution of endogenous wild-type Cx46. The Cx50^(Cx46/-) Cx46^(-/-) mice developed clear lenses (Figure IV-1A) similar to previously described lenses in knockover Cx50^(Cx46/Cx46) Cx46^(-/-) mice (Martinez-Wittinghan et al., 2003). In contrast, the Cx50^(G22R/-) Cx46^(-/-) mice developed severe cataracts and lens posterior rupture (Figure IV-1B). Interestingly, the Cx50^(G22R/Cx46) Cx46^(-/-) mice developed lenses with only very mild nuclear cataracts, and no posterior rupture (Figure IV-1C). Representative histological data of mice at postnatal day 14 showed that the Cx50^(G22R/-) Cx46^(-/-) lenses developed severely altered inner fibers, fiber degeneration, and lens posterior rupture (Figure IV-2A); however, the Cx50^(G22R/Cx46) Cx46^(-/-) lenses displayed normal fiber cells

without lens posterior rupture (Figure IV-2B). Thus, unlike the endogenous wild-type Cx46, the knock-in Cx46 subunits suppressed the severe cataract and prevented lens posterior rupture that occurred in the Cx50^(G22R/-) Cx46^(-/-) lenses.

Mixed expression of wild-type and mutant Cx50-G22R alleles does not affect embryonic fiber cell development

To determine if the Cx50-G22R mutation interacts with wild-type connexin proteins to alter embryonic lens fiber development, histological data from embryonic Cx50^(+/+) Cx46^(+/+) (Figure IV-3A), Cx50^(G22R/+) Cx46^(+/+) (Figure IV-3B), and Cx50^(G22R/G22R) Cx46^(+/+) (Figure IV-3C) lenses were analyzed. At day 15 of embryonic development, there were no discernable differences in fiber cell elongation or morphology when comparing heterozygous or homozygous mutant lenses to wild-type samples. These data imply that the N-terminal mutant, Cx50-G22R, does not affect embryonic primary fiber development *in vivo*.

Knock-in Cx46 stabilizes protein expression and restores typical gap junctions containing mutant Cx50-G22R subunits in the lens fiber cells

To understand the molecular mechanism underlying the ability of knock-in Cx46 subunits to rescue the lens phenotype, we characterized the distribution and expression of mutant Cx50-G22R subunits in the Cx50^(G22R/-) Cx46^(-/-) and Cx50^(G22R/Cx46) Cx46^(-/-) lenses by immunostaining and immunoblotting with a polyclonal Cx50 antibody that was previously shown to recognize the Cx50-G22R subunits (Chang et al., 2002). We first examined the subcellular distribution of Cx50-G22R subunits in frozen sections of Cx50^(G22R/Cx46) Cx46^(-/-) and Cx50^(G22R/-) Cx46^(-/-) lenses during the third week of postnatal development. Only very weak fluorescent signals corresponding to expression of the

Cx50-G22R protein were found in the most peripheral fiber cells of the Cx50^(G22R/-) Cx46^(-/-) lens (Figure IV-4A and 4C). In contrast, much stronger punctate signals of Cx50-G22R were located predominantly in the long side of both the peripheral and inner lens fiber cells of the Cx50^(G22R/Cx46) Cx46^(-/-) lens (Figure IV-4B and 4D). Consistent with the immunostaining data, western blotting further confirmed that the Cx50-G22R protein was poorly expressed in the membrane-enriched fraction of the Cx50^(G22R/-) Cx46^(-/-) lenses, but was obviously present in much higher amounts in the equally loaded, membrane-enriched fraction isolated from the Cx50^(G22R/Cx46) Cx46^(-/-) lenses (Figure IV-5). Moreover, immunoblotting showed that the knock-in Cx46 protein level remained largely unchanged in the Cx50^(G22R/Cx46) Cx46^(-/-) lenses compared to that in the Cx50^(Cx46/-) Cx46^(-/-) lenses. Thus, the presence of knock-in Cx46 in the lens restored or stabilized the expression of mutant Cx50-G22R subunits and targeted them to fiber cell membranes.

Co-expression of wild-type lens fiber connexins and Cx50-G22R subunits produces heteromeric gap junction channels *in vitro*

Based on our mouse data, we hypothesized that Cx50-G22R mutant subunits would alter channel formation and/or channel gating properties, contributing to the formation of the mutant lens phenotypes seen *in vivo*. To test this hypothesis, we examined the electrical properties of *Xenopus* oocytes expressing Cx50-G22R subunits alone or in conjunction with wild-type fiber connexins. Immunoblotting verified that wild-type and Cx50-G22R transcripts were efficiently translated in oocytes; protein expression was quantified by band densitometry, confirming that all conditions assayed expressed equivalent amounts of protein (Figure IV-6A).

We then measured junctional conductance between oocyte pairs injected with various combinations of wild-type and mutant transcripts (Figure IV-6B). Homotypic wild-type Cx50 and Cx46 channels exhibited mean conductance values of ~30 μ S and 19 μ S, respectively. Conversely, junctions comprised of Cx50-G22R subunits alone were uncoupled, exhibiting levels of gap junctional conductance indistinguishable from those of the water injected control pairs ($P > 0.05$).

Based on our data, we hypothesized that knock-in Cx46 subunits rescue the lens phenotype by interacting with Cx50-G22R subunits to form gap junction channels. To test this hypothesis, we examined the electrical coupling properties of paired *Xenopus* oocytes expressing Cx50-G22R subunits with or without wild-type Cx50 or Cx46 subunits. Mean junctional conductance measurements recorded from oocyte pairs co-injected with both wild-type Cx46 and mutant Cx50-G22R cRNAs developed heteromeric gap junctions with a mean conductance value of ~5 μ S, a level of coupling approximately 75% lower than that of the homotypic wild-type Cx46 channels. This reduction in coupling was statistically significant ($P < 0.05$), and occurred despite equal levels of Cx46 protein synthesis (Figure IV-6A).

Similarly, the mean conductance of channels containing wild-type and mutant Cx50 subunits was reduced by 50%, a significant reduction when compared to that of the homotypic wild-type Cx50 channels ($P < 0.05$). Since the levels of mutant and wild-type protein expression were nearly identical, the reduction in mean conductance cannot be attributed to an aberration in protein expression or increase in degradation. Therefore, we propose that this decrease in coupling is the result of the formation of functional heteromeric channels with variations in intrinsic channel gating properties.

Heteromeric gap junctions containing wild-type fiber connexins and Cx50-G22R subunits have altered voltage gating properties

If co-injected Cx50-G22R and wild-type Cx50 or Cx46 subunits interact to form heteromeric channels, the gating properties of the junctional conductance may be distinct from those of homotypic wild-type channels. To test this possibility, we examined the kinetics and steady-state properties of gap junctional voltage dependence in homotypic wild-type channels and co-injected oocyte pairs expressing both mutant and wild-type subunits using the dual whole-cell voltage clamp technique. When wild-type Cx50 channels were subjected to a series of voltage applications ranging from ± 20 mV to ± 120 mV, junctional current declined rapidly during larger voltage applications. Conversely, homotypic Cx46 gap junctions displayed a much slower decline in I_j at all comparable voltages. Interestingly, oocytes co-injected with both wild-type and mutant Cx50 transcripts displayed no identifiable change in current decay when compared to wild-type Cx50 channels. However, cells co-expressing wild-type Cx46 and Cx50-G22R showed junctional currents that declined considerably faster during larger voltage applications when compared to homotypic Cx46 channels (Figure IV-7A).

To further quantify these alterations in voltage sensitivity, the initial 500 milliseconds of current decay following a positive 80 mV voltage application was fit by a monoexponential function to determine the rate of channel closure (Figure IV-7B). While there were no significant changes in the mean time constant, τ , when homotypic Cx50 channels were compared to mixed channels expressing both mutant and wild-type Cx50 proteins ($P > 0.05$), comparison of homotypic wild-type Cx46 and heteromeric channels comprised of Cx46 and Cx50-G22R subunits revealed significantly different channel

closure times of 240 and 95 milliseconds, respectively ($P < 0.05$). In a similar fashion, a plot of steady-state junctional conductance, normalized to the values obtained at ± 20 mV, showed that the reductions in conductance for co-injected Cx50-G22R and Cx46 heteromeric channels were greater at all tested voltages than the reductions in steady-state G_j for Cx46 homotypic channels. As expected, our data revealed no drastic change in the equilibrium gating properties when homotypic Cx50 gap junctions and channels co-expressing wild-type and mutant Cx50 were compared (Figure IV-7C). These data clearly show that co-expression of Cx50-G22R with wild-type Cx46 results in significantly altered gating properties. Since Cx50-G22R is a functionally silent allele, the shifted gating properties are most consistent with the formation of heteromeric channels by the co-injected Cx50-G22R and Cx46 subunits. Meanwhile, the absence of detectable changes in the gating properties of mixed channels expressing wild-type and mutant Cx50 proteins indicated that the reduction in electrical coupling exhibited by mixed channels may be the result of a reduction in the amount of functional subunits contributing to channel formation or an aberration in gap junctional plaque formation.

Cx50-G22R localizes to form gap junctional plaques in transfected cells

It has been previously reported that mutant Cx50 proteins exhibit an altered ability to localize to the cell membrane, as well as a reduced capacity to form gap junctional plaques (Chang et al., 2002) (Xia et al., 2006b). In order to determine if the reductions in junctional conductance shown by channels of mixed connexin expression was the result of a failure to efficiently localize connexins to the plasma membrane, wild-type Cx46, Cx50 or Cx50-G22R cDNAs were subcloned into the pIRES2-EGFP vector and transiently expressed in transfected HeLa cells.

Immunofluorescent images revealed that all three connexins were sufficiently expressed *in vitro* (Figure IV-8). As expected, wild-type Cx46 (Figure IV-8A) and Cx50 (Figure IV-8B) subunits were properly targeted to plasma membrane, specifically at regions of cell to cell contact, a phenomenon consistent with the formation of gap junctions. Interestingly, Cx50-G22R proteins were also able to properly localize to sites of cell-cell apposition (Figure IV-8C). These data indicated that the reductions in coupling seen in the paired *Xenopus* assay were not due to a lost ability of Cx50-G22R subunits to form gap junctional plaques.

Discussion

This work directly demonstrates that the interaction of wild-type Cx46 and mutant Cx50 connexin subunits changes gap junction channel properties, thereby manipulating lens phenotypes. We have shown that the knock-in Cx46 subunits prevent severe cataracts and lens posterior rupture by restoring the gap junction structures containing Cx50-G22R subunits *in vivo*. Moreover, mutant Cx50-G22R subunits form functional heteromeric channels with wild-type Cx46 subunits in paired *Xenopus* oocytes *in vitro*. These heteromeric channels show a reduced junctional conductance, but faster gating kinetics and increased voltage sensitivity compared to homomeric channels formed by wild-type Cx46 subunits alone. Interestingly, the co-expression of wild-type and mutant Cx50 does not alter any of the voltage gating parameters assayed. Taken together, these findings suggest that the formation of heteromeric gap junctions by knock-in Cx46 and mutant Cx50-G22R subunits are part of the mechanism that contributes to the suppression of the abnormal lens phenotypes.

It is particularly intriguing that the knock-in Cx46 subunits behave differently from the endogenous Cx46 subunits in their interactions with the Cx50-G22R mutant. Previous publications (Chang et al., 2002) indicate that in *Lop10* homozygous mice, endogenous Cx46 subunits positively contribute to the severity of cataract formation and posterior rupture (Chang et al., 2002). In contrast, the knock-in Cx46 subunits actively suppress cataract formation and posterior rupture. Several differences between knock-in Cx46 and endogenous Cx46 can be derived from previous studies: 1) knock-in Cx46 subunits, on the endogenous Cx50 loci, exhibit an earlier expression pattern than the endogenous Cx46 subunits; 2) the knock-in Cx46 protein level is higher than that of

endogenous Cx46; 3) in the absence of endogenous Cx50, knock-in Cx46, but not endogenous Cx46, forms pH-sensitive channels between the lens fiber cells (Martinez-Wittinghan et al., 2004). This work provides yet another difference, in that only knock-in Cx46 subunits functionally interact with Cx50-G22R to suppress lens phenotypes.

Both endogenous Cx46 and knock-in Cx46 connexins are phosphorylated in the lens. However, mutant Cx50-G22R significantly reduces the phosphorylated forms of endogenous Cx46 connexin (Chang et al., 2002), but does not alter the migration of knock-in Cx46 (Figure IV-4). Thus, phosphorylation of knock-in Cx46 in the knock-in mice may be one of the crucial factors for why only the knock-in Cx46 interacts with mutant Cx50-G22R to target it to gap junctions *in vivo*. Alternatively, the higher expression level of knock-in Cx46 could be another important factor that contributes to phenotypic rescue in the Cx50^(G22R/Cx46) Cx46^(-/-) lenses, since gap junction channels formed by Cx46 alone are sufficient to maintain lens transparency if mutant Cx50 subunits are absent in the lens fibers.

This work provides direct evidence to support the hypothesis that the N-terminal domain of a connexin can modulate both the conductance and gating of gap junction channels formed by different subunits. The glycine 22 residue is an evolutionarily conserved residue in the N-terminal domain of Cx50 connexin. The N-terminus has been reported to form a part of the transjunctional voltage sensor and play a role in the gating of gap junction channels (Verselis et al., 1994). Electrophysiological studies of paired *Xenopus* oocytes provide crucial data showing that mutant Cx50-G22R subunits are able to form heteromeric gap junction channels with wild-type Cx46 subunits. However, these heteromeric channels have reduced macroscopic conductance and faster gating. These

observations may explain why the lens phenotypes are not fully rescued in the Cx50^(G22R/Cx46) Cx46^(-/-) mice.

The analysis of embryonic heterozygous and homozygous mutant lenses, in conjunction with the paired *Xenopus* oocyte assay examining the electrophysiological properties of gap junctions containing both wild-type and mutant Cx50 subunits, reveals that the interaction of these two proteins does not inhibit intrinsic channel function or cause morphological changes during embryonic development. A recent study characterizing the effects of an extracellular loop one mutant, Cx50-S50P, utilizes transgenic mice expressing different combinations of mutant and wild-type alleles to determine that the interaction of wild-type Cx50 and Cx50-S50P inhibits primary fiber cell during embryonic lens development (Xia et al., 2006c). Taken together, these data imply that mutations in different Cx50 domains mediate distinct mechanisms to control various aspects of lens development and homeostasis.

Different Cx46 (*GJA3*) and Cx50 (*GJA8*) mutations in humans and mice link various types of cataracts to these genes. To date, Cx50 mutations are reported in the N-terminal domain (G22R and R23T) (Chang et al., 2002) (Willoughby et al., 2003), the E1 loop (D47A, E48K, S50P, V64G and V64A) (Steele, Jr. et al., 1998) (Berry et al., 1999) (Xia et al., 2006c) (Zheng et al., 2005) (Graw et al., 2001), the second transmembrane domain (P88S) (Shiels et al., 1998), and the C-terminal intracellular domain (I247M) (Polyakov et al., 2001). Cx46 mutations are identified in the first transmembrane domain (F32L) (Jiang et al., 2003), E1 loop (P59L and N63S) (Bennett et al., 2004) (Mackay et al., 1999), E2 loop (P187L and N188T) (Rees et al., 2000) (Li et al., 2004), and C-terminal domain (S380fs) (Mackay et al., 1999). The unique properties of the heteromeric

channels containing a mixture of wild-type and mutant subunits suggest a molecular explanation for why different mutations of Cx46 or Cx50 cause a variety of cataract phenotypes in humans and mice. These data indicate that mutant connexin subunits can act as specific molecular tools that change the properties of gap junction channels and manipulate the cell-cell communication signals in the lens. Thus, we believe that the mouse mutant lines with different point mutations in Cx46 or Cx50 connexins provide extremely useful models for investigating the specific communication signals mediated by gap junction channels in the lens fiber cells and for understanding how changes in fiber-fiber communication leads to distinct cataract phenotypes. Finally, a better understanding of the underlying molecular mechanism for cataract formation may lead to the development of alternative approaches to prevent or delay cataract.

Figure IV-1. Knock-in Cx46 suppresses the severe cataract of the Cx50-G22R mutation. Lens photos show a comparison of three compound mutant lenses at the age of 3 weeks. (A) The Cx50^(Cx46^{-/-}) Cx46^(-/-) lens is transparent. (B) The Cx50^(G22R^{-/-}) Cx46^(-/-) lens has severe cataract with posterior rupture. (C) The Cx50^(G22R/Cx46) Cx46^(-/-) lens is intact with only a mild nuclear cataract. (Xia et al., 2006b)

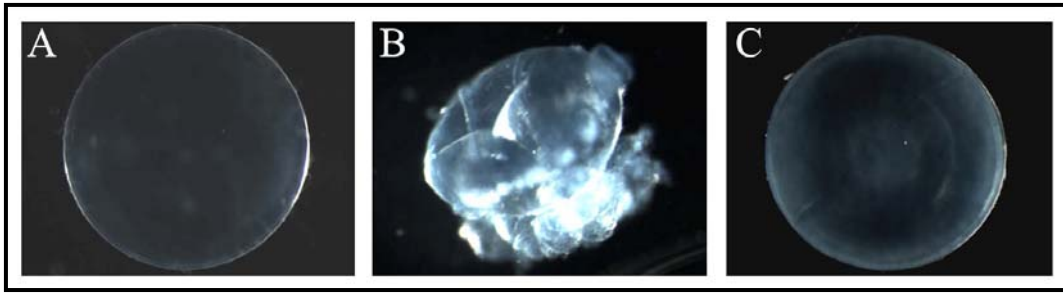


Figure IV-2. Histology reveals normal fiber morphology in the Cx50^(G22R/Cx46) Cx46^(-/-). (A) The Cx50^(G22R/-) Cx46^(-/-) lens of a 2-week old mouse has severely degenerated inner fibers and a ruptured posterior capsule. (B) Cx50^(G22R/Cx46) Cx46^(-/-) lens section shows relatively normal inner lens fibers without obvious cell degeneration. The abnormal central fibers could be due to sectioning artifacts or the mild nuclear cataract (Xia et al., 2006b).

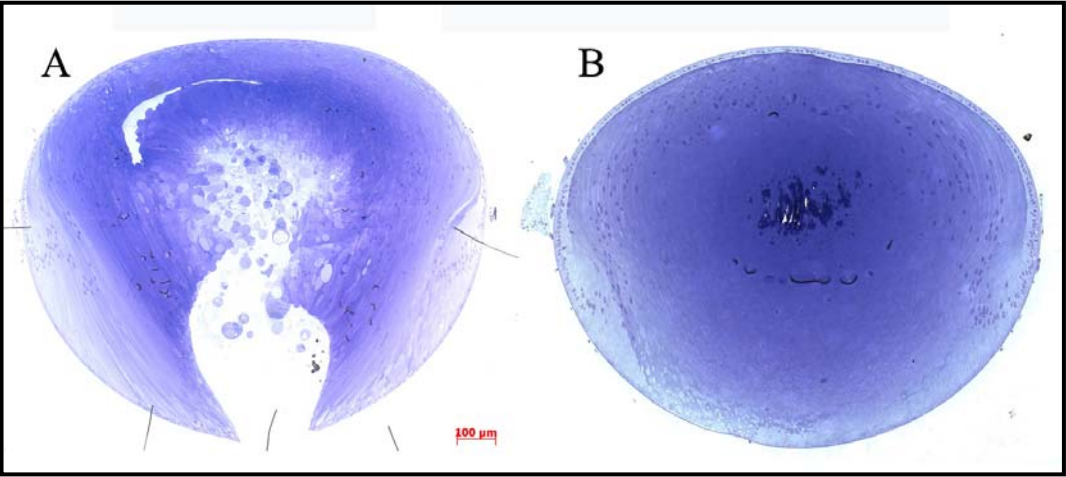


Figure IV-3 Histology reveals normal embryonic fiber development in wild-type ($Cx50^{+/+} Cx46^{-/-}$) (A), the $Cx50^{(G22R/+)} Cx46^{+/+}$ (B), and $Cx50^{(G22R/G22R)} Cx46^{+/+}$ (C) lenses at day 15 of embryonic development. All three lenses exhibit normal inner lens fibers without obvious cell degeneration or inhibition of primary fiber cell elongation.

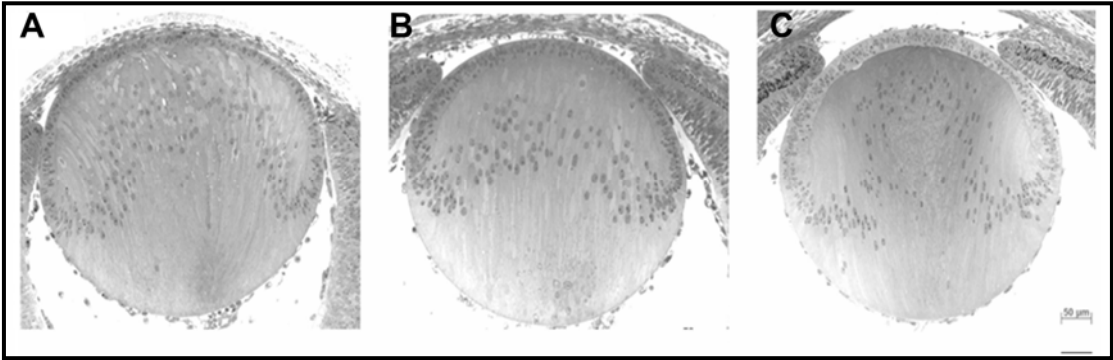


Figure IV-4. Immunohistochemical staining reveals that the knock-in Cx46 connexin restores the gap junctions consisting of the Cx50-G22R mutant subunits in lens fiber cells. The upper panel shows Cx50 staining (red) in the Cx50^(G22R/-) Cx46^(-/-) (A) and the Cx50^(G22R/Cx46) Cx46^(-/-) (B) lens cross sections. The lower panel shows the merged images of Cx50 connexin (red) and F-actin (FITC-phalloidin staining in green) in Cx50^(G22R/-) Cx46^(-/-) (C) and Cx50^(G22R/Cx46) Cx46^(-/-) (D) lens cross sections. Very small punctate fluorescent spots appear in only the peripheral fiber cells of the Cx50^(G22R/-) Cx46^(-/-) lens, while punctate fluorescent signals typical of gap junction channels are predominantly seen in the longer sides of the fiber cells of the Cx50^(G22R/Cx46) Cx46^(-/-) lens. Scale bar: 20 μm (Xia et al., 2006b).

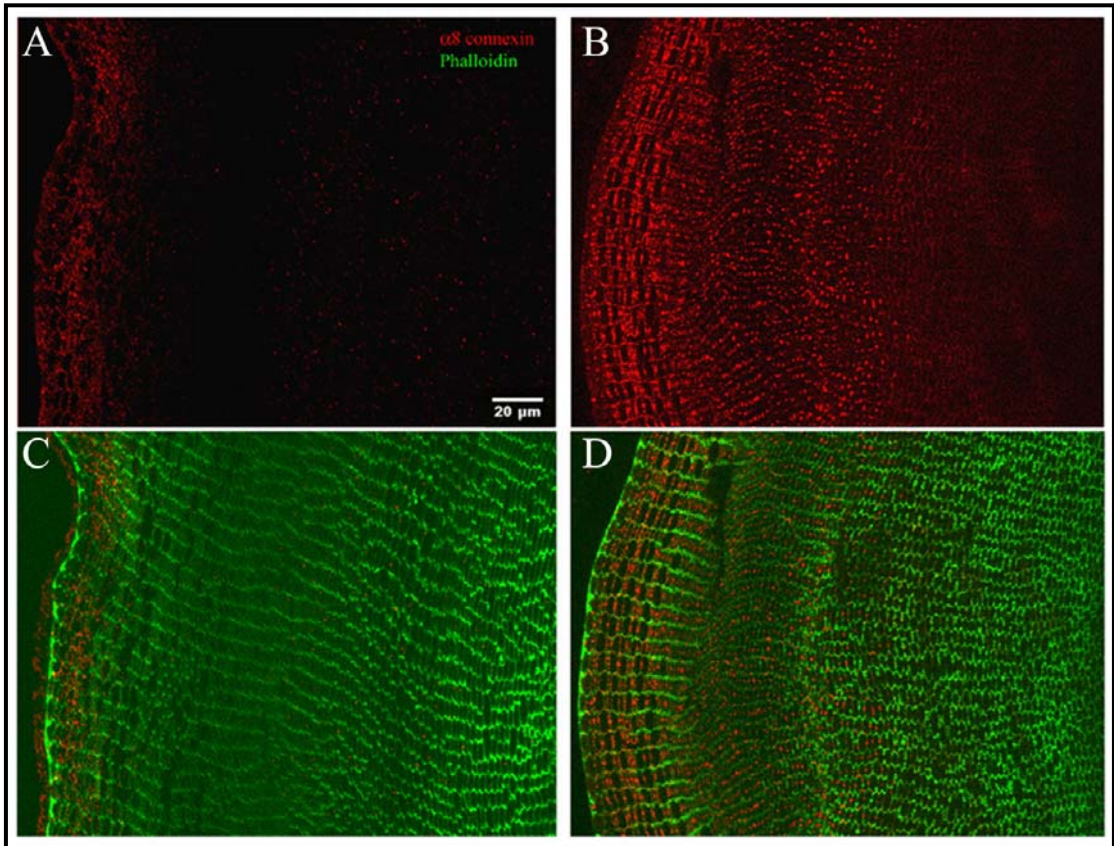


Figure IV-5. Western blot data show an increase in Cx50-G22R protein level in the Cx50^(G22R/Cx46) Cx46^(-/-) lens. Preparation of membrane protein-enriched samples from the lenses of different mice at 3 of weeks age are seen in: Lane 1: wild type Cx50^(+/+) Cx46^(+/+), Lane 2: Cx50^(Cx46/-) Cx46^(-/-), Lane 3: Cx50^(G22R/Cx46) Cx46^(-/-), and Lane 4: Cx50^(G22R/-) Cx46^(-/-). Equal portions of lens samples were loaded onto the gel and probed with an anti-Cx46 connexin antibody (A) and with an anti-Cx50 antibody (B). Lane 1 shows the wild-type control for endogenous Cx46 and Cx50. All three mutant mice contain no wild-type Cx46 and Cx50 alleles; the bands in lanes 2 and 3 of panel A are knock-in Cx46 proteins and the band in lane 3 of panel B is the Cx50-G22R mutant subunit. The molecular weight markers are listed on the left (Xia et al., 2006b).

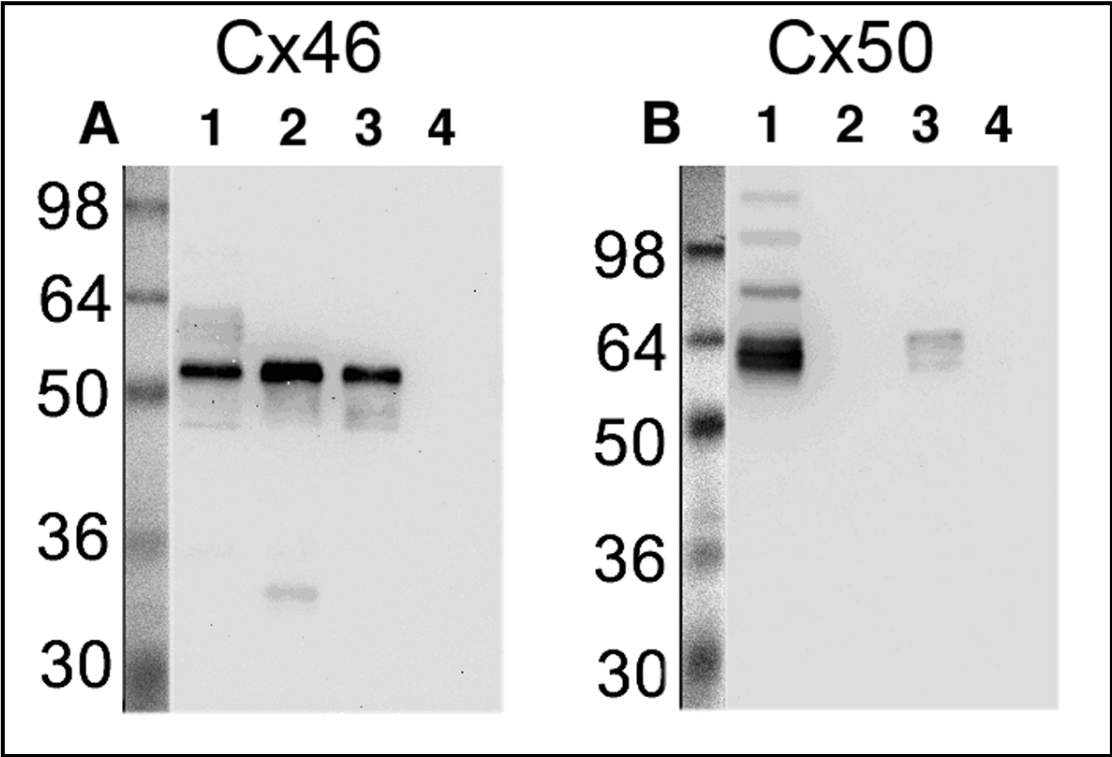


Figure IV-6. (A) Western blot analysis of *Xenopus* oocytes shows equivalent expression of wild-type Cx50, Cx46 or Cx50-G22R proteins when expressed alone or co-injected. Quantitation of mean band intensity by densitometry confirms that levels of connexin expression are not statistically different ($P > 0.05$) among all samples analyzed. Densitometry values are the mean \pm the standard error measurement of three independent experiments. (B) Cx50-G22R forms functional heteromeric channels with Cx46. Junctional conductance recordings from oocyte pairs expressing wild-type Cx46, wild-type Cx50, or Cx50-G22R alone or oocytes that co-express Cx50-G22R and either wild-type Cx46 or Cx50. Pairs containing wild-type Cx46 alone ($n = 20$) or co-injected with Cx50-G22R and Cx46 transcripts ($n = 57$) exhibit conductance values >100 fold higher than the water injected background value ($n = 40$). However, pairs co-expressing Cx46 and Cx50-G22R show a 75% reduction in mean conductance when compared to homotypic Cx46 channels ($P < 0.05$, Student's t-test). Cells paired to form homotypic Cx50-G22R ($n = 55$) channels fail to produce levels of coupling significantly higher than background ($P > 0.05$, Student's t-test). Mixed channels containing both wild-type and mutant Cx50 subunits ($n = 35$) exhibit a statistically significant 50% reduction in coupling when compared to homotypic wild-type Cx50 channels ($n = 28$) ($P < 0.05$, Student' t-test).

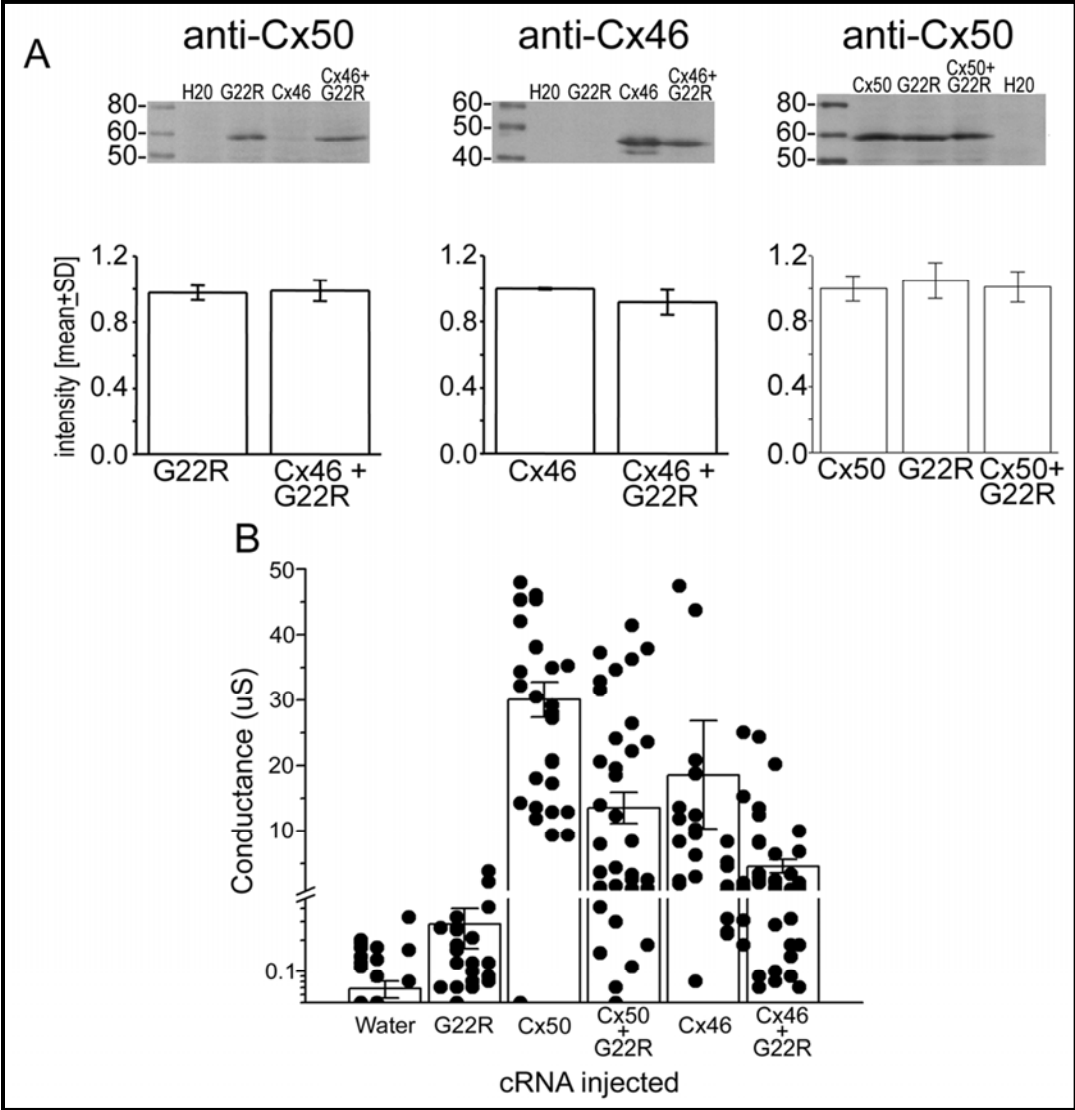


Figure IV-7. Voltage gating properties of homotypic and mixed channels. (A) The decay in junctional current (I_j) induced by transjunctional voltage (V_j) is plotted as a function of time for channels containing Cx46 or Cx50 alone or oocytes co-expressing both wild-type and mutant subunits. V_j is stepped to ± 120 mV in 20 mV increments. At all potentials, heteromeric channels containing Cx50-G22R and Cx46 show a more rapid current decay of greater magnitude. Conversely, I_j decay across mixed channels containing both wild-type and mutant Cx50 are unaltered. (B) Analysis of channel closure kinetics. Representative initial current decays for homotypic and heteromeric gap junctions after application of a +80mV transjunctional voltage are fit to a monoexponential decay to determine the mean time constant, τ . Heteromeric channels expressing Cx50-G22R and Cx46 close significantly faster than homotypic Cx46 junctions ($P < 0.05$, Student's t-test). Interestingly, channel closure kinetics do not reveal significant changes when we compare the mean channel closure times of homotypic Cx50 and mixed channels containing wild-type and mutant Cx50 ($P > 0.05$, Student's t-test). (C) Comparison of equilibrium conductance. Steady state conductance measured when current decay reaches equilibrium is normalized to the recordings at ± 20 mV, and plotted as a function of V_j . The steady-state reduction in conductance for heteromeric Cx50-G22R and Cx46 channels is greater than the reduction for homotypic Cx46 channels. However, steady-state voltage sensitivity is unaltered when homotypic wild-type Cx50 channels and heteromeric gap junctions are compared.

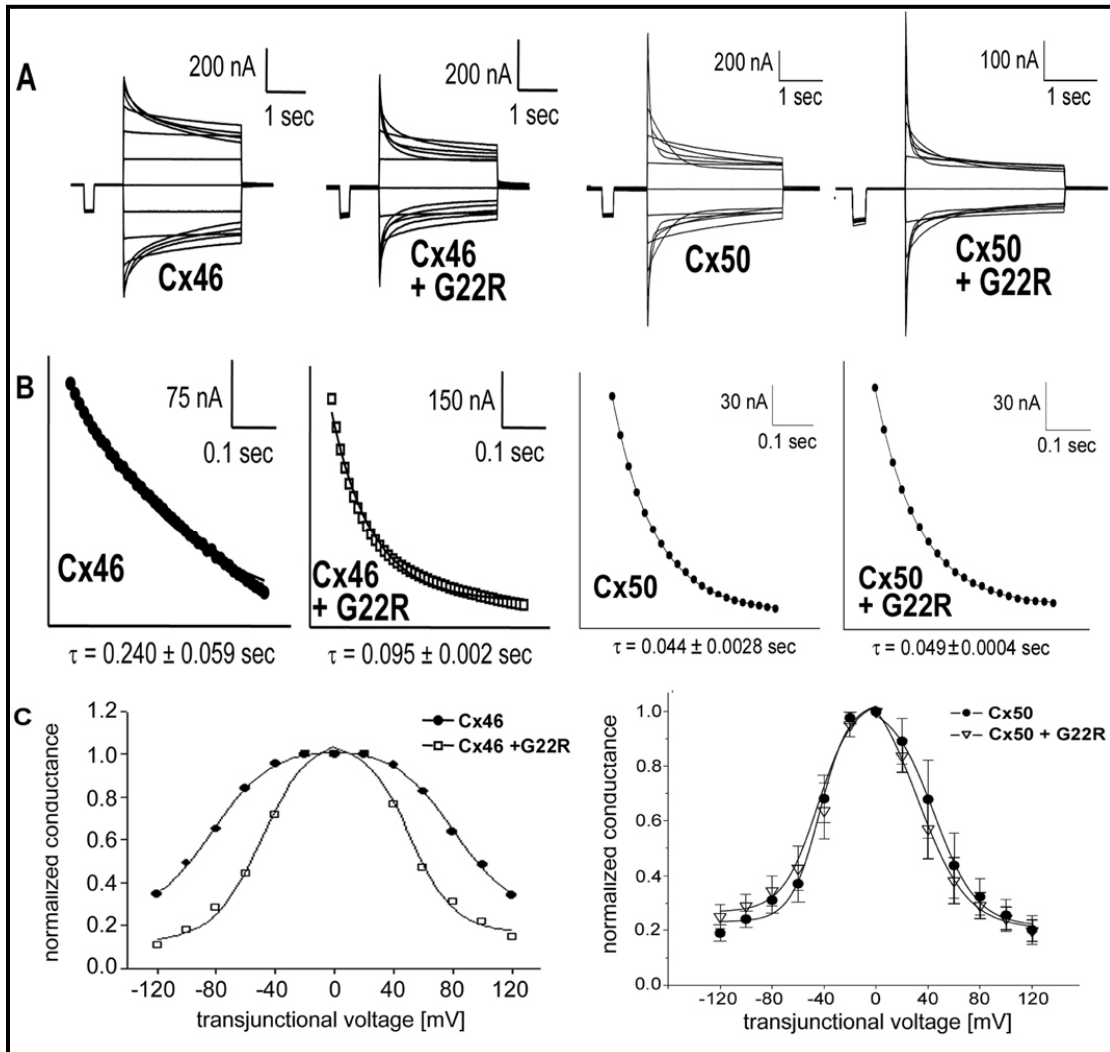
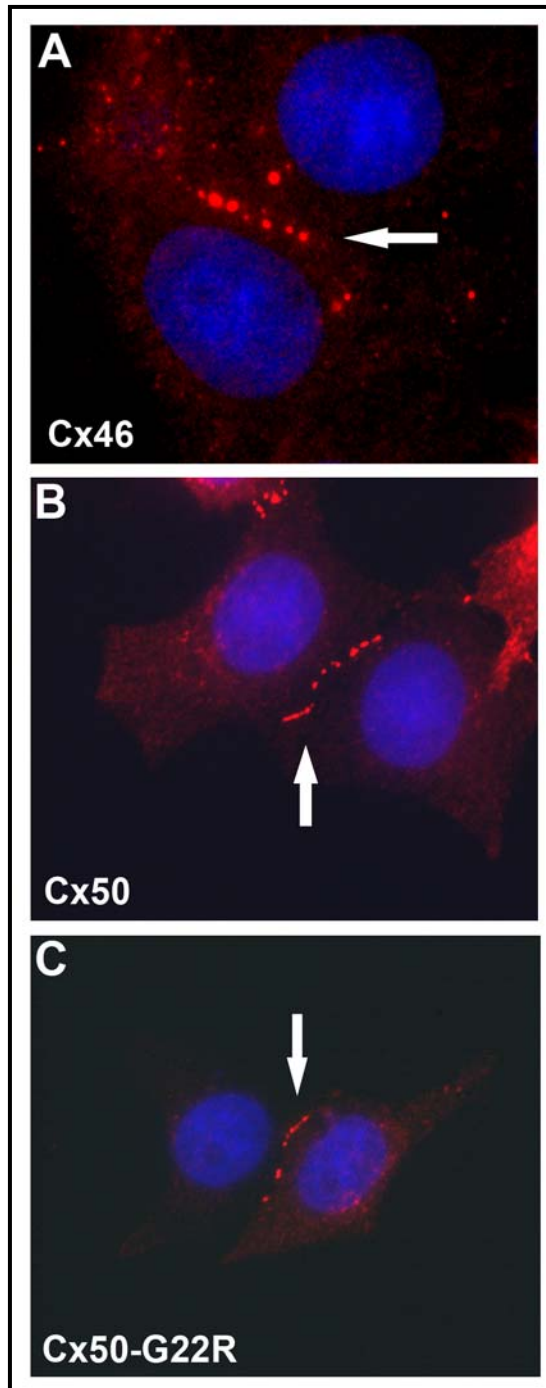


Figure IV-8. Mutant Cx50 localizes to the plasma membrane. Images (100x) of HeLa cells transiently transfected with either wild-type Cx46 (A), wild-type Cx50 (B), or mutant Cx50 (C) DNA. Blue represents DAPI staining of the nucleus, while red shows Cy3 staining of connexins. Overlay images of the transfections indicate efficient translation of all of the connexin proteins and their localization to the cell membrane, especially at areas of cell to cell apposition (arrows).



Chapter V

The cataract inducing Cx50-S50P mutation dominantly alters wild-type lens connexin channel gating

Abstract

Mutations within Cx50 have been linked to various cataract phenotypes. To determine the mechanism behind cataract formation, we used the paired *Xenopus* oocyte system in conjunction with transfected HeLa cells and genetically engineered mouse models to examine the functional characteristics of gap junctions expressing a cataract causing Cx50 mutant protein, Cx50-S50P. S50P subunits alone failed to induce electrical coupling. However, the mixed expression of S50P and either wild-type Cx50 or Cx46 subunits, paired to create heteromeric gap junctions, formed functional intercellular channels with altered voltage gating properties when compared to homotypic wild-type channels. Additionally, immunofluorescent microscopy showed that S50P subunits alone failed to localize to the plasma membrane, unlike Cx46, which concentrated at cell-cell appositions. S50P co-localized with wild-type Cx46 in both transfected HeLa cells *in vitro* and mouse lens sections *in vivo*. Taken together, these data define the electrophysiological properties and intracellular targeting of gap junctions formed by the heteromeric combination of Cx50 or Cx46 and S50P mutant proteins. Additionally, mixed channels displayed significantly altered gating properties, a phenomenon that may contribute to the cause of cataract associated with this mutation.

Results

The following chapter includes two immunofluorescent lens images incorporated as panels E and F of Figure V-7 that have been graciously contributed by our collaborators in the Gong Laboratory at the University of California-Berkeley. These data provide additional support for the hypotheses of this dissertation. For an in-depth description of the methodology used to attain these *in vivo* lens images, please refer to DeRosa et al. 2007 (DeRosa et al., 2007).

Connexin expression in *Xenopus* oocytes

The production of lens fiber connexins in *Xenopus* oocytes was examined via immunoblot analysis. Oocytes injected with water, wild-type Cx50, Cx46, or Cx50-S50P cRNA alone, and cells expressing both mutant and wild-type connexins were analyzed using a polyclonal antibody specific for the central cytoplasmic loop of mouse Cx50(White et al., 1992) or a polyclonal antibody raised against the extreme carboxy terminus of rat Cx46(Paul et al., 1991). Immunoblotting revealed an ~60 kDa band corresponding to Cx50 in oocyte samples injected with wild-type or mutant cRNA transcripts (Figure V-1A). An antibody specific for Cx46 detected two bands of ~46 kDa in samples injected with Cx46 cRNA alone or co-injected oocytes expressing Cx46 and Cx50-S50P (Figure V-1B). Expression levels were quantified using band densitometry on replicate immunoblots (n=3). A plot of the mean band intensity values (normalized to wild-type mean intensity value) (Figure V-1C) showed no significant reduction of Cx50 expression in oocytes injected with wild-type Cx50 or Cx50-S50P alone, nor was a reduction seen in co-injected samples expressing both wild-type and mutant Cx50 proteins ($P > 0.05$, ANOVA). Similarly, samples tested for Cx46 expression show

equivalent levels of Cx46 production (Figure V-1D) in samples injected with Cx46 alone or in conjunction with Cx50-S50P, as band densitometry showed no significant change in mean band intensity ($P > 0.05$, ANOVA). Thus, both wild-type and mutant transcripts were synthesized equally, and any alteration in channel function cannot be attributed to differences in protein expression.

Cx50-S50P fails to form functional channels in *Xenopus* oocytes

To test the hypothesis that the S50P mutation alters intercellular communication in the lens, we measured gap junctional conductance, G_j , in oocyte pairs injected with various combinations of lens fiber connexin cRNAs (Figure V-1E). Control oocyte pairs injected with anti-sense oligonucleotide and water showed negligible junctional conductance. Conversely, homotypic wild-type Cx50 or Cx46 channels displayed mean conductance values of ~ 26 and ~ 20 μS , respectively, a significant increase in G_j that is several hundred-fold greater than that of the background ($P < 0.05$, Student's t-test). Interestingly, cells injected with both wild-type and mutant Cx50 cRNA transcripts, paired to form heteromeric channels, exhibited a mean G_j of approximately 20 μS , which was not significantly different compared to homotypic Cx50 channels ($P > 0.05$, Student's t-test). Similarly, oocytes paired to form heteromeric gap junctions containing Cx46 and Cx50-S50P subunits displayed a mean conductance of 17 μS , a decrease in G_j not significantly different compared to the homotypic Cx46 channel ($P > 0.05$, Student's t-test). Homotypic channels comprised of mutant Cx50-S50P subunits produced a level of conductance significantly lower than that of homotypic wild-type Cx50, indicating that Cx50-S50P proteins alone fail to form functional intercellular channels ($P < 0.05$,

Student's t-test). Additionally, the heterotypic pairing of oocytes expressing Cx50 or Cx46 with those containing Cx50-S50P alone failed to significantly couple cells, as levels of junctional conductance were similar to that of the background measured in water-injected pairs. Co-injection of Cx50-S50P with wild-type Cx50 or Cx46 facilitated the formation of functional intercellular channels that displayed slight reductions in mean conductance compared to homotypic wild-type. These results show that mutant Cx50 subunits fail to form homotypic or heterotypic gap junctions on their own, and do not significantly inhibit conductance when co-expressed with wild-type lens fiber connexins.

Voltage gating behavior of wild-type and heteromeric channels

To characterize the electrophysiological properties of homotypic wild-type channels or heteromeric channels expressing both wild-type and mutant connexins, voltage gating was examined by subjecting oocyte pairs to a series of hyperpolarizing and depolarizing transjunctional voltages (V_j). Figure V-2 shows a comparison of representative traces of junctional currents (I_j) for oocyte pairs expressing homotypic Cx50 (Figure V-2A) and mixed gap junctions expressing wild-type and mutant Cx50 proteins (Figure V-2B). I_j decreased symmetrically with time in a voltage-dependent manner for both channel types and showed a more rapid current decline at greater V_j applications. To analyze channel closure kinetics, the initial 250 milliseconds of current decay was plotted against time and fit to a mono-exponential function to determine the time constant, tau (τ). Representative current decays were recorded during an application of a positive 80 mV voltage step for homotypic wild-type (Figure V-2C) and mixed channels, expressing both wild-type Cx50 and mutant subunits (Figure V-2D). Mixed channels closed 15% faster than wild-type channels with mean channel closure times of

61 and 52 milliseconds, respectively ($P < 0.05$, Student's t-test). At a larger transjunctional potential of 120 mV, both channel configurations closed faster than at 80 mV, exhibiting mean tau values of 34 and 25 milliseconds for homotypic wild-type (Figure V-2E) and co-injected (Figure V-2F) channels, respectively ($P < 0.05$, Student's t-test). These slight alterations in channel closure kinetics may indicate an interaction between Cx50-S50P and wild-type Cx50 subunits when the two proteins are co-expressed in cells.

The comparison of homotypic channels comprised of Cx46 (Figure V-3A) and heteromeric gap junctions containing Cx46 and Cx50-S50P subunits (Figure V-3B) revealed that heteromeric channels appeared to be more sensitive at larger voltage applications, ± 80 -120 mV, than their homotypic counterparts. Similarly, mixed channels expressing wild-type Cx46 and Cx50 (Figure V-3C) showed that larger voltage potentials resulted in a more rapid decline toward steady state when compared to heteromeric gap junctions containing wild-type Cx46 and S50P subunits. Comparison of the three representative I_j decays, Cx46 alone (Figure V-3D), gap junctions expressing both Cx46 and Cx50-S50P proteins (Figure V-3E), and channels comprised of wild-type Cx46 and Cx50 (Figure V-3F), via one-way analysis of variance (ANOVA) during an 80 mV voltage application reveal that there were statistically significant differences ($P < 0.05$) in the mean channel closure times for all three channel types analyzed. Similarly, when a 120 mV potential was applied to oocyte pairs connected by homotypic Cx46 gap junctions, a mean channel closure time of 126 milliseconds was recorded (Figure V-3G). Comparison of this tau value to channels comprised of wild-type Cx46 and S50P (90 milliseconds, Figure V-3H), and channels containing wild-type Cx46 and Cx50 (75

milliseconds, Figure V-3I), showed that there were statistically significant differences between the three mean tau values ($P < 0.05$, ANOVA). Thus, the behavior of mixed channels containing wild-type Cx46 and S50P were functionally distinct from either homotypic Cx46 channels or heteromeric gap junctions expressing wild-type Cx46 and Cx50 subunits. These data support the hypothesis that Cx50-S50P interacts with wild-type Cx46 to form functional gap junctions with unique voltage gating properties.

The steady state voltage gating behavior of these channels was examined by plotting V_j against G_j (normalized to the values obtained at ± 20 mV) and fitting the data to the Boltzmann equation (Figure V-4, Table V-1). Analysis of the equilibrium gating properties showed no drastic changes in the steady-state properties of homotypic Cx50 channels and mixed gap junctions co-expressing wild-type and mutant Cx50 (Figure V-4A). Conversely, mixed channels containing both Cx46 and Cx50-S50P subunits (Figure V-4B, closed circles) displayed a visible shift toward lower transjunctional voltages in the Boltzmann plot when compared to wild-type Cx46 channels (Figure V-4B, open squares), indicating that heteromeric channels were more voltage sensitive than the homotypic wild-type Cx46 junctions at all tested voltages. Heteromeric channels comprised of wild-type Cx46 and Cx50 (Figure V-4B, open diamonds) were similar to those containing Cx46 and Cx50-S50P at negative transjunctional potentials, but showed a statistically significant alteration in voltage sensitivity at larger positive potentials. ANOVA revealed that there were statistically significant differences between all three data sets at all positive potentials ≥ 60 mV ($P < 0.05$).

Taken together, these results provide evidence for the heteromeric interaction between wild-type lens fiber connexins and mutant Cx50-S50P subunits *in vitro*.

Interestingly, the co-expression of wild-type Cx46 and Cx50-S50P presents strong evidence for the functional interaction between these two proteins via the formation of functional intercellular channels with decreased junctional conductance, visibly altered junctional current decay, and significantly altered channel closure kinetics. In contrast, the co-expression of wild-type and mutant Cx50 provides less evidence for the interaction of wild-type Cx50 and Cx50-S50P subunits *in vitro*, as only slight shifts in the electrophysiological properties of these channels were seen.

Voltage-gating behavior of heterotypic channels

To determine whether the slight shift in mean channel closure time and the 20% reduction in conductance could be attributed to interaction of the S50P mutant with wild-type Cx50, we analyzed the voltage gating characteristics of heterotypic channels where homomeric Cx46 connexons were paired with either Cx50 homomeric hemichannels, or heteromeric connexons containing both wild-type and mutant Cx50 subunits. Junctional conductance measurements recorded from oocytes paired to form heterotypic channels (Figure V-5A) showed that heterotypic gap junctions containing wild-type Cx46 and wild-type Cx50 displayed a mean G_j value of $\sim 22 \mu\text{S}$, a significant increase in coupling when compared to the $10.5 \mu\text{S}$ exhibited by heterotypic channels containing wild-type and mutant Cx50 subunits ($P < 0.05$, Student's t-test). Both channel types displayed a level of conductance significantly higher than that of the water-injected negative controls ($P < 0.05$, Student's t-test). Representative current traces for heterotypic oocyte pairs derived from cells expressing only Cx46 and paired with oocytes containing wild-type Cx50 alone (Figure V-5B), or oocytes co-expressing both wild-type and mutant Cx50 transcripts (Figure V-5C), exhibited no obvious changes in junctional current decay for

all voltage applications assayed. To examine the gating properties of heterotypic gap junctions, equilibrium gating properties of these channels were analyzed by applying the Boltzmann equation (Figure V-5D). Heterotypic channels expressing both wild-type and mutant Cx50 proteins showed a slight, but statistically significant, increase in voltage dependence compared to heterotypic channels expressing wild-type Cx46 and Cx50 proteins alone, as indicated by the downward shift in the Boltzmann curve for positive values of V_j ($P < 0.05$, Student's t-test, Table V-1). Taken together, these data indicate that the reduction in G_j seen in mixed channels comprised of wild-type and mutant Cx50 proteins, as well as the slight alteration in voltage sensitivity was due to the heteromeric interaction of S50P subunits with wild-type Cx50.

Cx50-S50P requires Cx46 to form voltage sensitive hemichannels

Several studies have suggested that abnormal hemichannel activity may play a role in the development of connexin-related diseases (DeRosa et al., 2007; Jiang and Gu, 2005) (Gerido et al., 2007), and Cx46 and Cx50 have both been shown to form hemichannels *in vitro* (Ebihara and Steiner, 1993) (Beahm and Hall, 2002). To test if S50P formed functional hemichannels that may have contributed to the mutant lens phenotypes seen *in vivo*, whole-cell currents (I_m) were recorded from single oocytes expressing wild-type Cx46 or Cx50-S50P proteins alone or in combination (Figure V-6). Oocytes expressing wild-type Cx46 alone revealed slowly activated outward currents that increased as voltage applications became larger and more positive. Conversely, S50P-injected oocytes exhibited negligible current flow at all voltage potentials analyzed. Mixed expression of wild-type Cx46 and Cx50, or wild-type Cx46 and S50P, similarly displayed the presence of intermediate outward currents for both tested conditions. When

steady-state currents were plotted against membrane voltage, negligible membrane currents were displayed by cells expressing only Cx50-S50P, while cells injected with wild-type Cx46 transcripts exhibited large currents that increased with V_m . Reduced whole-cell currents were observed for cells expressing both wild-type lens fiber connexins and cells containing wild-type Cx46 and S50P proteins. These data suggest that S50P fails to form hemichannels alone, but can form heteromeric hemichannels with wild-type Cx46.

Aberrant localization of Cx50-S50P in transfected cells and in the lens

It has been previously reported that mutant Cx50 proteins exhibit an altered ability to localize to the cell membrane and a reduced capacity to form gap junctional plaques (Chang et al., 2002) (Xia et al., 2006c). To determine if the reductions in junctional conductance shown by channels of mixed connexin expression were the result of a failure to efficiently localize connexins to the plasma membrane, wild-type Cx46 and/or Cx50-S50P, subcloned into the pIRES2-EGFP and pCS2+ vectors, respectively, were expressed in transiently transfected HeLa cells.

Immunofluorescent images revealed sufficient connexin expression for both wild-type Cx46 (Figure V-7B and V-7D) and Cx50-S50P (Figure V-7A and V-7C) proteins. Cx50-S50P alone was unable to localize to sites of cell-cell apposition, instead accumulating in subcellular compartments surrounding the nucleus (Figure V-7A, arrow). Conversely, Cx46 subunits were properly targeted to plasma membrane regions of cell to cell interaction in 75% of the cell pairs analyzed (Table V-II), a phenomenon consistent with the formation of gap junctions (Figure V-7B). Interestingly, co-transfection of HeLa cells with both wild-type Cx46 and Cx50-S50P cDNA facilitated the co-localization of

these proteins at cell-to-cell interfaces in 74% of the pairs examined (Figure V-7C and V-7D, arrowheads).

Immunostaining of frozen lens sections further confirmed the notion that Cx50-S50P mutant proteins were stabilized in gap junction plaques by Cx46 *in vivo*. Fluorescent images showed that Cx50-S50P mutant proteins were only detected in the most superficial differentiating fiber cells of Cx50^(S50P/S50P) Cx46^(-/-) lenses, lacking both endogenous wild-type Cx50 and Cx46 alleles (Figure V-7F). Conversely, substantial staining was extended deeper into differentiating fibers of Cx50^(S50P/S50P) Cx46^(+/+) lenses that expressed endogenous wild-type Cx46 (Figure V-7E). Thus, both *in vivo* and *in vitro* findings support the hypothesis that the mutant Cx50-S50P protein has the ability to associate with wild-type Cx46 subunits, a phenomenon that may play a role in cataract formation.

Discussion

In this study, we use a dual whole-cell voltage clamp method to characterize the electrophysiological properties of gap junction channels between paired *Xenopus* oocytes injected with different combinations of wild-type and mutant connexins. Dual whole-cell voltage clamp is used extensively to analyze and obtain unique “electrical fingerprints” to identify functional differences between intercellular channels containing diverse connexin subunits (Bruzzone et al., 1996) (Harris, 2001) (Evans and Martin, 2002). While the transjunctional potentials created using this assay may not correlate with the endogenous resting potentials present in the mammalian lens, the distinct functional characteristics revealed by these techniques facilitate the detection of changes in intrinsic channel properties that can only result from the interaction of the Cx50-S50P mutant and wild-type Cx46 or Cx50 proteins. These functional interactions help explain the physiological pathologies that occur *in vivo*.

The data presented herein provide *in vitro* and *in vivo* evidence for the interaction between wild-type Cx50, wild-type Cx46 and mutant Cx50-S50P subunits. Furthermore, this study provides support for the hypothesis that a unique interaction between mutant and wild-type lens connexins modulates the aberrant lens phenotypes displayed by Cx50-S50P mutant mice (Xia et al., 2006c). Our findings show that while Cx50-S50P subunits alone fail to form functional intercellular channels or voltage activated hemichannels in *Xenopus* oocytes, or target to gap junctions in transfected HeLa cells, the mixed expression of wild-type lens fiber connexins and mutant Cx50-S50P subunits can form functional gap junctions that display levels of electrical coupling comparable to those recorded from homotypic wild-type channels. Additionally, heteromeric channels

containing S50P proteins and either wild-type Cx46 or Cx50 exhibit distinct voltage gating properties, and increase the mutant's ability to localize in junctional plaques. Together, these data imply that unique interactions between connexins in the lens play a crucial role in proper organ function and development.

Recent studies reveal that connexin diversity plays an integral role in the proper development and function of the mammalian lens, contributing to changes in channel gating and permeation (Le and Musil, 2001) (Rong et al., 2002) (Martinez-Wittinghan et al., 2003) (Gao et al., 2004) (White, 2003). In the past, different Cx50 variants have been indicated in the development of several distinct types of dominant cataract in mice (Steele, Jr. et al., 1998) (Graw et al., 2001) (Chang et al., 2002) (Xia et al., 2006c). Recent publications reveal that the combination of mutant Cx50-G22R (Xia et al., 2006b) or Cx50-S50P (Xia et al., 2006c) and wild-type lens fiber connexins leads to unique aberrations in lens development and function, and the presence of these mutant subunits in gap junction channels leads to alterations in channel gating properties and cell-cell communication *in vitro*. Similarly, mice heterozygous for the S50P mutation show a unique deficiency in primary fiber cell elongation, indicating that an interaction between the wild-type and mutant Cx50 subunits governs primary fiber cell development. Homozygous mutant mice exhibit lenses with a unique deficiency in secondary fiber cell development, a finding that suggests Cx50's involvement in a separate mechanism (Figure V-8) modulating secondary fiber cell development (Xia et al., 2006c) (Gong et al., 2007). Since the S50P mutant alone is nonfunctional and fails to properly localize to the membrane, we propose that the mutant must dominantly interact with wild-type subunits to impair lens development *in vivo*. This manuscript supports these hypotheses

and provides the mechanistic foundation for the unique cataract phenotypes exhibited by the S50P mutant mice.

Taken together, these data clearly demonstrate that Cx50 plays a crucial part in lens fiber cell development. The heterozygous mouse, Cx50^(S50P/+) Cx46^(-/-), displays a large cystic lumen between the anterior primary fiber cells and epithelium during embryonic development, while postnatal fiber cell development proceeds normally (Xia et al., 2006c). We propose that this phenomenon is governed by the unique interaction between the wild-type and mutant Cx50 subunits shown here, which leads to altered intercellular communication mediated by channels of mixed connexin expression. Similarly, we provide support for the hypothesis that Cx50 also plays a separate, distinct role in postnatal fiber cell development *in vivo*.

Interestingly, heterozygous mice, Cx50^(S50P/-) Cx46^(+/+), exhibit normal embryonic development in the presence of wild-type Cx46. However, these animals exhibit disrupted secondary fiber development as well as the presence of a dense nuclear cataract and posterior capsule rupture (Xia et al., 2006c). These findings, taken in conjunction with the data shown here, indicate an essential role for connexin diversity and Cx50-mediated intercellular communication in postnatal lens development.

In summary, these data indicate that mutant connexin subunits can interact with wild-type lens connexins to modulate both prenatal and postnatal lens development by altering channel function and cell-cell communication. Furthermore, varying the expression of wild-type lens connexins *in vivo* and *in vitro* demonstrates that wild-type Cx50 interacts with mutant Cx50-S50P in a manner that distinctly affects embryonic development via a slight alteration in channel gating, while a separate, unique interaction

between Cx50-S50P and wild-type Cx46 impairs postnatal lens fiber development via more profound alterations in intercellular communication. The distinctive properties of the heteromeric channels formed by wild-type and mutant lens connexins provide the basic molecular foundation behind a variety of unique cataract phenotypes attributed to various Cx50 mutations (Xu and Ebihara, 1999) (Xia et al., 2006c) (Arora et al., 2006) (Graw et al., 2001). These data indicate that mutant Cx50 proteins act as the molecular mechanism governing altered function of gap junction channels and aberrant intercellular communication in the lens. We believe that a better understanding of these underlying mechanisms may lead to the identification of molecular approaches to cataract prevention.

Figure V-1. Cx50-S50P fails to form functional intercellular channels. (A, B) Immunoblot analysis of oocytes shows equivalent levels of wild-type and mutant connexin expression for all conditions tested. (C, D) Band densitometry quantitatively confirmed that mean protein expression was not significantly changed ($P > 0.05$, ANOVA). (E) Junctional conductance measurements recorded from *Xenopus* oocyte pairs injected with wild-type Cx50, Cx46 or S50P transcripts alone or in combination. Cell pairs expressing wild-type Cx50 or Cx46 subunits alone form functional gap junctions with mean conductance values of approximately 26 and 20 μS , respectively. Oocytes co-injected with both wild-type and mutant Cx50 transcripts form channels with an $\sim 20\%$ decrease in G_j when compared to homotypic Cx50 gap junctions, a level of coupling significantly higher than that of the background ($P < 0.05$, Student's t-test), but not significantly different from homotypic Cx50 channels ($P > 0.05$, Student's t-test). Similarly, the co-expression of Cx46 and Cx50-S50P subunits does not significantly alter junctional conductance ($P > 0.05$, Student's t-test), as these channels exhibit a mean G_j of 17 μS . Heterotypic channels fail to form functional channels with levels of conductance significantly higher than that of water-injected negative controls ($P > 0.05$, Student's t-test). Cx50-S50P subunits alone fail to produce functional intercellular channels. Data points represent individual conductance measurements. Columns indicate the mean \pm SEM.

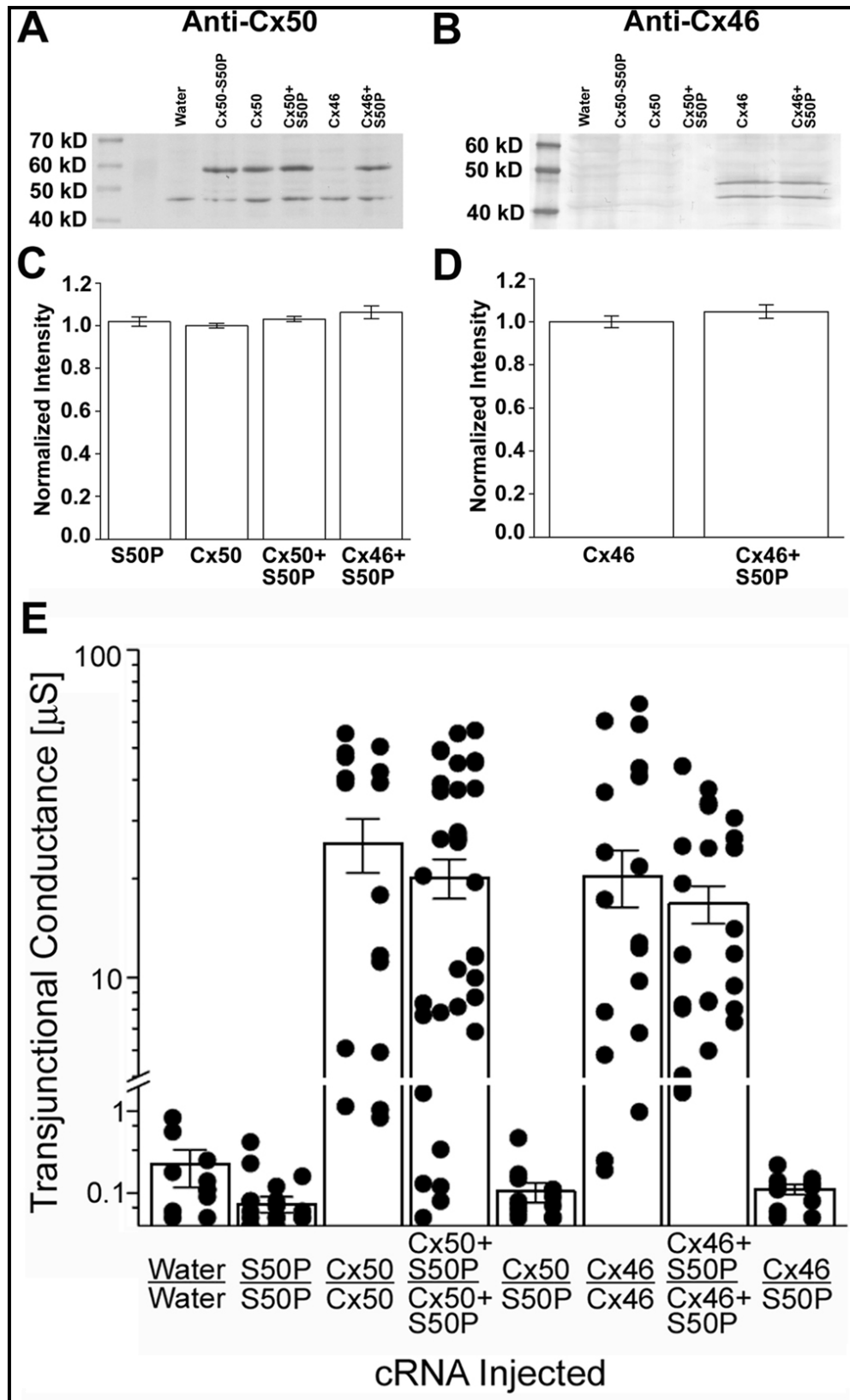


Figure V-2. Voltage gating properties of homotypic wild-type Cx50 channels and channels co-expressing Cx50-S50P and wild-type Cx50 subunits. Junctional current, measured and plotted as a function of time, indicates that channels co-expressing both wild-type and mutant Cx50 proteins (B) do not visibly alter current decay when compared to homotypic Cx50 channels (A). The mean time constant τ , determined by fitting representative current traces of the initial 250 milliseconds of I_j recordings to a monoexponential decay, is 52 ms ($n = 5$) when wild-type and mutant Cx50 transcripts are co-expressed (C). This value is significantly different ($P < 0.05$, Student's t-test) from the 61 millisecond mean channel closure time ($n = 4$) seen in the homotypic wild-type channel during an 80 mV potential. I_j measurements recorded during a 120 mV voltage application show a significant decrease in the mean τ value from 34 milliseconds for the (E) homotypic wild-type channel ($n = 4$) to 25 ms shown by the (F) co-injected gap junctions ($n = 5$, $P < 0.05$, Student's t-test).

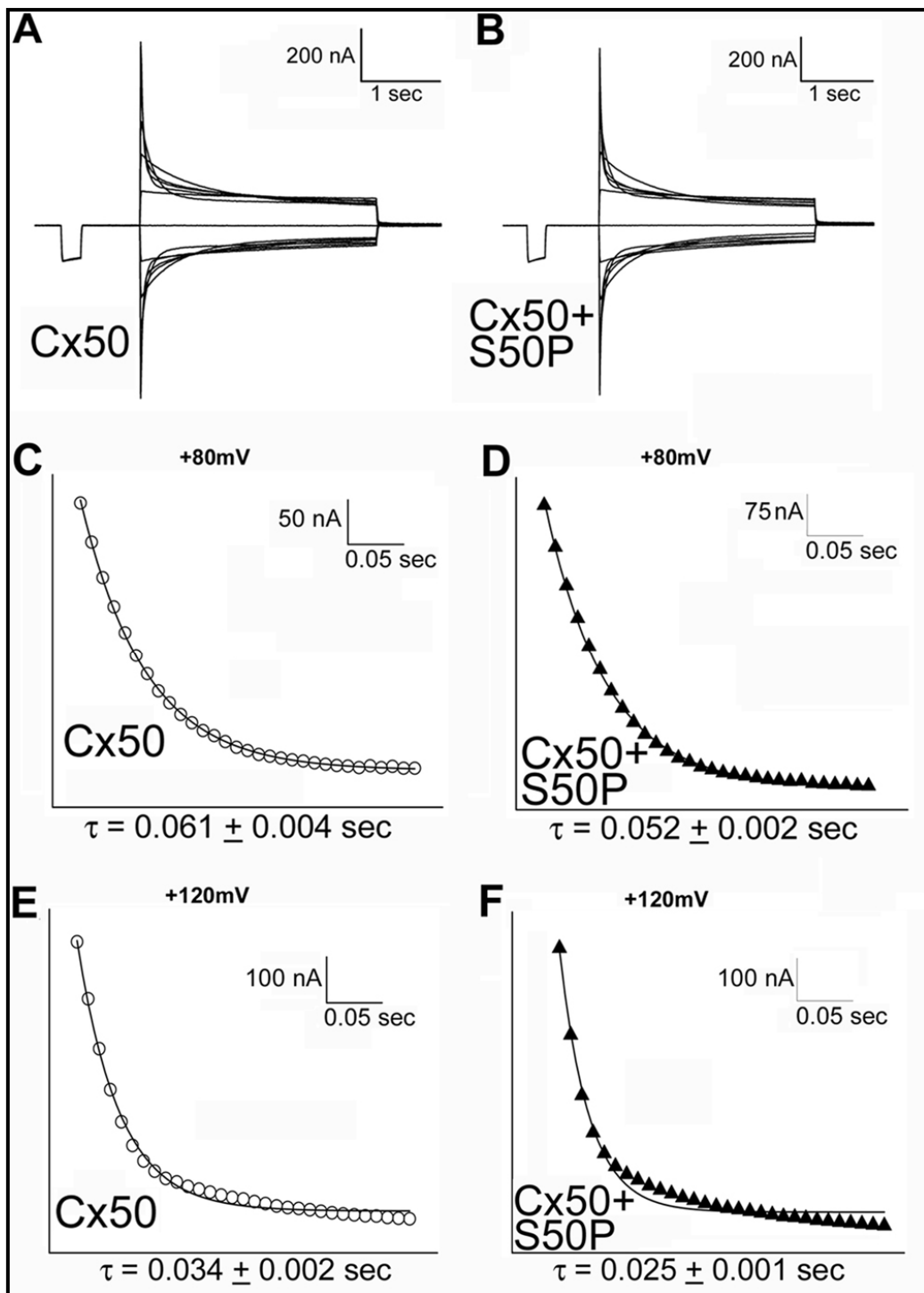


Figure V-3. Voltage gating properties of homotypic and heteromeric Cx46 channels. I_j values recorded from oocyte pairs were plotted as a function of time to reveal that channels expressing wild-type Cx46 alone (A) and mixed channels containing both Cx46 and Cx50-S50P proteins (B), as well as channels expressing wild-type Cx46 and Cx50 subunits (C), display altered voltage gating sensitivity, as co-injected pairs appear more responsive at larger voltage applications. Analysis of channel closure kinetics. The initial 250 mS of junctional current was fit to a monoexponential decay model to determine the mean time constant, tau. Representative I_j decays show that during an +80 mV potential, channels containing both Cx46 and Cx50-S50P subunits (E) close in 101 milliseconds, a value significantly faster than the 132 ms mean tau value exhibited by the homotypic Cx46 channel (D) ($P < 0.05$, ANOVA). Interestingly, channels co-expressing both wild-type Cx46 and Cx50 close in 85 ms (F), a rate approximately 16 and 36% faster than the mixed channels containing Cx46 and S50P or homotypic Cx46 gap junctions. Similarly, upon application of a V_j of 120 mV, homotypic Cx46 channels close in 126 ms (G), a mean channel closure time significantly slower than the 90 ms exhibited by the mixed channels containing wild-type Cx46 and S50P proteins (H) ($P < 0.05$, ANOVA). Heteromeric channels containing both wild-type Cx46 and Cx50 (I) display a mean tau value of 75 ms, a closure speed significantly faster than either the homotypic Cx46 or heteromeric Cx46 and S50P channel ($P < 0.05$, ANOVA). All means are derived from 4 independent experiments.

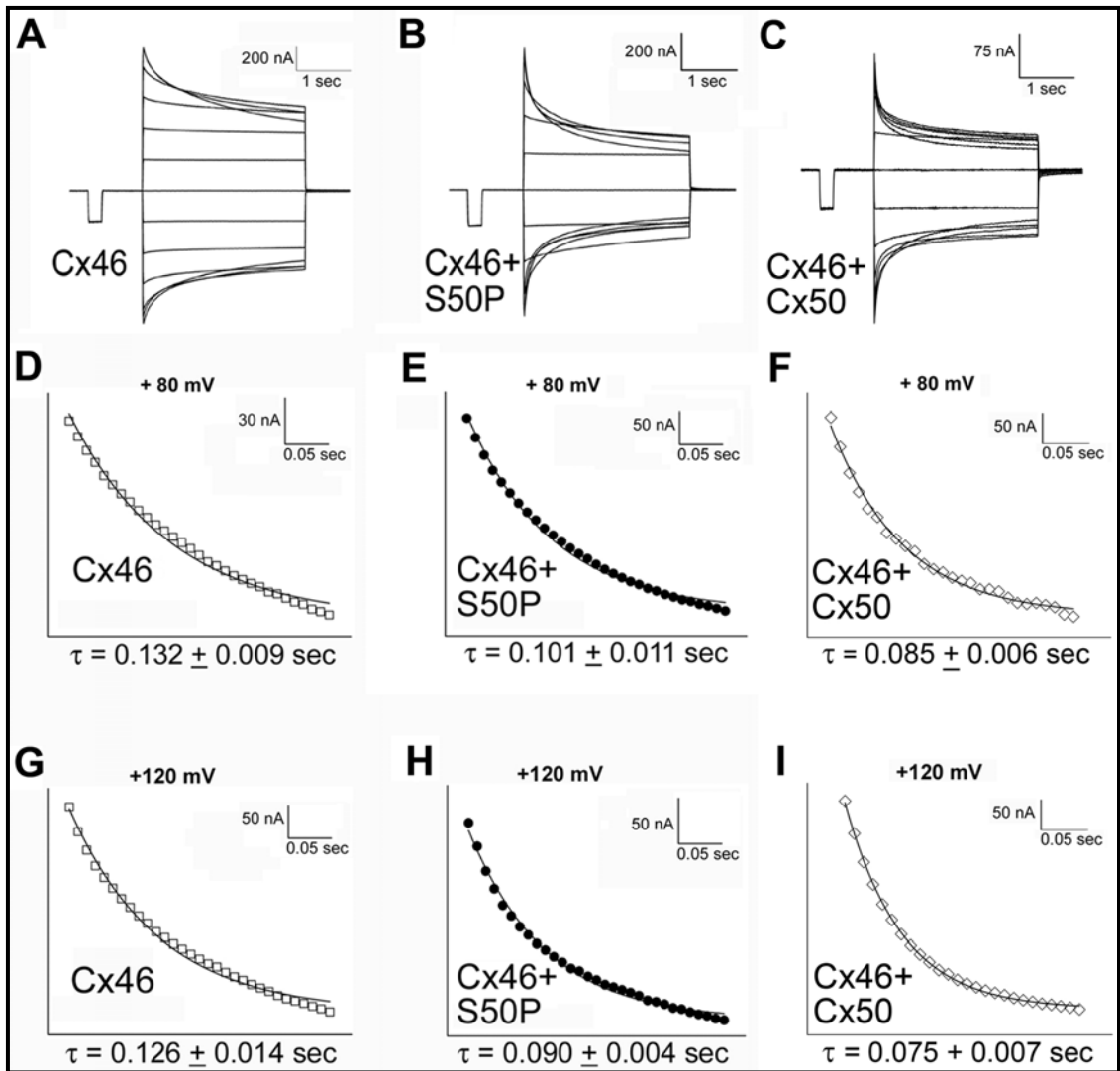


Figure V-4. Comparison of steady state conductance properties. Equilibrium gating properties were analyzed by plotting normalized junctional conductance against transjunctional voltage and fit to the Boltzmann equation. A comparison of homotypic wild-type Cx50 channels (n = 4) and mixed gap junctions containing both wild-type and mutant Cx50 subunits (n = 6) shows similar voltage sensitivity, indicated by the overlapping pattern of the two Boltzmann plots (A). The steady-state reduction in conductance is greater for mixed channels expressing both Cx46 and S50P subunits (n = 8) than for the homotypic Cx46 channel (n = 4), indicating an increase in voltage gating sensitivity for heteromeric channels. Equilibrium gating properties show modest changes at positive potentials when mixed channels containing both wild-type Cx46 and Cx50 (n = 6) are compared to heteromeric channels expressing wild-type Cx46 and S50P (B). Results are shown as the mean \pm SEM.

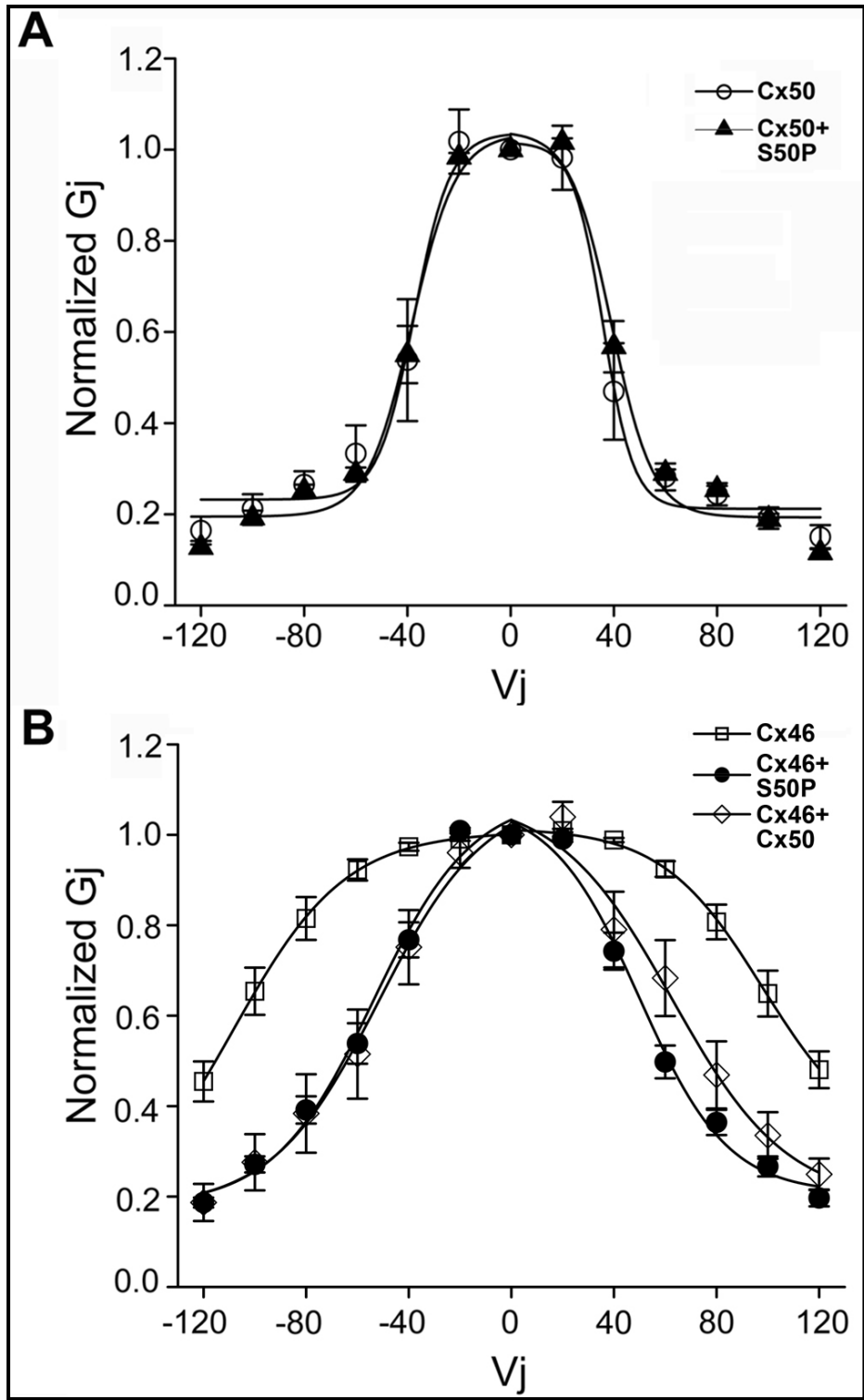


Figure V-5. Gating analysis of heterotypic wild-type and co-injected channels. G_j measurements were recorded from oocytes paired to form heterotypic wild-type or co-injected gap junctions. Cell pairs expressing wild-type Cx46 and Cx50 subunits form functional gap junctions with mean conductance values of approximately 22 μ S, a level of coupling significantly higher than that of the water-injected negative control ($P < 0.05$, Student's t-test). Co-injected heterotypic channels expressing both wild-type and mutant Cx50 transcripts form channels with an $\sim 50\%$ decrease in G_j as compared to wild-type heterotypic gap junctions, a level of coupling significantly higher than that of the background ($P < 0.05$, Student's t-test). Data points represent individual conductance measurements. Columns indicate the mean \pm SEM. Junctional currents recorded from oocyte pairs were plotted as a function of time to compare heterotypic gap junctions expressing wild-type Cx46 and Cx50 subunits (B) and heterotypic channels containing wild-type Cx46 and wild-type Cx50 and S50P mutant proteins (C). Representative I_j decays reveal that co-injected pairs appear more responsive at greater depolarizing voltage applications, and more asymmetric than heterotypic channels comprised of wild-type lens fiber connexins. Equilibrium gating properties were analyzed by plotting normalized junctional conductance against transjunctional voltage and fit to the Boltzmann equation. (D) The steady-state reduction in conductance is greater for channels expressing both wild-type Cx50 and Cx50-S50P subunits ($n = 6$) when compared to that of the heterotypic wild-type channel ($n = 5$), indicating an increase in voltage gating sensitivity for heterotypic channels containing the mutant protein.

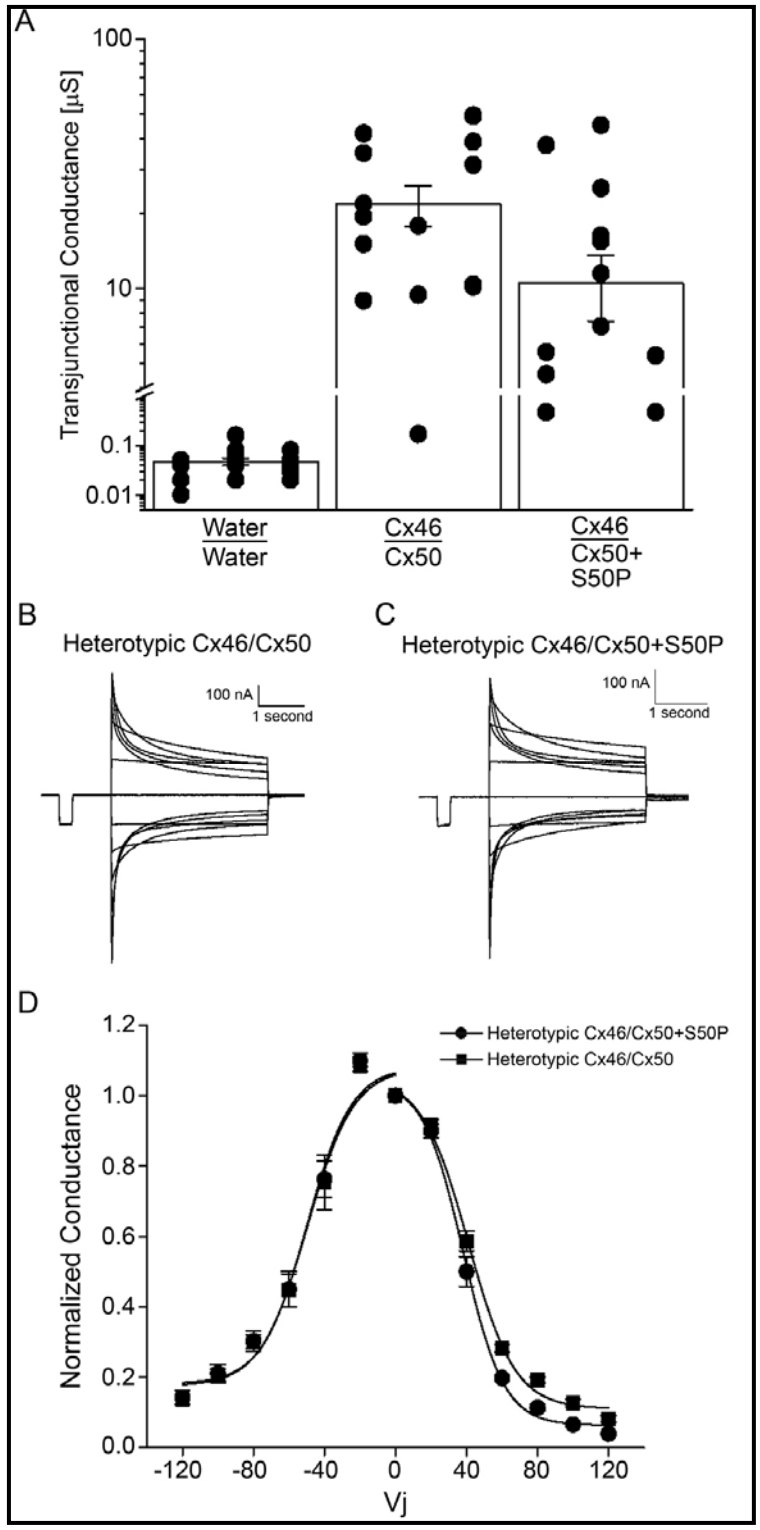


Figure V-6. S50P requires Cx46 to form functional hemichannels in *Xenopus* oocytes. (A) Single oocytes expressing wild-type Cx46 were clamped at a holding potential of -40 mV and subjected to voltage applications ranging from -30 to +60 mV in 10 mV steps. A representative trace displays voltage-induced outward membrane currents that increase in magnitude with time. In contrast, cells expressing S50P subunits alone show negligible membrane currents at all voltages analyzed (C). Voltage-induced membrane currents are seen in cells expressing either wild-type Cx50 and Cx46 (E) or wild-type Cx46 and S50P (F). Steady-state currents measured after 7 seconds of an initial voltage pulse were plotted as a function of membrane voltage. (B) Steady-state currents in wild-type Cx46-injected oocytes display increasing whole-cell currents at all positive voltage applications (n= 10, open squares). (D) Conversely, cells expressing S50P connexins alone exhibit negligible membrane currents at voltages analyzed (n= 7, closed triangles). (F) Wild-type Cx50 and Cx46 currents show an ~ 2 fold reduction compared to wild-type Cx46 injected cells at all voltages analyzed (n= 10, open diamonds) (H). Similarly, oocytes co-expressing wild-type Cx46 and S50P subunits induce whole-cell currents comparable to those exhibited by wild-type Cx50 and Cx46 co-injected oocytes (n= 10, closed circles). Data are the mean \pm SEM.

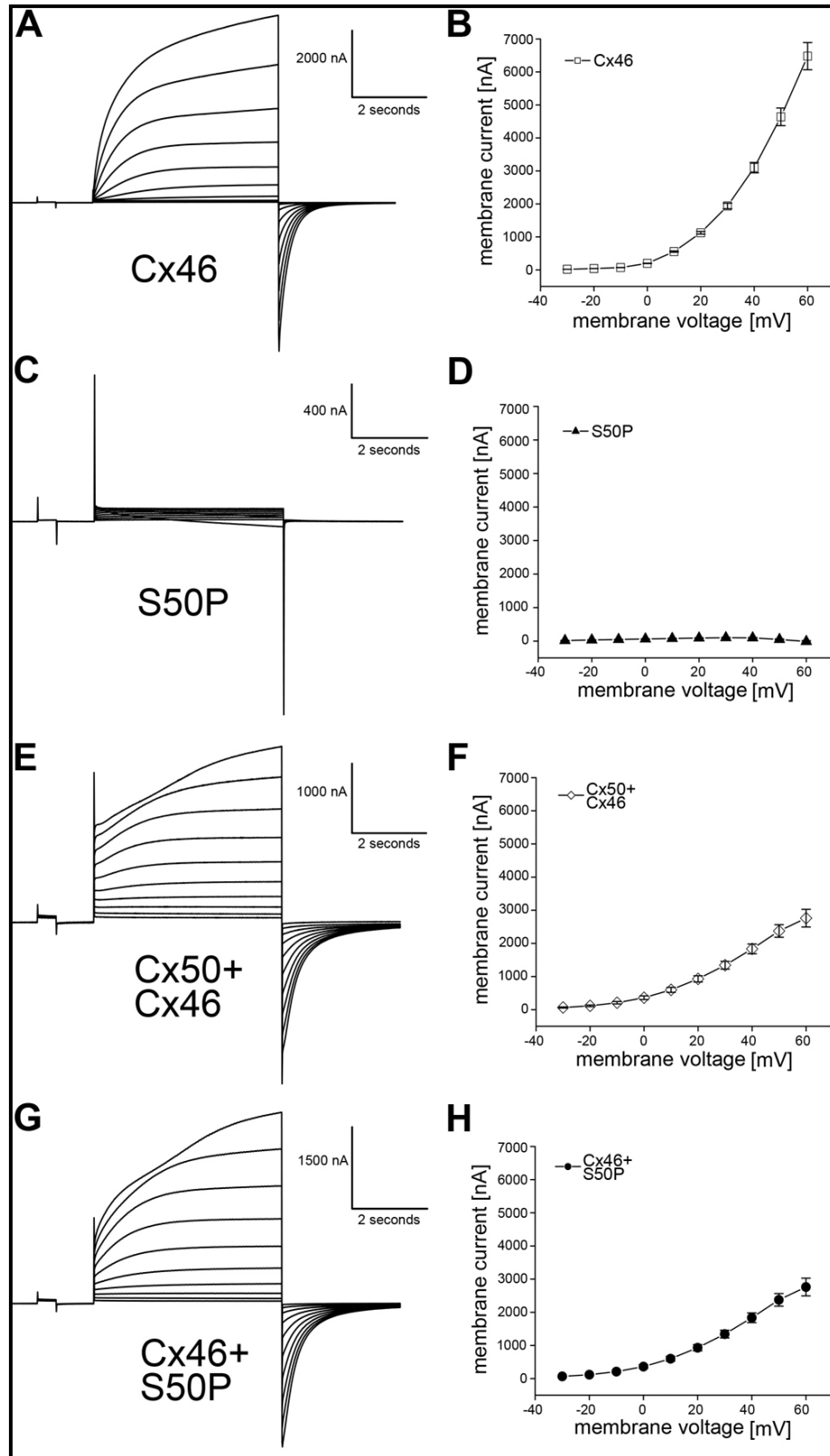


Figure V-7. Immunofluorescent imaging of Cx50-S50P *in vitro* and *in vivo*. Transiently transfected HeLa cells expressing Cx50-S50P (A) or wild-type Cx46 (B) proteins alone were immunostained and examined by fluorescent microscopy. Merged images exhibit Cy3 staining of connexins (red) and DAPI staining of cell nuclei (blue). The images show that Cx50-S50P alone fails to properly localize to the cell membrane at areas of cell-cell contact (A, arrow). Instead, connexin subunits accumulate in subcellular compartments surrounding the nucleus. Efficient translation of wild-type Cx46, and its subsequent localization to the membrane, specifically at areas of cell to cell apposition, is seen (B). HeLa cells co-transfected with both Cx50-S50P and wild-type Cx46 (C and D) show that in the presence of Cx46, S50P subunits co-localize to the membrane and form junctional plaques at areas of cell-cell contact (C, Cy2 staining of Cx50, green, D, Cy3 staining of Cx46, red, arrowheads). Fluorescent images of Cx50-S50P immunostaining in the bow region of homozygous mutant lenses with Cx46 (Cx50^(S50P/S50P) Cx46^(+/+)) (E) and without endogenous Cx46 (Cx50^(S50P/S50P) Cx46^(-/-)) (F). Lenses taken from mice on postnatal day 7 show more punctate Cx50 staining (green) that extends deeper into the differentiating fibers in the presence of wild-type Cx46 proteins (E). Frozen lens sections were co-stained with rhodamine-phalloidin (red) and DAPI (blue). A-D, scale bar = 5 μ m. E-F, scale bar=40 μ m.

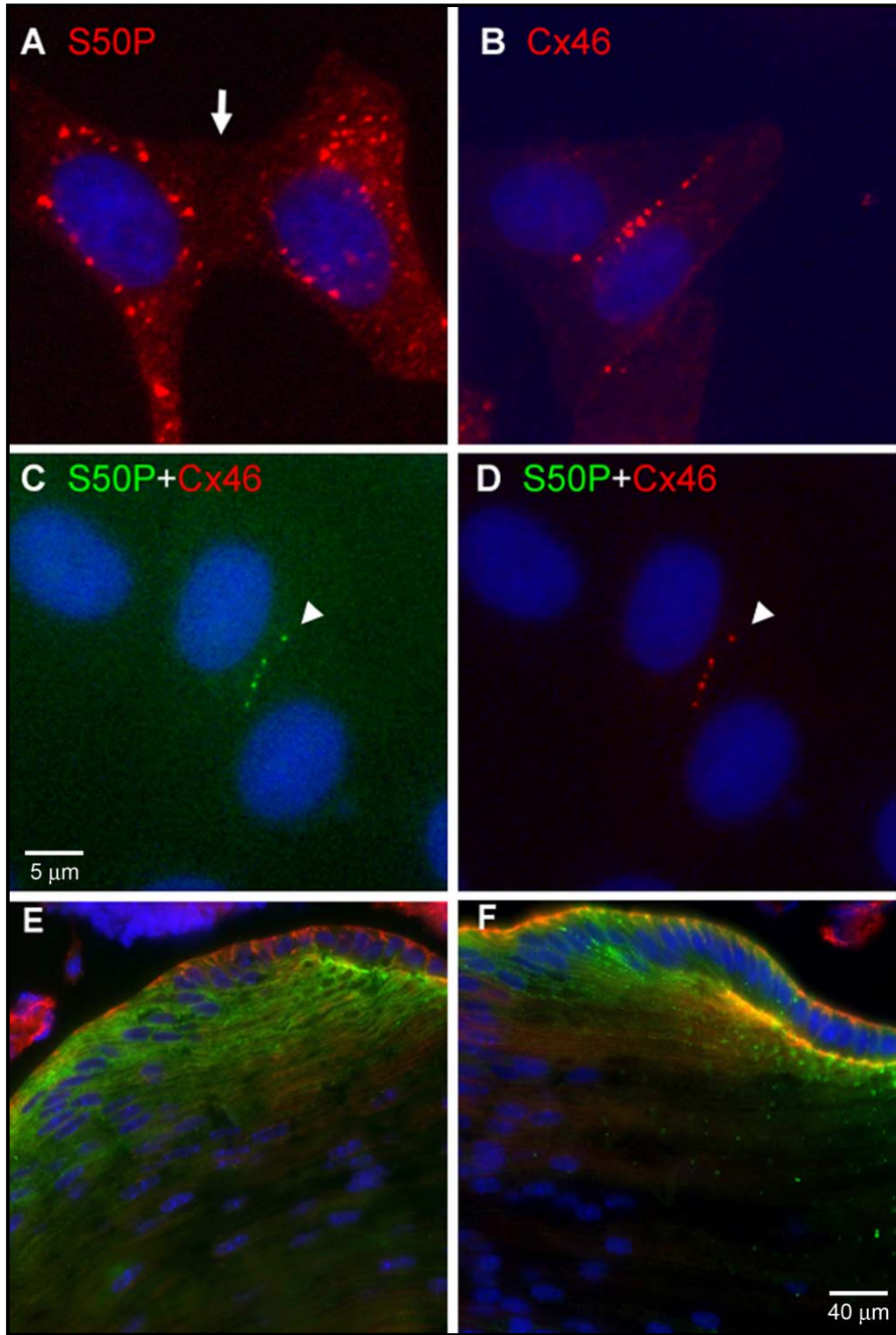


Figure V-8. Description of embryonic and adult lens phenotypes produced by mixing Cx50-S50P and wild-type lens fiber connexins. This model describes the embryonic and postnatal phenotypes of various mouse lenses created by breeding heterozygous mutant, Cx50^(S50P/+) Cx46^(+/+), and double knockout, Cx50^(-/-) Cx46^(-/-), mice. The drawing explains the proposed mechanism behind development of each unique phenotype based on the electrophysiological interactions documented herein.








Embryonic lens	Embryonic phenotype, proposed mechanism	Postnatal lens	Adult phenotype, proposed mechanism
 Cx50^(S50P/+) Cx46^(-/-) Cx50^(S50P/+) Cx46^(+/+)	abberant primary fiber cell elongation co-expression of wild-type and mutant Cx50 alters channel function	 Cx50^(S50P/-) Cx46^(+/+)	small lenses, with malformed secondary fibers and posterior capsule rupture co-expression of S50P and Cx46 form channels with altered function and gating properties, affecting only postnatal development
 Cx50^(S50P/-) Cx46^(+/+)	normal embryonic development mixing of S50P and wild-type Cx46 alters channel function without affecting embryonic development	 Cx50^(S50P/+) Cx46^(+/+)	small lenses with altered primary and secondary fibers the presence of S50P and wild-type lens connexins leads to altered channel function affecting both embryonic and postnatal development
 Cx50^(S50P/-) Cx46^(-/-) Cx50^(-/-) Cx46^(-/-)	normal embryonic development the expression of S50P alone does not affect embryonic lens development, similar to double knockout lens	 Cx50^(S50P/+) Cx46^(-/-)	small lenses with normal secondary fibers and disorganized primary fiber cells Mixing of wild-type and mutant Cx50 forms channels with altered gating properties that does not affect secondary fiber development
		 Cx50^(S50P/-) Cx46^(-/-) Cx50^(-/-) Cx46^(-/-)	small lenses with normal peripheral fibers and degenerate primary fiber cells, dense nuclear cataract S50P alone is a loss of function mutation that fails to form functional gap junctions producing a phenotype identical to that of the double knockout lens

Table V-1. Boltzmann parameters for wild-type and mixed channels. G_{jmin} represents the minimum conductance value, V_0 indicates the voltage measured midway through the G_j decline, and A denotes the cooperativity constant, reflecting the number of charges moving through the transjunctional field. Signs + and – for V_j indicate transjunctional membrane potential polarity.

Connexon	V_j	V_0	G_{jmin}	A
Homotypic				
Cx50	+	36	0.21	0.21
Cx50	-	-37	0.23	0.18
Cx46	+	98	0.31	0.07
Cx46	-	-108	0.13	0.05
Heteromeric				
Cx50+S50P	+	39	0.19	0.15
Cx50+S50P	-	-38	0.19	0.14
Cx46+S50P	+	50	0.21	0.07
Cx46+S50P	-	-54	0.18	0.07
Cx46+Cx50	+	63	0.19	0.06
Cx46+Cx50	-	-52	0.17	0.06
Heterotypic				
Cx46	-	-50	0.18	0.07
Cx50	+	41	0.11	0.07
Cx50+S50P	+	38	0.06	0.09

Table V-2: Quantitative analysis of gap junctional plaque formation in transiently transfected HeLa Cells.

Connexin Expressed	Junctional Plaques Present	No Junctional Plaques	Number of cell pairs analyzed
Cx50-S50P	0	18	18
Wild-type Cx46	12	4	16
Cx46 + Cx50-S50P	14	5	19

Chapter VI

The loss-of-function Cx50-R205G mutation dominantly alters wild-type lens connexin function

Abstract

Recent discovery of a novel C to G missense mutation in the Cx50 coding region was found to cause an autosomal semi-dominant cataract in mice. Here, we used the dual whole-cell voltage clamp technique in conjunction with the paired *Xenopus* oocyte assay to analyze the functional consequences of the Cx50-R205G mutation. We found that the R205G mutant acts as a dominant negative inhibitor of wild-type Cx50 with regard to channel function. Additionally, the Cx50-R205G mutant dominantly altered wild-type Cx46 channel gating when the two connexins were co-expressed *in vitro* to mimic heteromeric channel formation. Interestingly, the mutant R205G subunits were able to properly localize to the plasma membrane in transfected HeLa cells and showed no discernable reduction in translation compared to the wild-type Cx50 homolog. Taken together, these findings reveal that the Cx50-R205G mutation acts as a loss-of-function mutation with a strong dominant inhibition toward wild-type Cx50. Conversely, this mutant is able to interact with wild-type connexin46 to form functional intercellular channels with altered electrophysiological properties, a phenomenon that may play a role in the development of the unique cataract phenotype seen *in vivo*.

Results

Figure VI-1 in this chapter is an unpublished result of an ENU mutagenesis screen conducted in the laboratory of Dr. Xiaohua Gong. The lens pictures have been incorporated to provide a representation of the unique pathology associated with the Cx50-R205G mutation. The remaining Figures and Tables are all derived from my dissertation research.

The Cx50-R205G causes microphthalmia and cataract in the homozygous mutant mouse.

A cataractous mouse was identified from ENU-mutagenized mice by slit-lamp examination. This mouse was then bred with wild-type C57BL/6J mice, and half of the offspring developed similar ocular phenotypes. The F1 generation was backcrossed to generate mice homozygous for the R205G mutation. The homozygous mutant mice developed dense cataracts, severe microphthalmia, and a lamellar opacity in the lens cortex (Figure VI-1B). This mutation was mapped to a region on mouse chromosome three that corresponded to the Cx50 gene locus. DNA sequencing confirmed the presence of a single missense mutation (C-G) in the Cx50 coding region, resulting in the replacement of arginine by glycine at codon 205, in the second extracellular domain of the Cx50 peptide.

Functional expression of wild-type lens fiber connexins and mutant Cx50-R205G subunits in *Xenopus* oocytes

Genomic DNA isolated from homozygous mutant mice was subcloned and transcribed *in vitro*. These cRNA transcripts were then micro-injected into *Xenopus* oocytes, and protein expression was assayed via western blotting. Immunoblot data

showed that both wild-type and mutant connexin proteins were produced in oocytes injected with wild-type connexin transcripts alone, and in cells co-injected with both wild-type and mutant Cx50 cRNAs (Figure VI-2A, B). Connexin protein expression was then quantitatively analyzed by band densitometry (Figure VI-2C, D). These data confirmed that wild-type and mutant protein levels were not significantly different in oocytes injected with wild-type or mutant Cx50-R205G cRNAs alone or in cells co-injected with both wild-type and mutant connexins ($P > 0.05$). These findings implied that any alteration in channel function seen herein cannot be attributed to a change in connexin expression or increase in protein degradation for any of the conditions assayed.

We then measured junctional conductance by subjecting paired oocytes expressing connexin proteins to dual whole-cell voltage clamp (Figure VI-2E). Data showed that homotypic wild-type Cx50 and Cx46 channels displayed mean conductance values of 29 and 16.5 μS , respectively, measurements several hundred-fold higher than those recorded from water-injected pairs. By contrast, gap junctions comprised of Cx50-R205G subunits alone failed to electrically couple cells, as these pairs displayed a level of coupling not significantly greater than that of the water-injected negative controls ($P > 0.05$). Similarly, heterotypic cell pairs that had one cell injected with either wild-type Cx50 or Cx46 and the opposing cell expressing Cx50-R205G subunits failed to electrically couple. Co-injection of cells with wild-type and mutant connexin cRNAs enabled us to assay for any aberrations in electrical coupling between homotypic wild-type channels and gap junctions containing both mutant and wild-type subunits. A quantitative comparison of the mean conductance of homotypic Cx46 channels and mixed gap junctions co-expressing Cx50-R205G and wild-type Cx46 proteins revealed

no significant reduction in mean G_j for co-injected channels ($P > 0.05$). Conversely, co-expression of wild-type and mutant Cx50 in oocytes failed to electrically couple cells, indicated by the insignificant increase in junctional conductance when compared to the water-injected negative controls ($P > 0.05$). These data imply that Cx50-R205G acts as a dominant negative repressor of wild-type Cx50 *in vitro* with respect to channel formation, a phenomenon that may contribute to cataract development in the mutant mice. Since R205G did not abolish intercellular channel formation when co-expressed with Cx46, we hypothesize that Cx50-R205G may be capable of forming heteromeric channels with Cx46 in *Xenopus* oocytes, and that these unique gap junctions may display altered channel gating properties.

Heteromeric Cx46 and Cx50-R205G channels exhibit unique voltage gating properties

To determine if the intercellular channels formed by the co-expression of wild-type Cx46 and Cx50-R205G displayed distinct gating properties, the electrophysiological characteristics of homotypic Cx46 channels and gap junctions of mixed connexin expression were analyzed (Figure VI-3). The application of a series of transjunctional voltages (0 mV to ± 120 mV) caused a slow decay of junctional current toward steady-state at all potentials analyzed in homotypic Cx46 channels (Figure VI-3A). Conversely, oocytes co-injected with Cx46 and Cx50-R205G transcripts (Figure VI-3B) exhibited a visible change in the rate of I_j decay when compared to homotypic Cx46 channels.

This finding was further quantified by the examination of channel gating kinetics. The initial 300 milliseconds of I_j decay was fit by a monoexponential decay function to determine the mean time constant, tau (τ). These data revealed that gap junctions

containing wild-type Cx46 and Cx50-R205G subunits closed significantly faster than homotypic Cx46 channels ($P < 0.05$), as the mean tau value for co-injected pairs was ~215 milliseconds (Figure VI-3D), a value over 100 milliseconds faster than that of the homotypic wild-type Cx46 channels (Figure VI-3C). These data support the hypothesis that a unique interaction between wild-type Cx46 and Cx50-R205G subunits leads to alterations in intrinsic channel function.

If wild-type Cx46 and Cx50-R205G proteins interact to form functional gap junctions with unique electrophysiological properties, an analysis of the equilibrium gating properties of cells expressing Cx46 and Cx50-R205G subunits may show distinct changes in the steady-state reduction in junctional conductance when compared to homotypic Cx46 channels. To test this hypothesis, the steady-state junctional conductance was measured during the application of voltage pulses ranging from ± 20 to ± 120 mV. Recordings were then normalized to the values obtained at ± 20 mV and plotted against V_j . These data showed that the reductions in equilibrium conductance for co-injected Cx50-R205G and Cx46 heteromeric channels were greater than the reductions for Cx46 homotypic channels at all tested voltages (Figure VI-3E). The co-expression of Cx50-R205G and wild-type Cx46 resulted in significantly altered gating properties. Since Cx50-R205G is functionally silent with regard to channel function, these shifted gating properties are most consistent with the formation of heteromeric channels by the co-injection of Cx50-R205G and Cx46 subunits.

Cx50-R205G is efficiently translated and properly localizes to the plasma membrane

Some mutant Cx50 proteins are deficient in their ability localize to the cell membrane, and also exhibit a reduced capacity to form gap junctional plaques (Chang et

al., 2002) (Xia et al., 2006c) (Xia et al., 2006b). To determine if the failure to form functional intercellular channels is due to a deficiency in the ability of Cx50-R205G subunits to efficiently localize to the plasma membrane, wild-type and mutant fiber connexins (subcloned into the pIRES2-EGFP vector) were expressed in transiently transfected HeLa cells and analyzed via immunofluorescent microscopy. Transfected HeLa cells were fixed and treated with either a polyclonal rabbit anti-mouse Cx50 antibody (White et al., 1992) or a polyclonal rabbit anti-rat Cx46 antibody followed by the application of a Cy3-conjugated fluorescent secondary antibody. These cells were then viewed and photographed to determine any changes in connexin protein expression and localization. These data qualitatively showed that the Cx50-R205G mutant and wild-type lens fiber connexins were efficiently translated *in vitro* and localized to the plasma membrane specifically at areas of cell to cell apposition (Figure VI-4). Additionally, the capability of Cx50-R205G mutant connexons to properly localize to the plasma membrane indicated that the inability of these subunits to form functional intercellular channels when co-expressed with wild-type Cx50 in paired *Xenopus* oocytes was not due to a deficiency in mutant protein trafficking.

Discussion

Gap junctions formed by Cx43, Cx46, and Cx50 subunits provide the lens with an intercellular network that governs the transport of essential small molecules, cellular waste, and fluids between the metabolically active epithelium and the mature fibers found at the lens core. Lens fiber cells are coupled by gap junctions comprised of both Cx50 and Cx46, while lens epithelial cells are joined by channels expressing Cx43 and Cx50 subunits. Cx50-R205G was identified as a non-functional subunit that not only acts as dominant negative repressor of wild-type Cx50, but also dominantly alters wild-type Cx46 channel function *in vitro*. These unique functions may directly mediate primary and secondary fiber cell development and promote cataractogenesis *in vivo*.

These data reveal that the combination of Cx50-R205G and wild-type Cx50 subunits inhibits channel gating without preventing gap junctional plaque formation *in vitro*. Thus, we hypothesize that the developmental anomalies seen in the secondary lens fiber cells, specifically the lamellar opacity seen in the cortical fibers, may be attributable to a loss of gap junction-mediated coupling between epithelial cells and secondary fiber cells *in vivo*. Additionally, we have found that while co-expression of Cx50-R205G and wild-type Cx46 subunits forms functional intercellular channels that display a mean junctional conductance similar to that of the homotypic wild-type Cx46 channel, these channels exhibit significant changes in intrinsic channel gating properties. These results suggest that gap junctions formed by Cx50-R205G and wild-type Cx46 subunits alter a unique mechanism required for the maintenance of primary fiber cell development and homeostasis. These data, taken in conjunction with the *in vivo* lens data, indicate that the formation of heteromeric gap junctions by wild-type Cx46 and mutant Cx50-R205G

subunits may provide part of the mechanism that contributes to the development of the dense nuclear cataract seen in the mature fibers of homozygous mutant lenses. Further elucidation of the interactions between Cx50-R205G and wild-type Cx46 and Cx50 could be obtained by interbreeding these mutant animals with the connexin knock-in and knockout mice.

Currently, six Cx50 mutants have been linked to dominant cataracts in humans (Xia et al., 2006c) (Polyakov et al., 2001) (Rees et al., 2000) (Shiels et al., 1998) (Willoughby et al., 2003) (Zheng et al., 2005), and four Cx50 mutants have been shown to cause different dominant cataracts in mice (Steele, Jr. et al., 1998) (Graw et al., 2001) (Chang et al., 2002) (Xia et al., 2006c). This work characterizes the functional properties of a novel Connexin50 mutation and identifies the second extracellular loop domain as a possible location for an important docking site for other Cx50 subunits, and a possible location for a voltage gating sensor that dominantly alters heteromeric channel formation with wild-type Cx46 subunits. Moreover, these data provide further support for our general hypothesis that mutated connexins may act as molecular tools for changing the physiological properties of gap junctions and altering intercellular communication in the lens.

Figure VI-1 Homozygous mutant lenses develop microphthalmia and cataract. Whole lens images, looking down on the equatorial edge of a wild-type mouse lens (A) and a homozygous mutant lens ($Cx50^{(R205G/R205G)} Cx46^{(+/+)}$) (B) at postnatal day 21, show that the mutant lens displays severe microphthalmia, dense nuclear cataract, and a mild lamellar opacity in the lens cortex. (Dr. Xiaohua Gong, unpublished data)

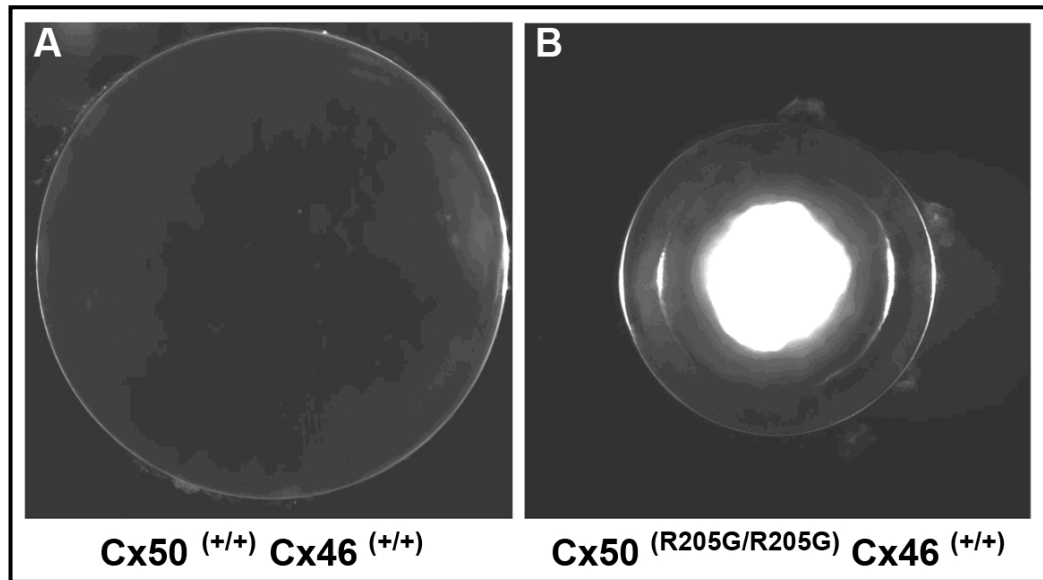


Figure VI-2 Functional expression of wild-type lens fiber connexins and mutant Cx50-R205G subunits in *Xenopus* oocytes. Immunoblot analysis of oocytes shows equivalent levels of wild-type and mutant Cx50 when expressed alone or in co-injected cells (A). Similarly, western blotting demonstrates similar levels of wild-type Cx46 in both conditions assayed (B). Band densitometry quantitatively confirms that mean protein expression does not change significantly (C, D) ($P > 0.05$). (E) Junctional conductance measurements recorded from *Xenopus* oocyte pairs injected with wild-type Cx50, Cx46 or R205G transcripts alone or in combination. Cell pairs expressing wild-type Cx50 or Cx46 subunits alone form functional gap junctions with mean conductance values of approximately 30 and 17 μS , respectively. Oocytes co-injected with both wild-type and mutant Cx50 transcripts fail to form functional gap junction channels, exhibiting a level of coupling not significantly higher than that of the background ($P > 0.05$). Conversely, the co-expression of Cx46 and Cx50-R205G subunits do not significantly alter junctional conductance ($P > 0.05$), as these channels exhibit a mean G_j of 16 μS . Heterotypic channels fail to form functional channels, with levels of conductance not significantly higher than that of the water-injected negative controls ($P > 0.05$). Cx50-R205G subunits alone fail to produce functional intercellular channels. Data points represent individual conductance measurements. Data are the mean \pm SEM of four individual experiments.

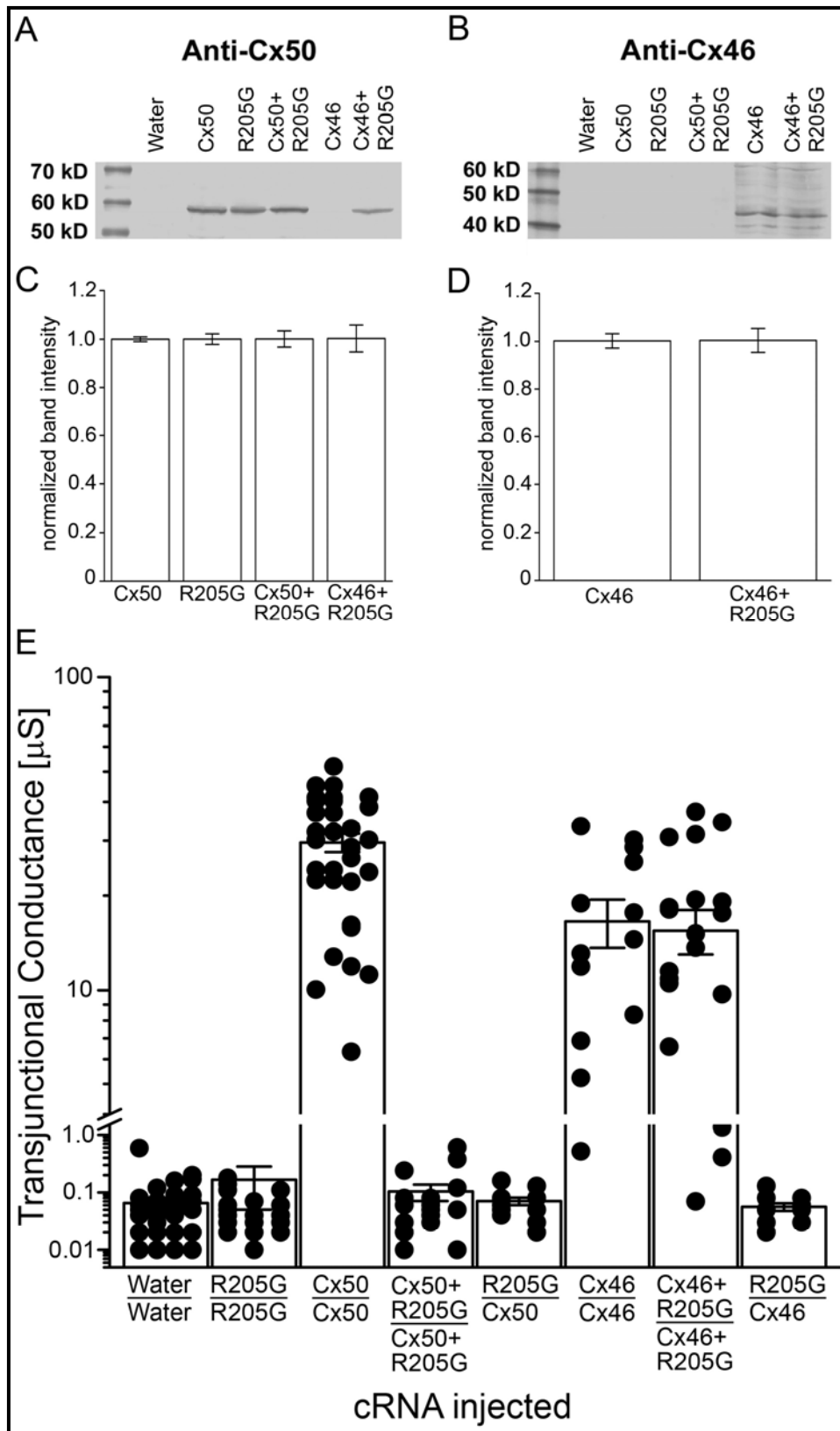


Figure VI-3. Voltage gating properties of homotypic Cx46 and heteromeric wild-type Cx46 and Cx50-R205G channels. The decay in junctional current (I_j) induced by transjunctional voltage (V_j) was plotted as a function of time for gap junctions comprised of Cx46 (A) and Cx50-R205G and Cx46 (B). Voltage was stepped to ± 120 mV in 20 mV increments. At all voltage applications $> \pm 20$ mV, mixed channels showed a more rapid current decay toward steady-state. Analysis of channel closure kinetics. Representative traces displayed the initial 250 ms of current decay recorded after application of a +120 mV transjunctional voltage for gap junctions containing wild-type Cx46 alone (n=5) (C), and heteromeric channels expressing both Cx46 and Cx50-R205G (n=5) (D). Current traces were fit to a monoexponential decay function to determine the mean time constant, τ . Heteromeric Cx46 and Cx50-R205G channels closed $\sim 25\%$ faster than homotypic Cx46 junctions, displaying a significant increase in mean channel closure time ($P < 0.05$). Comparison of equilibrium conductance (E). Steady-state conductance was measured when current decay reached equilibrium, normalized to the values at ± 20 mV, and plotted as a function of V_j . The steady-state reduction in conductance for heteromeric Cx46 and Cx50-R205G channels (n=8) was greater than the reduction for homotypic wild-type Cx46 channels (n=5).

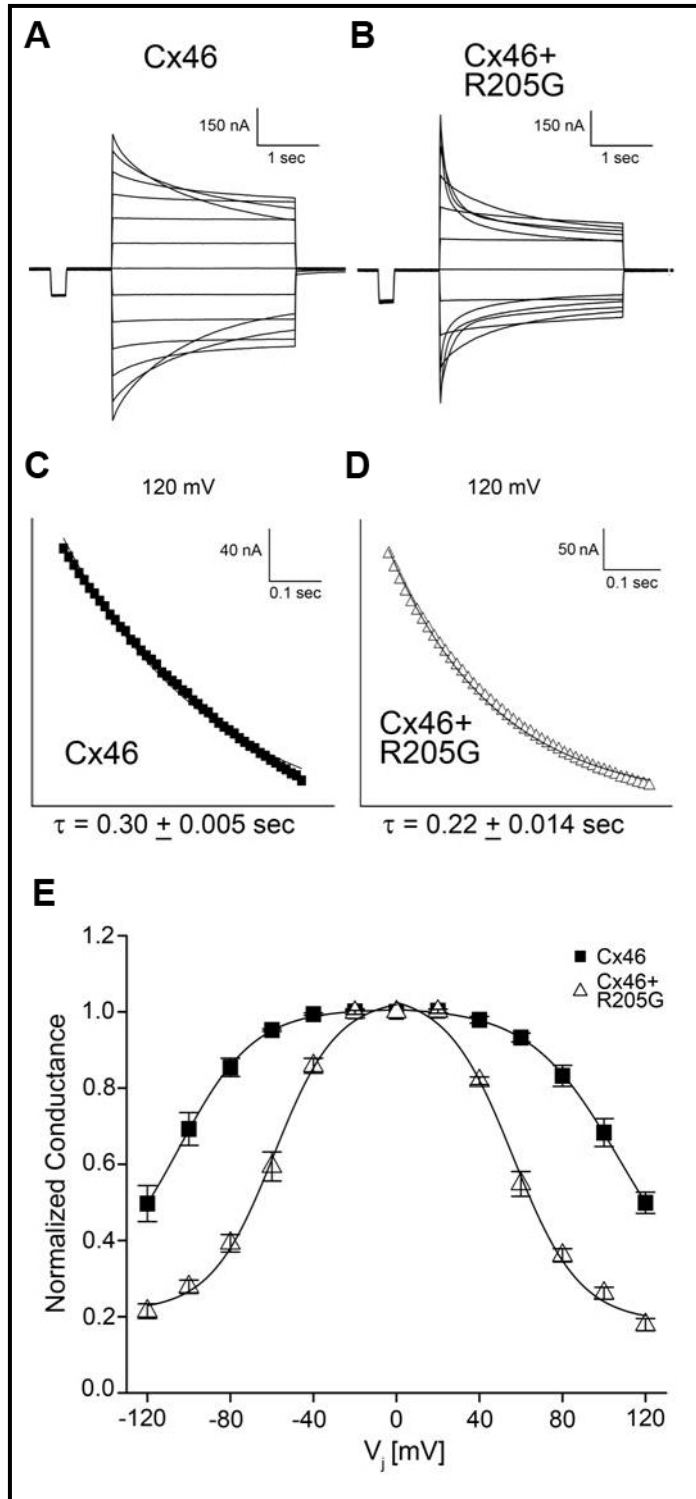


Figure VI-4. Immunofluorescent imaging of wild-type and mutant connexins in transiently transfected HeLa cells. Transiently transfected HeLa cells expressing Cx50-R205G (top), wild-type Cx50 (middle) or wild-type Cx46 (bottom) proteins were immunostained and examined by fluorescent microscopy. Merged images taken at 100x displayed Cy3 staining of lens connexins (red) and DAPI staining of cell nuclei (blue). Overlay images showed that all three connexins were efficiently translated and localized to the membrane, specifically at areas of cell to cell apposition (arrows).

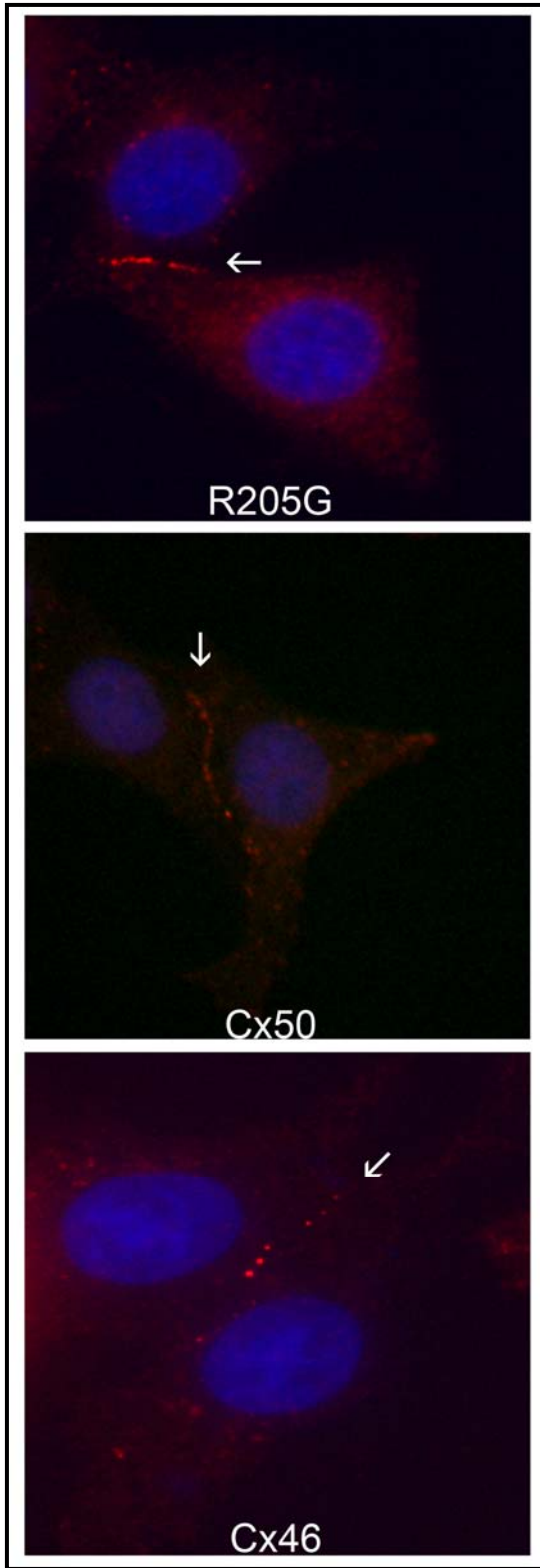


Table VI 1. Boltzmann parameters for wild-type and mixed channels. $G_{j\min}$ represents the minimum conductance value, V_0 indicates the voltage measured midway through the G_j decline, and A denotes the cooperativity constant, reflecting the number of charges moving through the transjunctional field. Signs + and – for V_j indicate transjunctional membrane potential polarity.

Connexion	V_j	V₀	G_{jmin}	A
Cx46	+	107	0.21	0.04
Cx46	-	-105	0.28	0.04
R205G+Cx46	+	56	0.19	0.05
R205G+Cx46	-	-59	0.21	0.06

Chapter VII

Functional characterization of a naturally occurring Cx50 truncation

Abstract

Lens connexins undergo proteolytic cleavage of their C-termini during fiber maturation. While the functional significance of this is unknown, cleavage has been correlated with changes in channel gating properties. This study evaluates the functional consequences of this endogenous truncation by characterizing the properties of a C-terminally truncated Cx50 protein. Our data show that Cx50tr290 channels exhibited an 86-89% reduction in mean macroscopic conductance compared to full-length Cx50. Heterotypic channels formed functional gap junctions, displayed an intermediate level of coupling, and exhibited unaltered voltage gating properties. C-terminal truncation did not alter single channel gating characteristics or unitary conductance. Interestingly, both truncated and full-length Cx50 channel conductance was reversibly blocked by cytoplasmic acidification. C-terminal truncation of Cx50 did not inhibit formation of homotypic or heterotypic channels. However, a significant decrease in conductance was observed for truncated channels, a phenomenon independent of alterations in voltage gating sensitivity, kinetics, or chemical gating. These results provide a plausible explanation for the 50% decrease in junctional coupling observed during lens fiber maturation.

Results

In the following chapter, I have included several figures that are the work of a close collaborator, Dr. Miduturu Srinivas. These data provide support for the main hypothesis of this chapter. For an in-depth description of the methodology used to obtain Figures VII-5-7, please refer to DeRosa et al. 2006 (DeRosa et al., 2006). Figures VII-1-4 and 8 are from my own experimental data.

Expression of Connexin Proteins in *Xenopus* Oocytes

Translation of connexin cRNAs was quantified by immunoblot analysis of oocytes injected with full-length Cx50, Cx50tr290, or water, using a polyclonal Cx50 antibody raised against an epitope in the central cytoplasmic loop of mouse Cx50 (White et al., 1992). The antibody recognized a 63-kDa band corresponding to full-length Cx50 (◀) and a 32-kDa band corresponding to Cx50tr290 (<◁) in oocyte samples injected with their respective cRNAs (Figure VII-1A). The antibody also detected a nonspecific band in all three samples (denoted by the asterisk). Expression levels were quantified by measuring band densitometry, and a plot of the mean band density values (Figure VII-1B) showed no significant difference in full-length Cx50 and Cx50tr290 protein expression ($P > 0.05$; Student's t test). Thus, both proteins were synthesized at equal levels, and any alteration in channel function caused by truncation could not be attributed to differences in protein expression.

Truncated Cx50 Channel Formation in *Xenopus* Oocytes

The ability to form intercellular channels was tested by whole-cell voltage clamp of paired *Xenopus* oocytes (Figure VII-2). As expected, full-length Cx50 pairs formed functional channels with a mean intercellular conductance of 23.8 μS , a value several

hundred-fold higher than the water-injected negative control pairs (0.06 μ S). Cells injected with Cx50tr290 cRNA exhibited a mean conductance value of 3.4 μ S, which was approximately 50-fold higher than background, but significantly decreased compared to full-length Cx50 (86% reduction; $P < 0.05$). Heterotypic cell pairs, in which one cell contributed full-length Cx50 and the other expressed Cx50tr290, displayed a mean conductance of 6.2 μ S. This 100-fold increase over background was intermediate between the homotypic full-length and truncated measurements. The level of heterotypic coupling was significantly decreased compared with full-length Cx50 ($P < 0.05$), but not Cx50tr290, homotypic channels ($P > 0.05$). These results show that Cx50tr290 forms functional gap junctions in homotypic and heterotypic pairs, but the mean gap junctional conductance was significantly decreased in both channel configurations.

Voltage Gating Behavior of Full-Length and Truncated Cx50 Channels in *Xenopus* Oocytes

To characterize the functional properties of full-length and truncated Cx50 proteins, voltage gating was examined by subjecting oocyte pairs to a series of hyperpolarizing and depolarizing transjunctional voltages (V_j). Figure VII-3 shows a comparison of representative traces of junctional currents (I_j) for oocyte pairs expressing homotypic Cx50 (Figure VII-3A), homotypic Cx50tr290 (Figure VII-3B), or heterotypic Cx50/Cx50tr290 (Figure VII-3C) gap junctions. I_j decreased symmetrically with time in a voltage-dependent manner for all channel types, with a more rapid decline in current at greater transjunctional potentials. To analyze channel-closure kinetics, the initial 200 ms current decay was plotted against time and fit to a mono-exponential function to determine the time constant tau (τ). Figure VII-3 shows representative current decays

after application of a positive 80 mV voltage step for truncated (Figure VII-3D), full-length (Figure VII-3E), and heterotypic (Figures VII-3F and 3G) Cx50 channels. All channel types exhibited a mean τ of 44 to 46 ms at this V_j step, and no significant changes in channel-closure kinetics resulted from truncation of the C-terminus of Cx50 ($P > 0.05$). The steady-state voltage gating behavior of these channels was examined by plotting V_j against G_j (normalized to the values obtained at ± 20 mV), and fitting the data to the Boltzmann equation (Figure VII-3H). Equilibrium voltage conductance was similar; Boltzmann parameters are listed in (Table VII-1). These data show that C-terminal truncation of Cx50 did not alter voltage gating in homotypic or heterotypic channels.

Localization and Functional Expression of Cx50tr290 in Mammalian Cells

The expression and intracellular targeting of connexin proteins was further analyzed in HeLa cells transiently transfected with full-length Cx50 or Cx50tr290 DNA. Immunofluorescent images revealed qualitatively similar levels of connexin expression for full-length (Figure VII-4A and 4C) and truncated (Figure VII-4B and 4D) Cx50 proteins. Punctate staining (Figure VII-4, arrows) indicated that Cx50 and Cx50tr290 were properly targeted to the plasma membrane, especially at regions of cell-to-cell apposition. Thus, truncated Cx50 proteins were expressed and successfully trafficked to the cell membrane in a manner indistinguishable from that of full-length Cx50. The ability of Cx50tr290 to form functional channels in mammalian cells was tested by dual whole-cell patch-clamp measurements of transiently transfected N2A cell pairs (Figure VII-5). All green fluorescence protein (GFP)-positive cell pairs expressing full-length Cx50 were electrically coupled, with a mean conductance of 17.5 nS. Most (68%) GFP-

labeled cell pairs expressing Cx50tr290 also formed functional channels, though with a mean level of coupling an order of magnitude lower (1.9 nS) than the full-length Cx50 value. This 89% reduction in mean G_j was statistically significant ($P < 0.05$), and correlated well with the 86% coupling decrease recorded between *Xenopus* oocyte pairs (Figure VII-2). These results indicate that cell pairs expressing truncated Cx50 have significantly decreased coupling even though expression or localization of the protein was unaltered.

Electrophysiological Properties of Truncated Cx50 Channels in Mammalian Cells

Voltage gating characteristics of Cx50tr290 channels expressed in N2A cells were determined with dual whole-cell patch clamp. A recording of junctional currents from an N2A cell pair expressing truncated Cx50 channels (Figure VII-6A) indicated that I_j decreased symmetrically over time in a voltage-dependent manner, with a swifter current decay at larger transjunctional voltage applications. Examination of Cx50tr290 gating kinetics revealed a τ of 44 ms after an 80 mV potential was applied (Figure VII-6B). Analysis of the steady state G_j/V_j relationship (Figure VII-6C) showed that truncated channels displayed voltage gating similar to that previously reported for full-length Cx50 (Srinivas et al., 1999), as indicated by the Boltzmann parameters provided in (Table VII-1). Taken together, these data suggested that C-terminal truncation did not alter voltage-dependent gating in transfected mammalian cells, a finding consistent with our data from paired *Xenopus* oocytes (Figure VII-3).

Unitary Conductance and Single-Channel Gating of Cx50tr290

To examine the functional role of the carboxyl tail of Cx50 in single-channel conductance and gating, current traces were recorded from paired N2A cells transfected

with full-length or Cx50tr290 cDNA using dual whole-cell patch clamp. Representative Cx50tr290 and full-length Cx50 single-channel current traces are illustrated in (Figure VII-7). Amplitude histograms for the single-channel currents recorded at the V_j s of -25 mV (Figure VII-7A) and -50 mV (Figure VII-7B) had distinct peaks that corresponded to the open-channel levels at 5.2 and 10.4 pA, respectively, and yielded a unitary conductance of 210 pS, a value similar to that found for full-length Cx50 channel currents (see Figure VII-7E for a recording of Cx50 channels at a V_j of -40 mV). Gating of Cx50 channels was also unaffected by cleavage. The Cx50tr290 channels were primarily in the fully open state at the smaller V_j pulse of -25 mV, but transitioned to a subconductance state at the larger driving voltage (-50 mV), as previously described for full-length Cx50 channels (Srinivas et al., 1999). Additionally, (Figure VII-7C) shows that during a 100-second recording of a single Cx50tr290 channel at a V_j of -30 mV, the truncated channels spent long periods of time in the fully open state, with only brief transitions into subconducting or nonconducting states. An expanded portion of the 100-second record (Figure VII-7D) showed that the truncated channel spent 88% of the time in the fully open state, similar to full-length Cx50 channels (Srinivas et al., 1999). Therefore, truncation did not affect the single channel conductance or gating properties of Cx50.

pH Gating Sensitivity of Truncated Cx50 Channels

The functional significance of the Cx50 carboxyl tail on pH gating was examined by perfusing *Xenopus* oocyte pairs with 100% CO_2 -saturated external solution. Full-length and Cx50tr290-injected oocyte pairs exhibited a rapid decline in G_j over time on perfusion with 100% CO_2 (Figure VII-8A). Junctional coupling recovered when the extracellular medium was switched back to the original MB medium. These data

indicated that C-terminal truncation of murine connexin50 at amino acid 290 did not inhibit the chemical gating properties of gap junction channels in paired *Xenopus* oocytes.

Human Cx50 has been reported to be insensitive to cytosolic acidification on truncation (Xu et al., 2002), a discrepancy with our data that may have resulted from the use of an ammonium exchange technique to produce a calculated reduction in intracellular pH (Xu et al., 2002), or from intrinsic differences between the human and murine truncated Cx50 proteins. To distinguish between these two possibilities, we made a human Cx50tr294 construct and expressed it in *Xenopus* oocytes. Like its mouse counterpart, human Cx50tr294 induced coupling between paired oocytes with a mean conductance of 5.9 μ S (Figure VII-8B). Perfusion of human truncated Cx50 pairs with 100% CO₂-saturated medium resulted in a greater than 90% reduction in coupling that recovered on washout of CO₂ (Figure VII-8C). These data show that truncation of human Cx50 did not abolish pH sensitivity.

Discussion

We mimic the naturally occurring C-terminal cleavage of Cx50 and characterize the functional properties of the resultant channels *in vitro* to further elucidate the role of truncation in lens fiber maturation. Immunoblotting confirms that full-length and truncated Cx50 expression levels are not statistically different, and immunocytochemistry shows that truncated proteins target to sites of cell–cell contact. Interestingly, intercellular conductance measurements show that Cx50tr290 proteins form functional gap junctions with an 86% to 89% reduction in junctional conductance from that of the full-length channel, a phenomenon that has not been reported. This reduction in coupling does not result from decreased unitary conductance, improper targeting, or dramatic alterations in voltage or chemical gating.

Previous studies of truncated lens connexins have shown that cleavage of the C-termini does not abolish channel-forming ability (Lin et al., 1998) (Stergiopoulos et al., 1999) (Xu et al., 2002) (Eckert, 2002), a finding that coincides with the data described in this study. However, we report a significant decrease in macroscopic gap junctional conductance produced by Cx50tr290 as compared to full-length channels in two different expression functional systems. Furthermore, we observe a 210-pS unitary conductance for Cx50tr290 channels, a value very close to the 220-pS conductance previously reported for full-length mouse Cx50 channels (Srinivas et al., 1999). Thus, C-terminal cleavage is seen to reduce macroscopic coupling without affecting unitary conductance, a phenomenon that may link the endogenous cleavage of Cx50 to the observed 50% decrease in junctional coupling at the differentiating-to-mature fiber transition during lens fiber maturation. This idea is further supported by coupling measurements in Cx46 and

Cx50 knockout lenses, which show the deletion of Cx46 to eliminate coupling in the mature fibers, whereas knockout of Cx50 produces only a marginal reduction (Baldo et al., 2001) (Gong et al., 1998). These data have been interpreted to link the 50% drop in coupling during fiber maturation to a loss of functional Cx50 channels. The large reduction in macroscopic coupling seen in Cx50tr290 is consistent with the idea that the endogenous cleavage of Cx50 could negatively regulate channel activity, possibly through a reduction in the number of functional channel subunits.

No role for the carboxyl terminus in voltage gating has been identified by previous studies of cleaved lens fiber connexins (Xu et al., 2002) (Stergiopoulos et al., 1999) (Lin et al., 1998) (Eckert, 2002). In agreement with this earlier work, we find channel gating and kinetics to be nearly identical when full-length and truncated electrophysiology data are compared. Transjunctional current recordings collected at different transjunctional potentials reveal indistinguishable symmetrical traces for both channel sets, supporting the conclusion that the endogenous C-terminal truncation does not affect voltage-dependent gating. This has been further confirmed by studies of heterotypic channels displaying no asymmetry in their junctional currents, suggesting that Cx50tr290 can interact with full-length Cx50 without alteration of gating properties.

In marked contrast to voltage gating, previous studies of truncated lens connexins have reached conflicting conclusions regarding the role of the C-terminus in chemical gating of junctional conductance by pH (Lin et al., 1998) (Stergiopoulos et al., 1999) (Xu et al., 2002) (Eckert, 2002). The intracellular pH in the lens core is more acidic than that in the cortex, and impedance studies have shown that junctional coupling in the mature fibers of the core is less sensitive to pH (Mathias et al., 1997). One hypothesis is that

cleavage of lens fiber connexins reduced sensitivity to pH gating. This is supported by some studies showing that cleavage of the carboxyl terminus of Cx50 abolishes pH gating in vitro (Lin et al., 1998) (Xu et al., 2002). However, others have found that truncated lens connexins retain their sensitivity to cytosolic acidification, and that pH gating is largely unaffected by carboxyl terminal cleavage (Stergiopoulos et al., 1999) (Eckert, 2002).

One source of variation in the aforementioned studies may be the Cx50 isoform being assayed. We report that the murine and human truncated Cx50 retain pH sensitivity, a finding that agrees with Stergiopoulos et al. (Stergiopoulos et al., 1999), who also tested mouse Cx50. In contrast, the human and ovine isoforms have both been reported to be insensitive to the effects of cytosolic acidification on truncation (Lin et al., 1998) (Xu et al., 2002). Although the Cx50 orthologs are highly conserved, the exact sites of truncation vary among species. In mice, the endogenous truncation sites are at amino acids 290 and 300, corresponding to positions 284 and 294 in human Cx50. Our data suggest that truncated Cx50 channels retain pH sensitivity regardless of species, and imply that differences in experimental design underlie the conflicting results. In this context, it is worth noting that early reports of pH insensitivity of chick lens connexins (Rup et al., 1993) were subsequently shown to be premature on further analysis (Jiang et al., 1995). A greater source of variability may come from the methodology used to reduce intracellular pH. Xu et al. (Xu et al., 2002) used an ammonium exchange technique, while the other studies relied on superfusion of CO₂-saturated solution (Lin et al., 1998) (Stergiopoulos et al., 1999); the efficiency and degree of acidification could vary between methods. Although we did not directly verify the acidification of the cytoplasm, our results are in

good agreement with those of Stergiopoulos et al., (Stergiopoulos et al., 1999) the only study that directly measured intracellular pH, and indicate that truncated Cx50 is still pH gated, though with a modest shift in pKa.

The greatest consequence of Cx50 truncation is a significant reduction in macroscopic conductance. This correlates well with the ~50% drop in gap junctional conductance observed *in vivo* during fiber maturation. Further experimentation on the functional significance of C-terminal cleavage may benefit from the generation and analysis of genetically engineered animals expressing forms of Cx50 that are either permanently truncated, or have mutated calpain cleavage sites that prevent truncation.

Figure VII-1. Western blot analysis of *Xenopus* oocyte extracts indicates similar expression of full-length (Cx50) and truncated (Cx50tr290) proteins. (A) Oocytes were collected and membrane fractions were prepared. Equal amounts of the preparations were loaded into each lane for each condition. Western blots were probed with a polyclonal rabbit anti-mouse Cx50 antiserum. Full-length (◄) and truncated (◄) Cx50 proteins were efficiently translated. *Antibody detection of a nonspecific band. (B) Quantitation of protein expression by densitometry showed equivalent levels of connexin expression. Levels of synthesis of full-length and truncated Cx50 proteins were not statistically different ($P > 0.05$). Densitometry values are the mean \pm SE of four independent experiments that were normalized to the mean band intensity of the full-length sample.

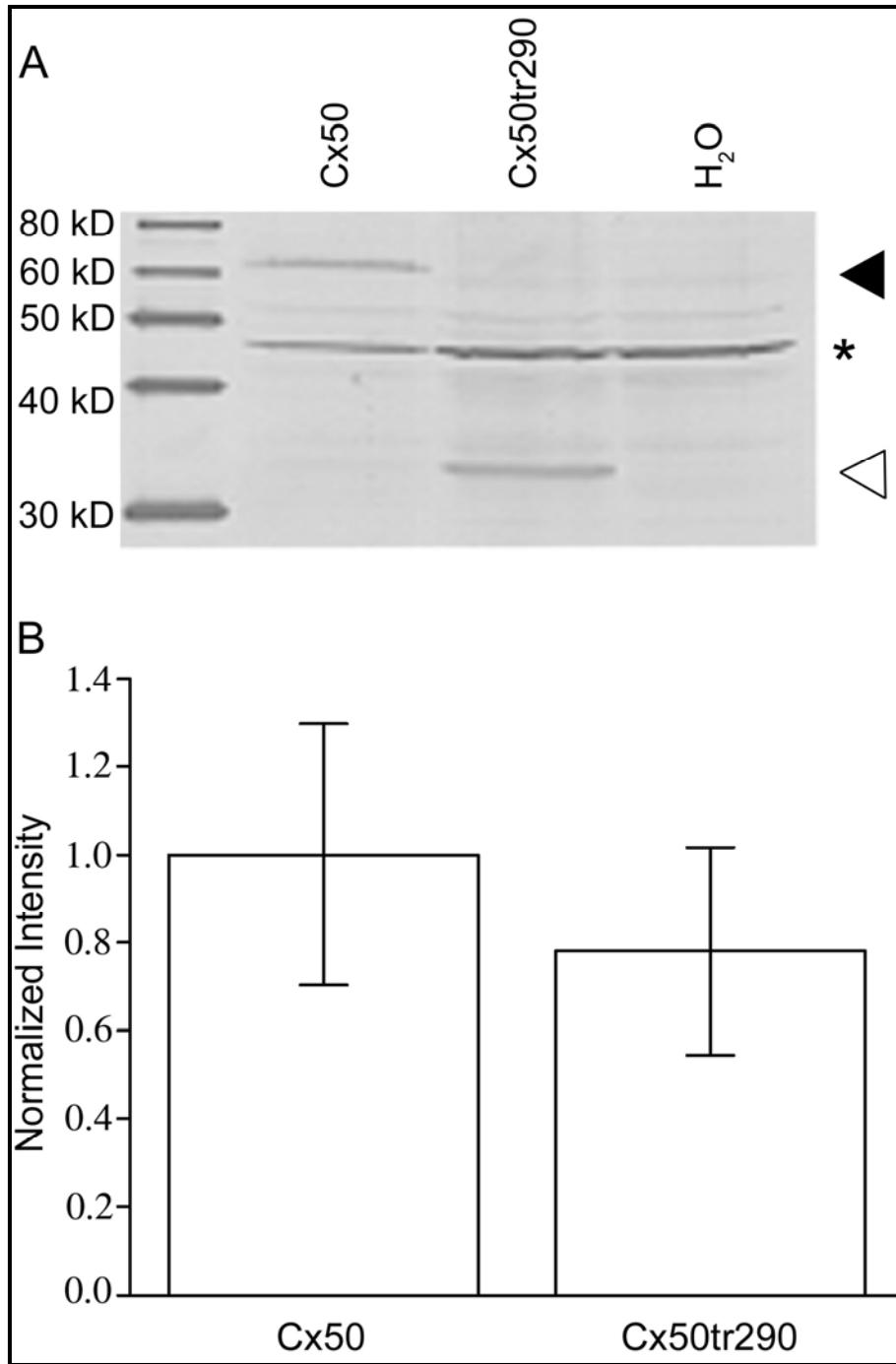


Figure VII-2. Truncated Cx50 forms functional intercellular channels. Junctional conductance values were measured between oocyte pairs injected with full-length Cx50, Cx50tr290, or water. Full-length Cx50 and Cx50tr290 channels exhibited mean conductance values 400- or 50-fold greater than water-injected controls. Heterotypic channels formed by pairing two oocytes-one expressing full-length Cx50, the other injected with truncated Cx50 cRNA displayed an intermediate level of coupling that was 100-fold higher than background. Columns are the mean \pm SE. Data points within each column represent the individual conductance values for each condition tested.

Figure VII-3. Voltage-gating properties of full-length, truncated, and heterotypic Cx50 channels. Junctional currents (I_j) induced by transjunctional voltages (V_j) were plotted as a function of time. For homotypic channels composed of full-length Cx50 (A), Cx50tr290 (B), and heterotypic (C) channels, rapid current decay was seen at large voltages (± 80 – 120 mV), whereas modest voltages (± 20 – 60 mV) exhibited a slower decline in junctional current. No qualitative changes in channel voltage gating were seen among the three channel types. Channel kinetics were analyzed by fitting the initial 200 ms of current decay recorded at $+80$ mV to a monoexponential model for cell pairs expressing truncated (D), full-length (E), and heterotypic channels (F, G). Channel closure kinetics were not affected by C-terminal truncation. Tau (τ) values represent the mean \pm SE of six independent I_j traces. Equilibrium-gating properties were analyzed by plotting normalized steady state conductance against transjunctional voltage and fitting to the Boltzmann equation (H). Comparison between full-length and truncated channels showed similar voltage sensitivity. Boltzmann parameters are given in Table VII-1.

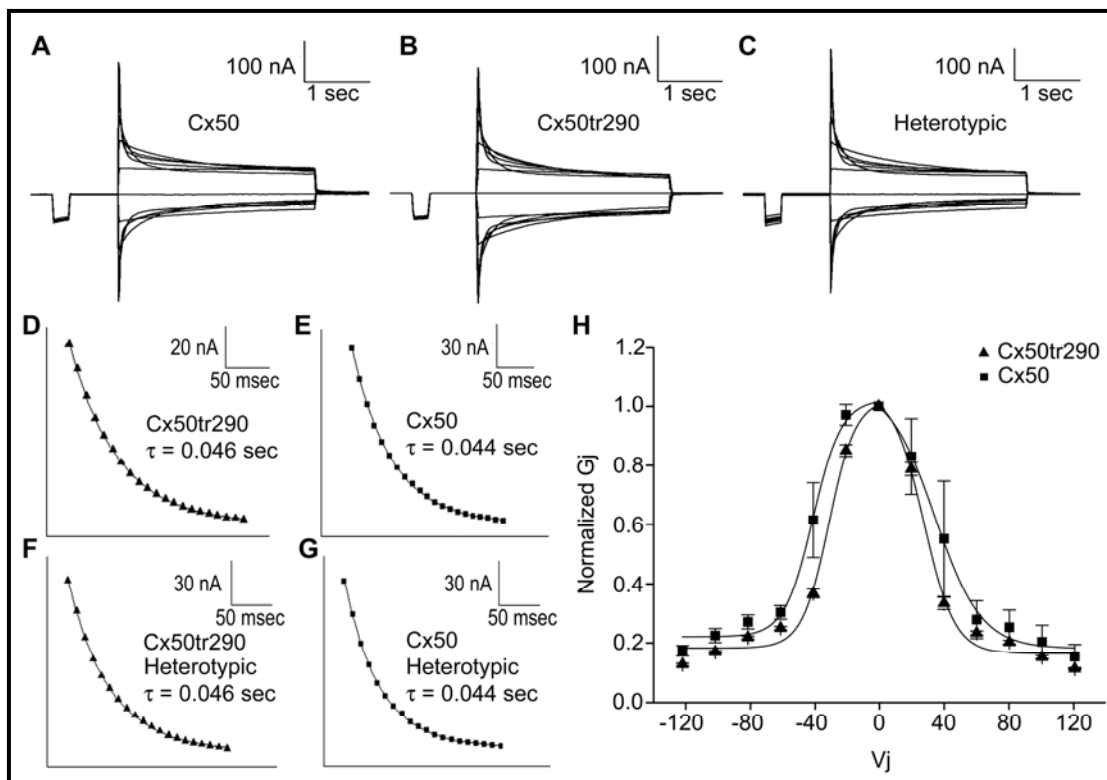


Figure VII-4. Immunofluorescence imaging of Cx50 in transfected HeLa cells. Transiently transfected HeLa cells expressing full-length Cx50 (A, C) or Cx50tr290 (B, D) proteins were immunostained and examined by fluorescence microscopy. Merged images taken at x100 (A, B) and x60 (C, D) exhibited Cy3 staining of connexins (red) and DAPI staining of cell nuclei (blue). All images showed that full-length and truncated Cx50 were efficiently translated and localized to the membrane, specifically at areas of cell-to-cell apposition (arrows).

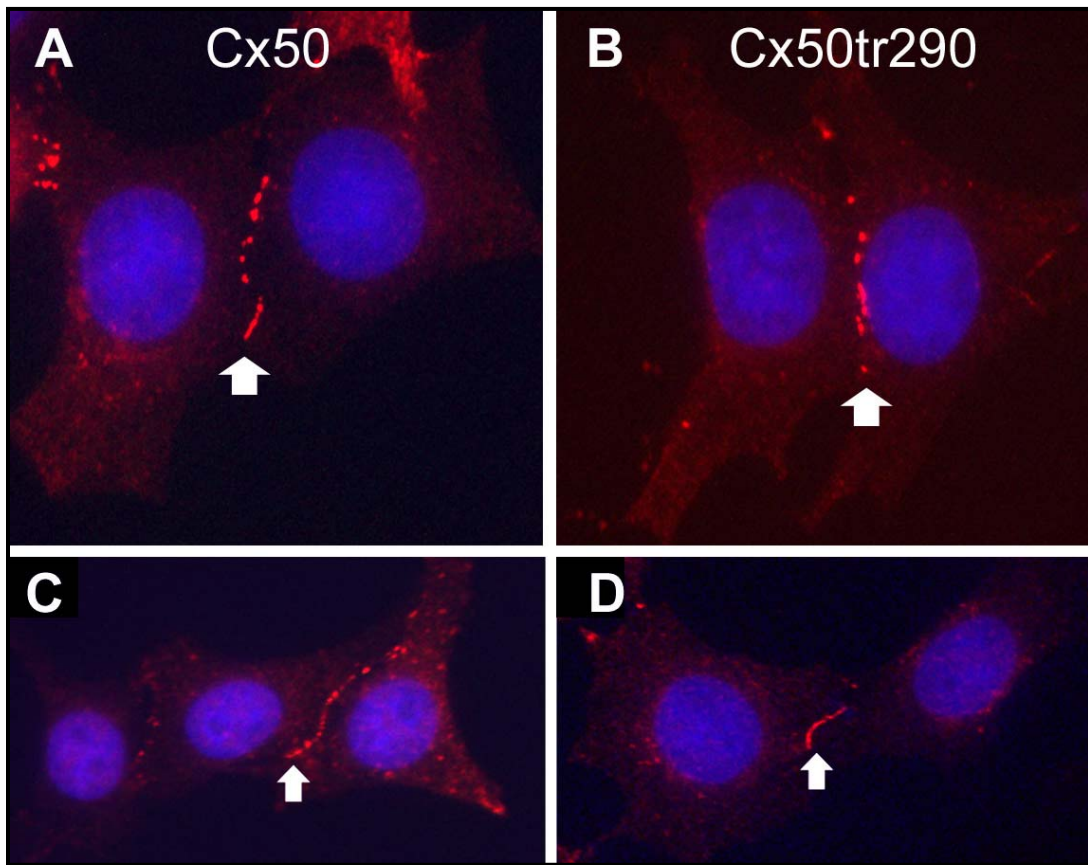


Figure VII-5. Cx50tr290 subunits form functional intercellular channels with reduced coupling in N2A cell pairs. G_j was measured using dual whole-cell patch clamp on transiently transfected N2A cells expressing either full-length or truncated Cx50 proteins. Full-length Cx50 channels displayed a mean conductance of 17.5 nS, a significantly higher level of coupling than the 1.9 nS shown by truncated Cx50 channels ($P < 0.05$). Columns are the mean \pm SE. Symbols within each column represent individual conductance values. Uncoupled pairs are represented on the x -axis.

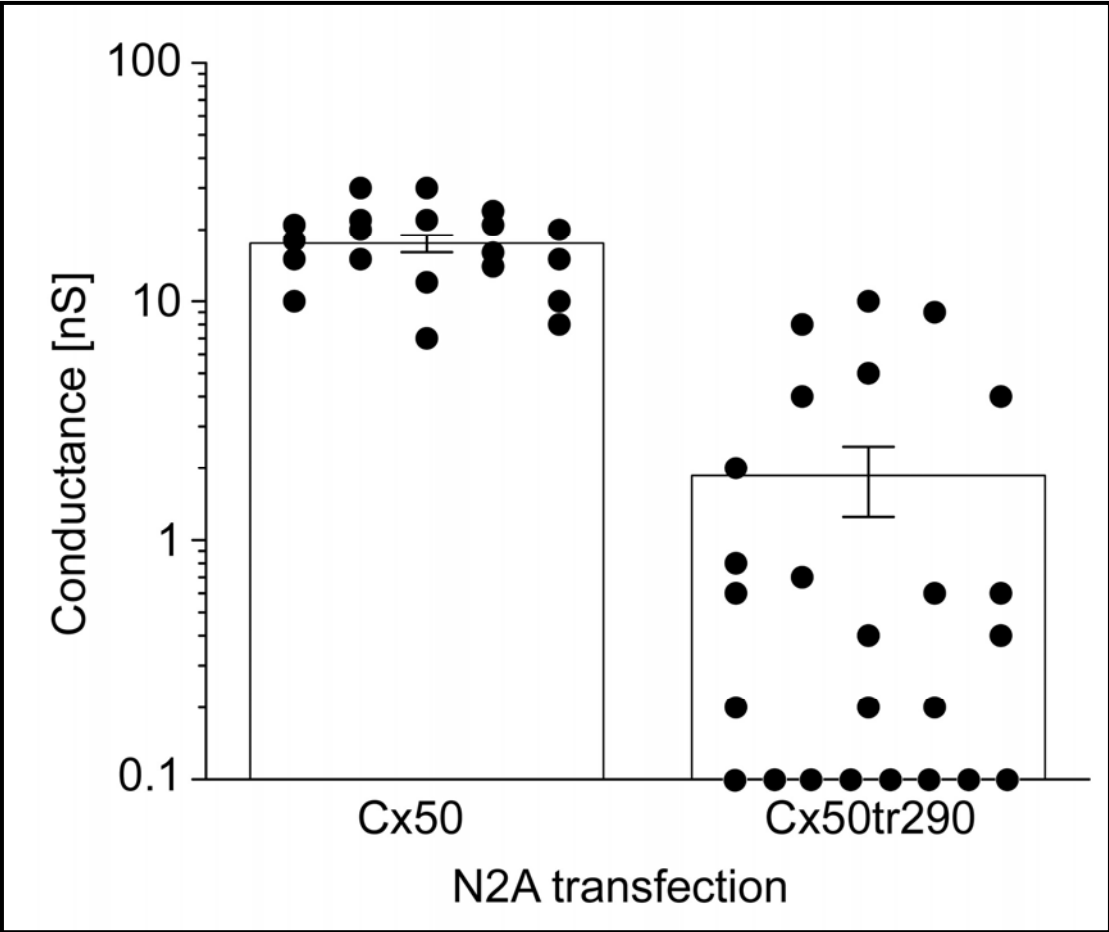


Figure VII-6. Voltage dependence and gating kinetics of truncated Cx50 channels in transfected cells. Representative current traces recorded from transiently transfected N2A cell pairs expressing Cx50tr290 subunits (A). Junctional currents recorded during a series of transjunctional voltage applications ranging from +120 to -120 mV in 20 mV intervals were plotted as a function of time. Gating properties were symmetrical at positive and negative polarities. Cx50tr290 channel closure kinetics were analyzed at a transjunctional potential of 80 mV by fitting to a monoexponential decay (B) and were similar to full-length and truncated Cx50 channels expressed in oocytes. Normalized steady state conductance was plotted against transjunctional voltage and analyzed using the Boltzmann equation (C), whose parameters are given in Table VII-1. Voltage gating sensitivity of Cx50tr290 channels was largely unchanged when compared with full-length Cx50 junctions. Voltage dependence and gating kinetics of truncated Cx50 channels in transfected cells. Representative current traces recorded from transiently transfected N2A cell pairs expressing Cx50tr290 subunits (A). Junctional currents were recorded during a series of transjunctional voltage applications ranging from +120 mV to -120 in 20 mV intervals and plotted as a function of time. The gating properties were symmetrical at both positive and negative polarities. Cx50tr290 channel closure kinetics were analyzed at a transjunctional potential of 80 mV by fitting to a monoexponential decay (B) and were similar to full-length and truncated Cx50 channels expressed in oocytes. Normalized steady state conductance was plotted against transjunctional voltage and analyzed using the Boltzmann equation (C) whose parameters are given in Table VII-I. The voltage gating sensitivity of Cx50tr290 channels was largely unchanged when compared to full-length Cx50 junctions.

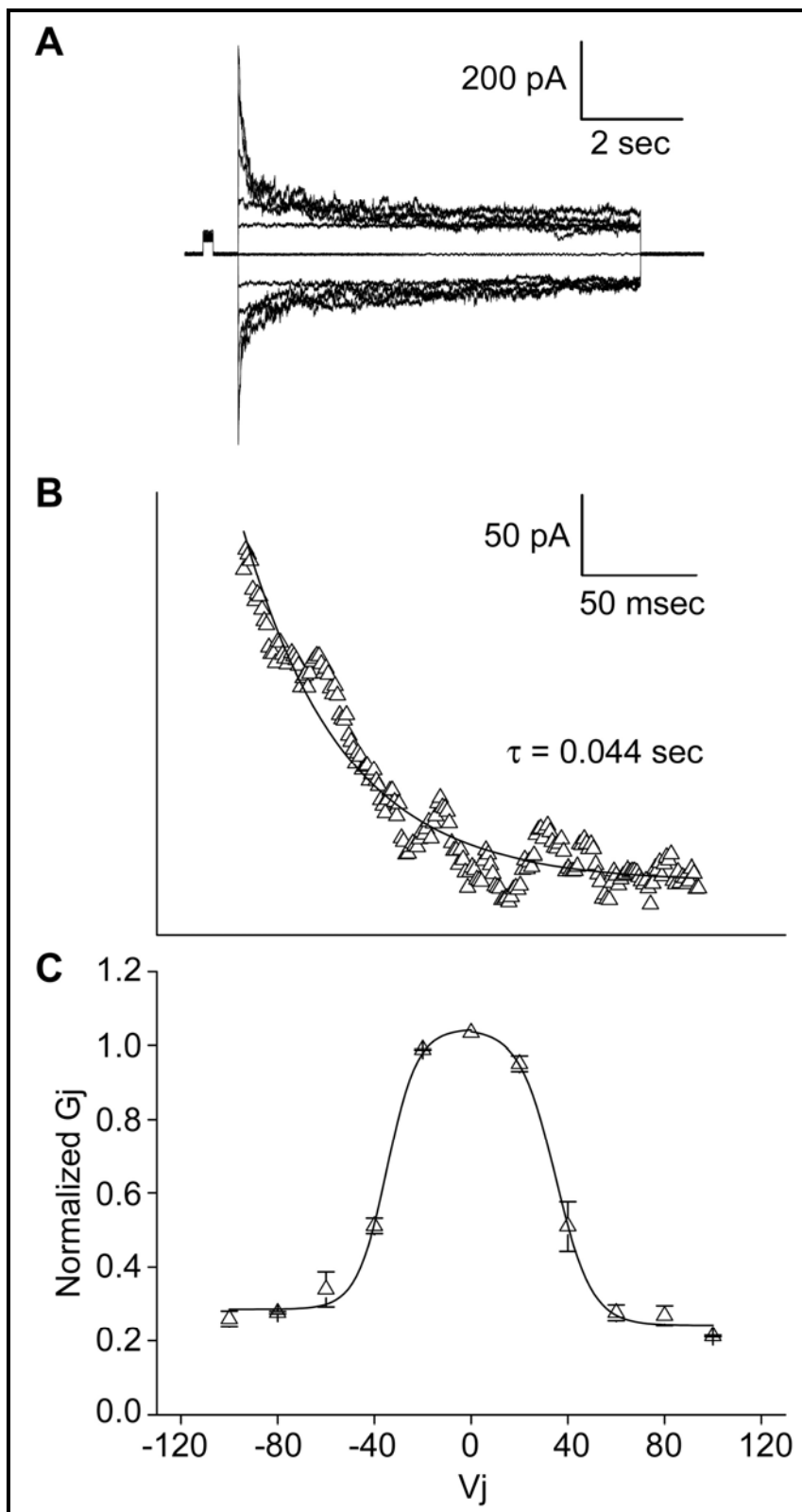


Figure VII-7. Cx50tr290 and full-length Cx50 have identical single-channel properties. Junctional currents recorded from single channels containing of Cx50tr290 at three different transjunctional voltages. Cx50tr290 channels were primarily open at -25 mV (A), but transitioned to lower conductance states at -50 mV (B) and showed a unitary conductance of 210 pS. During an extended recording of a single Cx50tr290 channel at -30 mV (C), the truncated channels remained in the fully open state, with only brief transitions into lower conducting states. An expanded portion of the record (D) showed only two brief transitions (asterisk) to substates. Full-length Cx50 single-channel current recordings at -40 mV had a peak at 8.4 pA, corresponding to a unitary conductance of 210 pS (E). All-point histograms are plotted on the right.

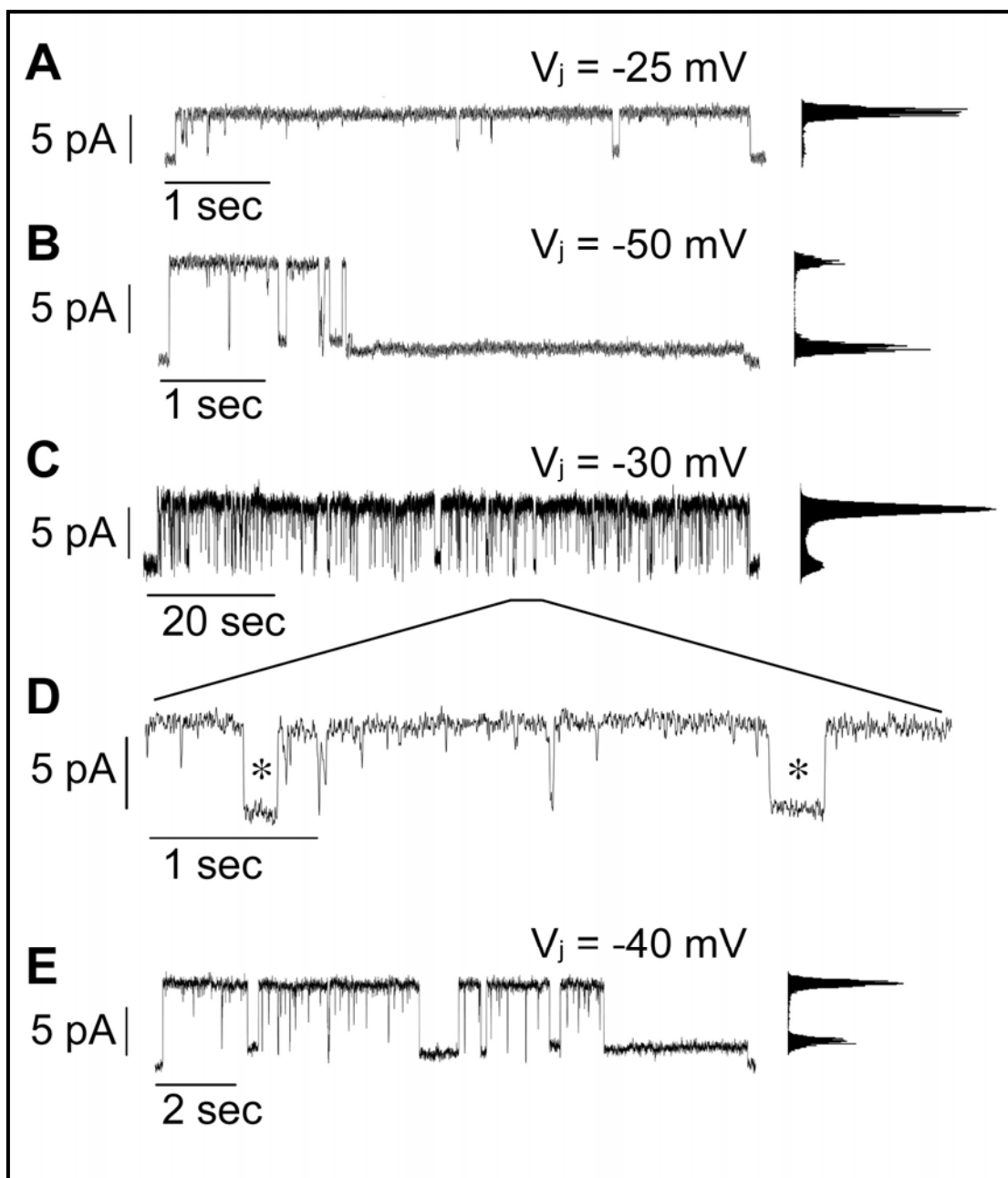


Figure VII-8. pH gating sensitivity of full-length and truncated Cx50 channels. (A) Full-length and Cx50tr290 channels rapidly closed during cytoplasmic acidification, indicating that C-terminal truncation did not eliminate pH gating sensitivity. On washout, transjunctional conductance recovered. Human truncated Cx50 forms pH-sensitive intercellular channels. Human Cx50tr294 channels exhibited a mean conductance of 5.9 μ S, a value 100-fold higher than water-injected controls (B). Human Cx50tr294 channels reversibly closed during cytoplasmic acidification indicating that, like murine Cx50, C-terminal truncation did not abolish pH gating (C). Data are the mean \pm SE of 3 to 10 pairs.

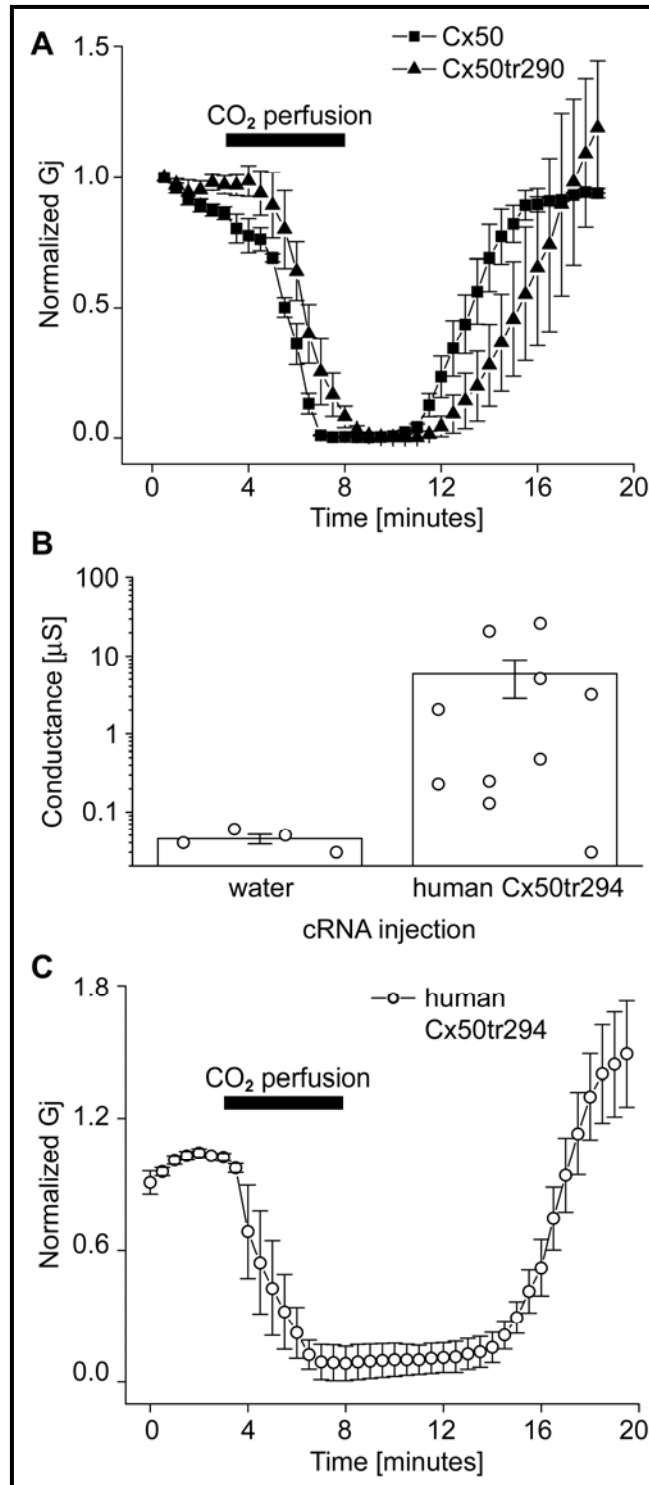


Table VII-I. Boltzmann Parameters for Full-length and Truncated Cx50 Channels

G_{jmin} represents the minimum conductance value, V_0 indicates the voltage measured midway through the G_j decline, and A denotes the cooperativity constant, reflecting the number of charges moving through the transjunctional field. Plus and minus signs for V_j indicate transjunctional membrane potential polarity. * Data taken from (Srinivas et al., 1999).

Connexon	V_j	V_0	G_{jmin}	A
Xenopus Oocytes				
Cx50	+	34	0.16	0.06
Cx50	-	-40	0.20	0.09
Cx50tr290	+	28	0.14	0.11
Cx50tr290	-	-30	0.16	0.12
N2A cells				
Cx50*	+	38	0.21	0.16
Cx50*	-	-37	0.22	0.15
Cx50tr290	+	35	0.24	0.11
Cx50tr290	-	-35	0.29	0.22

Chapter VIII

Concluding remarks

Summary of analysis

Gap junctions link the cytoplasm of adjacent cells, creating a regulated pathway that governs numerous biological processes such as tissue homeostasis in many organisms. While great strides have been made in revealing the structural organization, docking process, and biochemical or electrical properties of gap junction channels, much remains undiscovered. Previous studies have identified more than 20 highly homologous members of the connexin gene family in humans and mice, as the primary component of gap junction channels (Willecke et al., 2002). Each connexin is arranged with two conserved extracellular loops, four transmembrane domains, and a cytoplasmic intercellular loop, as well as internal amino and carboxyl termini that vary greatly across connexin orthologs. Three-dimensional electron crystallography reveals that gap junctions form via the association of two hexameric transmembrane channels called connexons (Leube, 1995) (Traub et al., 1998) (Unwin, 1989) (Unger et al., 1999). Within the channel, each of the aforementioned connexin domains is expected to play a unique role in gap junction function. The transmembrane domains will undoubtedly contribute to lining the channel pore, and some may even participate in hexamer oligomerization. The N-terminus is highly conserved across species and was found to play a role in membrane insertion, voltage gating, and calmodulin binding (Torok et al., 1997) (Purnick et al., 2000) (Rubin et al., 1992) (Peracchia and Peracchia, 2005). The amino acid composition of a connexin's cytoplasmic loop is highly variable, and recent evidence implies that the intracellular loop may govern channel permeability, a finding that coincides with data showing that channel permeability is connexin dependent (Koumi et al., 1995). The presence of three conserved cysteines in each of the two extracellular loops of all

connexin species is presumably crucial for connexon docking in the extracellular space between neighboring cells (Foote et al., 1998) (Hennemann et al., 1992). The cytosolic C-terminus is the most variable domain among connexins. Due to variation in peptide length, the universal role of this domain remains unclear. However, in alpha connexins (Cx43, Cx46, Cx50), the C-terminus contains many phosphorylation sites that may govern electrical coupling (Lampe and Lau, 2000) (Lampe et al., 2000) (Fishman et al., 1991), as well as endogenous truncation sites correlating with an alteration in channel pH gating sensitivity (Stergiopoulos et al., 1999) (Xu et al., 2002) and electrical coupling (DeRosa et al., 2006). The variability and overlap in the functions of each connexin domain suggest a need for the functional characterization of these specific protein domains.

This dissertation utilizes four different Cx50 protein variants containing alterations in the cytosolic amino or carboxy termini, as well as both extracellular loops. Through the use of disease-causing mutations and naturally occurring post-translational modifications, we provide further insight toward uncovering the physiological relevance of these distinct connexin50 protein domains.

Analysis of Cx50 amino-terminal mutants reveal that mutation of this domain affects channel voltage gating (Peracchia and Peracchia, 2005). Thus, we hypothesize that Cx50-G22R mutant subunits will alter the electrical gating properties of gap junction channels in the lens. Our electrophysiological data indicate that Cx50-G22R is a loss of function mutation, as expression of this protein alone fails to electrically couple cells. However, the mixed expression of Cx50-G22R and wild-type Cx46 fiber connexins creates functional gap junction channels with significant reductions in conductance and

distinct alterations voltage gating properties when compared to homotypic Cx46 channels. Conversely, co-expression of wild-type Cx50 and Cx50-G22R mutant subunits does not produce any obvious changes in channel function when compared to homotypic wild-type Cx50 channels, other than an attenuated ability to electrically couple cells. The unaltered gating properties of mixed channels expressing wild-type and mutant Cx50 subunits, in conjunction with the G22R mutant protein's ability to localize to the plasma membrane and form junctional plaques, suggests that decreased mixed channel coupling may result from fewer functional connexin subunits contributing to channel formation. Additional support for this hypothesis may come from dye permeation studies using transfected cells or transgenic mouse lenses expressing both wild-type and mutant Cx50 proteins. Presumably, these studies will show discernable differences in the diffusion rates of molecular or ionic tracer dyes when homotypic and mixed channels are analyzed. Conversely, the data herein suggest that endogenous wild-type Cx46 and Cx50-G22R mutant subunits interact to form functional heteromeric gap junctions with unique gating characteristics, a phenomenon that may contribute to the aberrant ocular phenotypes seen *in vivo*. Similarly, our data imply that knock-in Cx46 subunits interact with mutant Cx50-G22R subunits to form heteromeric channels that partially restore intercellular communication between lens fiber cells, providing a possible mechanism behind the partial rescue of the mutant lens phenotype. These findings add to the growing body of literature establishing the N-terminal domain of numerous connexins as a significant regulator of channel voltage gating (Peracchia and Peracchia, 2005) (Purnick et al., 2000) (Verselis et al., 1994) (Bruzzone et al., 2003), as we definitively describe changes in the electrical properties of gap junctions containing Cx50-G22R mutant subunits.

Genetic mutations in either of the two extracellular loops have revealed that these domains play a critical role in the docking of two hemichannels between adjacent cells (Foote et al., 1998) (Martin et al., 2000) (Yeager and Nicholson, 1996). The extracellular domains of α -connexins are highly conserved and mutations of charged amino acids in either of the extracellular loops are associated with congenital cataracts in both mice (Xu and Ebihara, 1999) and humans (Berry et al., 1999). Electrophysiological examination of these mutant connexins imply a possible role for the first extracellular domain of Cx50 in channel gating (Xu and Ebihara, 1999).

This dissertation analyzes the effects of two extracellular loop mutants, Cx50-S50P (E1) and Cx50-R205G (E2) on channel gating, gap junctional plaque formation, and lens development and function. The data herein imply that the extracellular domains of Cx50 govern an interaction with other Cx50 proteins, as co-expression of Cx50-S50P and wild-type Cx50 subunits inhibit embryonic fiber cell development by dominantly altering wild-type channel gating. Additionally, mutant Cx50-R205G acts as a dominant negative inhibitor of wild-type Cx50 channel function *in vitro*. Similarly, we show that mutation of either of Cx50's extracellular loops does not inhibit interaction with wild-type Cx46 subunits, but co-expression of these mutant subunits and Cx46 results in significant alterations in channel function. These findings support prior suppositions stating that the extracellular domains of α -connexins play a role in connexin oligomerization, electrical coupling and gap junctional plaque formation (Steele, Jr. et al., 1998) (Berry et al., 1999) (Graw et al., 2001) (Shiels et al., 1998) (Foote et al., 1998) (Martin et al., 2000) (Yeager and Nicholson, 1996) (Xu and Ebihara, 1999).

There is a growing amount of literature regarding the physiological relevance of numerous connexin family members' carboxy-termini (Lampe and Lau, 2000) (Kwak et al., 1995) (Stergiopoulos et al., 1999) (Xu et al., 2002) (Lin et al., 1998) (DeRosa et al., 2006) (Revilla et al., 2000). The high variation in amino acid sequences in the C-terminus implies that the functional differences exhibited by connexins may manifest in this domain. Previous studies of α -connexins containing genetic or post-translational variations in their C-termini have reveal many roles for this cytoplasmic domain, such as regulation of voltage-dependent gating (Revilla et al., 2000), protein phosphorylation (Lampe and Lau, 2000) (Kwak et al., 1995), and chemical gating by H^+ ions (Stergiopoulos et al., 1999) (Xu et al., 2002) (Lin et al., 1998) (DeRosa et al., 2006). This dissertation helps clarify several of the discrepancies created by previous laboratories regarding the endogenous truncation of Cx50's carboxy terminus.

Here we reproduce the naturally occurring C-terminal cleavage of Cx50 and characterize the functional properties of the resulting channels *in vitro* to verify the role of truncation during lens fiber cell maturation. Junctional conductance measurements reveal that truncated Cx50 subunits form functional intercellular channels that exhibit an 86-89% reduction in electrical coupling when compared to that of the full-length protein. Dual whole-cell patch clamp analysis shows that this reduction does not result from decreased unitary conductance, improper targeting, or dramatic alterations in voltage or chemical gating. Thus, C-terminal truncation appears to cause a reduction of macroscopic coupling without intrinsic channel function, a phenomenon that could link the endogenous cleavage of Cx50 to the observed 50% decrease in junctional coupling at the DF-MF transition during lens development (Mathias et al., 1991) (Baldo and Mathias,

1992). Furthermore, our data suggest that both human and mouse isoforms of Cx50 retain pH sensitivity after truncation. Interestingly, the intracellular pH in the lens core is more acidic than in the cortex, and impedance studies show that junctional coupling in the mature fibers of the core is less sensitive to pH (Baruch et al., 2001). Dye permeation and electrophysiological examination of transgenic mice lenses expressing only truncated Cx50 subunits may vastly improve the current understanding of the precise physiological relevance of the C-termini of lens fiber connexins.

Chapter IX

References

1. **Anand, R. J. and Hackam, D. J.** (2005). The role of gap junctions in health and disease. *Crit Care Med.* 33, S535-S538.
2. **Arora, A., Minogue, P. J., Liu, X., Reddy, M. A., Ainsworth, J. R., Bhattacharya, S. S., Webster, A. R., Hunt, D. M., Ebihara, L., Moore, A. T. et al.** (2006). A novel GJA8 mutation is associated with autosomal dominant lamellar pulverulent cataract: further evidence for gap junction dysfunction in human cataract. *J. Med. Genet.* 43, e2.
3. **Baldo, G. J., Gong, X., Martinez-Wittinghan, F. J., Kumar, N. M., Gilula, N. B. and Mathias, R. T.** (2001). Gap junctional coupling in lenses from alpha(8) connexin knockout mice. *J. Gen. Physiol* 118, 447-456.
4. **Baldo, G. J. and Mathias, R. T.** (1992). Spatial variations in membrane properties in the intact rat lens. *Biophys. J.* 63, 518-529.
5. **Baruch, A., Greenbaum, D., Levy, E. T., Nielsen, P. A., Gilula, N. B., Kumar, N. M. and Bogyo, M.** (2001). Defining a link between gap junction communication, proteolysis, and cataract formation. *J. Biol. Chem.* 276, 28999-29006.
6. **Bassnett, S.** (2002). Lens organelle degradation. *Exp. Eye Res.* 74, 1-6.
7. **Beahm, D. L. and Hall, J. E.** (2002). Hemichannel and junctional properties of Connexin50. *Biophys. J.* 82, 2016-2031.
8. **Bennett, M. V.** (1994). Connexins in disease. *Nature* 368, 18-19.
9. **Bennett, M. V., Rubin, J. B., Bargiello, T. A. and Verselis, V. K.** (1993). Structure-function studies of voltage sensitivity of connexins, the family of gap junction forming proteins. *Jpn. J. Physiol* 43 Suppl 1, S301-S310.
10. **Bennett, T. M., Mackay, D. S., Knopf, H. L. and Shiels, A.** (2004). A novel missense mutation in the gene for gap-junction protein alpha3 (GJA3) associated with autosomal dominant "nuclear punctate" cataracts linked to chromosome 13q. *Mol. Vis.* 10, 376-382.

11. **Bergoffen, J., Scherer, S. S., Wang, S., Scott, M. O., Bone, L. J., Paul, D. L., Chen, K., Lensch, M. W., Chance, P. F. and Fischbeck, K. H.** (1993). Connexin mutations in X-linked Charcot-Marie-Tooth disease. *Science* 262, 2039-2042.

12. **Berry, V., Mackay, D., Khaliq, S., Francis, P. J., Hameed, A., Anwar, K., Mehdi, S. Q., Newbold, R. J., Ionides, A., Shiels, A. et al.** (1999). Connexin50 mutation in a family with congenital "zonular nuclear" pulverulent cataract of Pakistani origin. *Hum. Genet.* 105, 168-170.

13. **Bevans, C. G., Kordel, M., Rhee, S. K. and Harris, A. L.** (1998). Isoform composition of connexin channels determines selectivity among second messengers and uncharged molecules. *J. Biol. Chem.* 273, 2808-2816.

14. **Bruzzone, R., Veronesi, V., Gomes, D., Bicego, M., Duval, N., Marlin, S., Petit, C., D'Andrea, P. and White, T. W.** (2003). Loss-of-function and residual channel activity of connexin26 mutations associated with non-syndromic deafness. *FEBS Lett.* 533, 79-88.

15. **Bruzzone, R., White, T. W. and Paul, D. L.** (1996). Connections with connexins: the molecular basis of direct intercellular signaling. *Eur. J. Biochem.* 238, 1-27.

16. **Bukauskas, F. F., Elfgang, C., Willecke, K. and Weingart, R.** (1995). Biophysical properties of gap junction channels formed by mouse connexin40 in induced pairs of transfected human HeLa cells. *Biophys. J.* 68, 2289-2298.

17. **Candia, O. A. and Zamudio, A. C.** (2002). Regional distribution of the Na(+) and K(+) currents around the crystalline lens of rabbit. *Am. J. Physiol Cell Physiol* 282, C252-C262.

18. **Cao, F., Eckert, R., Elfgang, C., Nitsche, J. M., Snyder, S. A., ulser, D. F., Willecke, K. and Nicholson, B. J.** (1998). A quantitative analysis of connexin-specific permeability differences of gap junctions expressed in HeLa transfectants and *Xenopus* oocytes. *J. Cell Sci.* 111 (Pt 1), 31-43.

19. **Chang, B., Wang, X., Hawes, N. L., Ojakian, R., Davisson, M. T., Lo, W. K. and Gong, X.** (2002). A Gja8 (Cx50) point mutation causes an alteration of alpha 3 connexin (Cx46) in semi-dominant cataracts of Lop10 mice. *Hum. Mol. Genet.* 11, 507-513.

20. **DeRosa, A. M., Mui, R., Srinivas, M. and White, T. W.** (2006). Functional characterization of a naturally occurring Cx50 truncation. *Invest Ophthalmol. Vis. Sci.* 47, 4474-4481.
21. **DeRosa, A. M., Xia, C. H., Gong, X. and White, T. W.** (2007). The cataract-inducing S50P mutation in Cx50 dominantly alters the channel gating of wild-type lens connexins. *J. Cell Sci.*
22. **Donaldson, P., Kistler, J. and Mathias, R. T.** (2001). Molecular solutions to mammalian lens transparency. *News Physiol Sci.* 16, 118-123.
23. **Dunia, I., Cibert, C., Gong, X., Xia, C. H., Recouvreur, M., Levy, E., Kumar, N., Bloemendal, H. and Benedetti, E. L.** (2006). Structural and immunocytochemical alterations in eye lens fiber cells from Cx46 and Cx50 knockout mice. *Eur. J. Cell Biol.* 85, 729-752.
24. **Ebihara, L. and Steiner, E.** (1993). Properties of a nonjunctional current expressed from a rat connexin46 cDNA in *Xenopus* oocytes. *J. Gen. Physiol* 102, 59-74.
25. **Eckert, R.** (2002). pH gating of lens fibre connexins. *Pflugers Arch.* 443, 843-851.
26. **Evans, W. H. and Martin, P. E.** (2002). Gap junctions: structure and function (Review). *Mol. Membr. Biol.* 19, 121-136.
27. **Fishman, G. I., Moreno, A. P., Spray, D. C. and Levinwand, L. A.** (1991). Functional analysis of human cardiac gap junction channel mutants. *Proc. Natl. Acad. Sci. U. S. A* 88, 3525-3529.
28. **Foote, C. I., Zhou, L., Zhu, X. and Nicholson, B. J.** (1998). The pattern of disulfide linkages in the extracellular loop regions of connexin 32 suggests a model for the docking interface of gap junctions. *J. Cell Biol.* 140, 1187-1197.
29. **Gao, J., Sun, X., Martinez-Wittinghan, F. J., Gong, X., White, T. W. and Mathias, R. T.** (2004). Connections between connexins, calcium, and cataracts in the lens. *J. Gen. Physiol* 124, 289-300.

30. **Gao, J., Sun, X., Yatsula, V., Wymore, R. S. and Mathias, R. T.** (2000). Isoform-specific function and distribution of Na/K pumps in the frog lens epithelium. *J. Membr. Biol.* 178, 89-101.
31. **Gerido, D. A., DeRosa, A. M., Richard, G. and White, T. W.** (2007). Aberrant hemichannel properties of Cx26 mutations causing skin disease and deafness. *Am. J. Physiol Cell Physiol.*
32. **Gerido, D. A. and White, T. W.** (2004). Connexin disorders of the ear, skin, and lens. *Biochim. Biophys. Acta* 1662, 159-170.
33. **Goldberg, G. S., Lampe, P. D. and Nicholson, B. J.** (1999). Selective transfer of endogenous metabolites through gap junctions composed of different connexins. *Nat. Cell Biol.* 1, 457-459.
34. **Gong, X., Baldo, G. J., Kumar, N. M., Gilula, N. B. and Mathias, R. T.** (1998). Gap junctional coupling in lenses lacking alpha3 connexin. *Proc. Natl. Acad. Sci. U. S. A* 95, 15303-15308.
35. **Gong, X., Cheng, C. and Xia, C. H.** (2007). Connexins in Lens Development and Cataractogenesis. *J. Membr. Biol.*
36. **Gong, X., Li, E., Klier, G., Huang, Q., Wu, Y., Lei, H., Kumar, N. M., Horwitz, J. and Gilula, N. B.** (1997). Disruption of alpha3 connexin gene leads to proteolysis and cataractogenesis in mice. *Cell* 91, 833-843.
37. **Goodenough, D. A.** (1992). The crystalline lens. A system networked by gap junctional intercellular communication. *Semin. Cell Biol.* 3, 49-58.
38. **Graw, J., Loster, J., Soewarto, D., Fuchs, H., Meyer, B., Reis, A., Wolf, E., Balling, R. and Hrabe, d. A.** (2001). Characterization of a mutation in the lens-specific MP70 encoding gene of the mouse leading to a dominant cataract. *Exp. Eye Res.* 73, 867-876.
39. **Grujters, W. T., Kistler, J., Bullivant, S. and Goodenough, D. A.** (1987). Immunolocalization of MP70 in lens fiber 16-17-nm intercellular junctions. *J. Cell Biol.* 104, 565-572.

40. **Harris, A. L.** (2001). Emerging issues of connexin channels: biophysics fills the gap. *Q. Rev. Biophys.* 34, 325-472.
41. **Hennemann, H., Dahl, E., White, J. B., Schwarz, H. J., Lalley, P. A., Chang, S., Nicholson, B. J. and Willecke, K.** (1992). Two gap junction genes, connexin 31.1 and 30.3, are closely linked on mouse chromosome 4 and preferentially expressed in skin. *J. Biol. Chem.* 267, 17225-17233.
42. **Hopperstad, M. G., Srinivas, M. and Spray, D. C.** (2000). Properties of gap junction channels formed by Cx46 alone and in combination with Cx50. *Biophys. J.* 79, 1954-1966.
43. **Jacobs, M. D., Soeller, C., Cannell, M. B. and Donaldson, P. J.** (2001). Quantifying changes in gap junction structure as a function of lens fiber cell differentiation. *Cell Commun. Adhes.* 8, 349-353.
44. **Jiang, H., Jin, Y., Bu, L., Zhang, W., Liu, J., Cui, B., Kong, X. and Hu, L.** (2003). A novel mutation in GJA3 (connexin46) for autosomal dominant congenital nuclear pulverulent cataract. *Mol. Vis.* 9, 579-583.
45. **Jiang, J. X. and Goodenough, D. A.** (1996). Heteromeric connexons in lens gap junction channels. *Proc. Natl. Acad. Sci. U. S. A* 93, 1287-1291.
46. **Jiang, J. X. and Gu, S.** (2005). Gap junction- and hemichannel-independent actions of connexins. *Biochim. Biophys. Acta* 1711, 208-214.
47. **Jiang, J. X., White, T. W. and Goodenough, D. A.** (1995). Changes in connexin expression and distribution during chick lens development. *Dev. Biol.* 168, 649-661.
48. **Kelsell, D. P., Dunlop, J., Stevens, H. P., Lench, N. J., Liang, J. N., Parry, G., Mueller, R. F. and Leigh, I. M.** (1997). Connexin 26 mutations in hereditary non-syndromic sensorineural deafness. *Nature* 387, 80-83.
49. **Kistler, J., Berriman, J., Evans, C. W., Gruijters, W. T., Christie, D., Corin, A. and Bullivant, S.** (1990). Molecular portrait of lens gap junction protein MP70. *J. Struct. Biol.* 103, 204-211.

50. **Konig, N. and Zampighi, G. A.** (1995). Purification of bovine lens cell-to-cell channels composed of connexin44 and connexin50. *J. Cell Sci.* 108 (Pt 9), 3091-3098.
51. **Koumi, S., Backer, C. L. and Arentzen, C. E.** (1995). Characterization of inwardly rectifying K⁺ channel in human cardiac myocytes. Alterations in channel behavior in myocytes isolated from patients with idiopathic dilated cardiomyopathy. *Circulation* 92, 164-174.
52. **Kwak, B. R., Hermans, M. M., De Jonge, H. R., Lohmann, S. M., Jongsma, H. J. and Chanson, M.** (1995). Differential regulation of distinct types of gap junction channels by similar phosphorylating conditions. *Mol. Biol. Cell* 6, 1707-1719.
53. **Lampe, P. D. and Lau, A. F.** (2000). Regulation of gap junctions by phosphorylation of connexins. *Arch. Biochem. Biophys.* 384, 205-215.
54. **Lampe, P. D., Tenbroek, E. M., Burt, J. M., Kurata, W. E., Johnson, R. G. and Lau, A. F.** (2000). Phosphorylation of connexin43 on serine368 by protein kinase C regulates gap junctional communication. *J. Cell Biol.* 149, 1503-1512.
55. **Le, A. C. and Musil, L. S.** (2001). A novel role for FGF and extracellular signal-regulated kinase in gap junction-mediated intercellular communication in the lens. *J. Cell Biol.* 154, 197-216.
56. **Leube, R. E.** (1995). The topogenic fate of the polytopic transmembrane proteins, synaptophysin and connexin, is determined by their membrane-spanning domains. *J. Cell Sci.* 108 (Pt 3), 883-894.
57. **Li, Y., Wang, J., Dong, B. and Man, H.** (2004). A novel connexin46 (GJA3) mutation in autosomal dominant congenital nuclear pulverulent cataract. *Mol. Vis.* 10, 668-671.
58. **Lin, J. S., Eckert, R., Kistler, J. and Donaldson, P.** (1998). Spatial differences in gap junction gating in the lens are a consequence of connexin cleavage. *Eur. J. Cell Biol.* 76, 246-250.

59. **Lin, J. S., Fitzgerald, S., Dong, Y., Knight, C., Donaldson, P. and Kistler, J.** (1997). Processing of the gap junction protein connexin50 in the ocular lens is accomplished by calpain. *Eur. J. Cell Biol.* 73, 141-149.
60. **Mackay, D., Ionides, A., Kibar, Z., Rouleau, G., Berry, V., Moore, A., Shiels, A. and Bhattacharya, S.** (1999). Connexin46 mutations in autosomal dominant congenital cataract. *Am. J. Hum. Genet.* 64, 1357-1364.
61. **Martin, P. E., Steggle, J., Wilson, C., Ahmad, S. and Evans, W. H.** (2000). Targeting motifs and functional parameters governing the assembly of connexins into gap junctions. *Biochem. J.* 350 Pt 3, 943.
62. **Martinez-Wittinghan, F. J., Sellitto, C., Li, L., Gong, X., Brink, P. R., Mathias, R. T. and White, T. W.** (2003). Dominant cataracts result from incongruous mixing of wild-type lens connexins. *J. Cell Biol.* 161, 969-978.
63. **Martinez-Wittinghan, F. J., Sellitto, C., White, T. W., Mathias, R. T., Paul, D. and Goodenough, D. A.** (2004). Lens gap junctional coupling is modulated by connexin identity and the locus of gene expression. *Invest Ophthalmol. Vis. Sci.* 45, 3629-3637.
64. **Mathias, R. T., Rae, J. L. and Baldo, G. J.** (1997). Physiological properties of the normal lens. *Physiol Rev.* 77, 21-50.
65. **Mathias, R. T., Riquelme, G. and Rae, J. L.** (1991). Cell to cell communication and pH in the frog lens. *J. Gen. Physiol* 98, 1085-1103.
66. **Menko, A. S.** (2002). Lens epithelial cell differentiation. *Experimental Eye Research* 75, 485-490.
67. **Moreno, A. P., Saez, J. C., Fishman, G. I. and Spray, D. C.** (1994). Human connexin43 gap junction channels. Regulation of unitary conductances by phosphorylation. *Circ. Res.* 74, 1050-1057.
68. **Niessen, H., Harz, H., Bedner, P., Kramer, K. and Willecke, K.** (2000). Selective permeability of different connexin channels to the second messenger inositol 1,4,5-trisphosphate. *J. Cell Sci.* 113 (Pt 8), 1365-1372.

69. **Paul, D. L., Ebihara, L., Takemoto, L. J., Swenson, K. I. and Goodenough, D. A.** (1991). Connexin46, a novel lens gap junction protein, induces voltage-gated currents in nonjunctional plasma membrane of *Xenopus* oocytes. *J. Cell Biol.* 115, 1077-1089.
70. **Paznekas, W. A., Boyadjiev, S. A., Shapiro, R. E., Daniels, O., Wollnik, B., Keegan, C. E., Innis, J. W., Dinulos, M. B., Christian, C., Hannibal, M. C. et al.** (2003). Connexin 43 (GJA1) mutations cause the pleiotropic phenotype of oculodentodigital dysplasia. *Am. J. Hum. Genet.* 72, 408-418.
71. **Peracchia, C., Chen, J. T. and Peracchia, L. L.** (2004). CO(2) sensitivity of voltage gating and gating polarity of gapjunction channels--connexin40 and its COOH-terminus-truncated mutant. *J. Membr. Biol.* 200, 105-113.
72. **Peracchia, C. and Peracchia, L. L.** (2005). Inversion of both gating polarity and CO2 sensitivity of voltage gating with D3N mutation of Cx50. *Am. J. Physiol Cell Physiol* 288, C1381-C1389.
73. **Piatigorsky, J.** (1981). Lens differentiation in vertebrates. A review of cellular and molecular features. *Differentiation* 19, 134-153.
74. **Polyakov, A. V., Shagina, I. A., Khlebnikova, O. V. and Evgrafov, O. V.** (2001). Mutation in the Connexin50 gene (GJA8) in a Russian family with zonular pulverulent cataract. *Clin. Genet.* 60, 476-478.
75. **Purnick, P. E., Benjamin, D. C., Verselis, V. K., Bargiello, T. A. and Dowd, T. L.** (2000). Structure of the amino terminus of a gap junction protein. *Arch. Biochem. Biophys.* 381, 181-190.
76. **Reaume, A. G., de Sousa, P. A., Kulkarni, S., Langille, B. L., Zhu, D., Davies, T. C., Juneja, S. C., Kidder, G. M. and Rossant, J.** (1995). Cardiac malformation in neonatal mice lacking connexin43. *Science* 267, 1831-1834.
77. **Rees, M. I., Watts, P., Fenton, I., Clarke, A., Snell, R. G., Owen, M. J. and Gray, J.** (2000). Further evidence of autosomal dominant congenital zonular pulverulent cataracts linked to 13q11 (CZP3) and a novel mutation in connexin46 (GJA3). *Hum. Genet.* 106, 206-209.

78. **Revilla, A., Bennett, M. V. and Barrio, L. C.** (2000). Molecular determinants of membrane potential dependence in vertebrate gap junction channels. *Proc. Natl. Acad. Sci. U. S. A* 97, 14760-14765.
79. **Rong, P., Wang, X., Niesman, I., Wu, Y., Benedetti, L. E., Dunia, I., Levy, E. and Gong, X.** (2002). Disruption of Gja8 (alpha8 connexin) in mice leads to microphthalmia associated with retardation of lens growth and lens fiber maturation. *Development* 129, 167-174.
80. **Rubin, J. B., Verselis, V. K., Bennett, M. V. and Bargiello, T. A.** (1992). A domain substitution procedure and its use to analyze voltage dependence of homotypic gap junctions formed by connexins 26 and 32. *Proc. Natl. Acad. Sci. U. S. A* 89, 3820-3824.
81. **Runge, P. E., Hawes, N. L., Heckenlively, J. R., Langley, S. H. and Roderick, T. H.** (1992). Autosomal dominant mouse cataract (Lop-10). Consistent differences of expression in heterozygotes. *Invest Ophthalmol. Vis. Sci.* 33, 3202-3208.
82. **Rup, D. M., Veenstra, R. D., Wang, H. Z., Brink, P. R. and Beyer, E. C.** (1993). Chick connexin-56, a novel lens gap junction protein. Molecular cloning and functional expression. *J. Biol. Chem.* 268, 706-712.
83. **Sellitto, C., Li, L. and White, T. W.** (2004). Connexin50 is essential for normal postnatal lens cell proliferation. *Invest Ophthalmol. Vis. Sci.* 45, 3196-3202.
84. **Shiels, A., Mackay, D., Ionides, A., Berry, V., Moore, A. and Bhattacharya, S.** (1998). A missense mutation in the human connexin50 gene (GJA8) underlies autosomal dominant "zonular pulverulent" cataract, on chromosome 1q. *Am. J. Hum. Genet.* 62, 526-532.
85. **Spray, D. C., Harris, A. L. and Bennett, M. V.** (1981). Equilibrium properties of a voltage-dependent junctional conductance. *J. Gen. Physiol* 77, 77-93.
86. **Srinivas, M., Costa, M., Gao, Y., Fort, A., Fishman, G. I. and Spray, D. C.** (1999). Voltage dependence of macroscopic and unitary currents of gap junction channels formed by mouse connexin50 expressed in rat neuroblastoma cells. *J. Physiol* 517 (Pt 3), 673-689.

87. **Srinivas, M., Kronengold, J., Bukauskas, F. F., Bargiello, T. A. and Verselis, V. K.** (2005). Correlative studies of gating in Cx46 and Cx50 hemichannels and gap junction channels. *Biophys. J.* 88, 1725-1739.
88. **Steele, E. C., Jr., Lyon, M. F., Favor, J., Guillot, P. V., Boyd, Y. and Church, R. L.** (1998). A mutation in the Connexin50 (Cx50) gene is a candidate for the No2 mouse cataract. *Curr. Eye Res.* 17, 883-889.
89. **Stergiopoulos, K., Alvarado, J. L., Mastroianni, M., Ek-Vitorin, J. F., Taffet, S. M. and Delmar, M.** (1999). Hetero-domain interactions as a mechanism for the regulation of connexin channels. *Circ. Res.* 84, 1144-1155.
90. **Tamiya, S., Dean, W. L., Paterson, C. A. and Delamere, N. A.** (2003). Regional distribution of Na,K-ATPase activity in porcine lens epithelium. *Invest Ophthalmol. Vis. Sci.* 44, 4395-4399.
91. **Torok, K., Stauffer, K. and Evans, W. H.** (1997). Connexin 32 of gap junctions contains two cytoplasmic calmodulin-binding domains. *Biochem. J.* 326 (Pt 2), 479-483.
92. **Traub, O., Hertlein, B., Kasper, M., Eckert, R., Krisciukaitis, A., Hulser, D. and Willecke, K.** (1998). Characterization of the gap junction protein connexin37 in murine endothelium, respiratory epithelium, and after transfection in human HeLa cells. *Eur. J. Cell Biol.* 77, 313-322.
93. **Unger, V. M., Kumar, N. M., Gilula, N. B. and Yeager, M.** (1999). Three-dimensional structure of a recombinant gap junction membrane channel. *Science* 283, 1176-1180.
94. **Unwin, N.** (1989). The structure of ion channels in membranes of excitable cells. *Neuron* 3, 665-676.
95. **Valiunas, V., Beyer, E. C. and Brink, P. R.** (2002). Cardiac gap junction channels show quantitative differences in selectivity. *Circ. Res.* 91, 104-111.
96. **Veenstra, R. D.** (1996). Size and selectivity of gap junction channels formed from different connexins. *J. Bioenerg. Biomembr.* 28, 327-337.

97. **Veenstra, R. D., Wang, H. Z., Beyer, E. C. and Brink, P. R.** (1994). Selective dye and ionic permeability of gap junction channels formed by connexin45. *Circ. Res.* 75, 483-490.
98. **Verselis, V. K., Ginter, C. S. and Bargiello, T. A.** (1994). Opposite voltage gating polarities of two closely related connexins. *Nature* 368, 348-351.
99. **White, T. W.** (2002). Unique and redundant connexin contributions to lens development. *Science* 295, 319-320.
100. **White, T. W.** (2003). Nonredundant gap junction functions. *News Physiol Sci.* 18, 95-99.
101. **White, T. W. and Bruzzone, R.** (2000a). Gap junctions: fates worse than death? *Curr. Biol.* 10, R685-R688.
102. **White, T. W. and Bruzzone, R.** (2000b). Intercellular communication in the eye: clarifying the need for connexin diversity. *Brain Res. Brain Res. Rev.* 32, 130-137.
103. **White, T. W., Bruzzone, R., Goodenough, D. A. and Paul, D. L.** (1992). Mouse Cx50, a functional member of the connexin family of gap junction proteins, is the lens fiber protein MP70. *Mol. Biol. Cell* 3, 711-720.
104. **White, T. W., Bruzzone, R., Goodenough, D. A. and Paul, D. L.** (1994a). Voltage gating of connexins. *Nature* 371, 208-209.
105. **White, T. W., Bruzzone, R., Wolfram, S., Paul, D. L. and Goodenough, D. A.** (1994b). Selective interactions among the multiple connexin proteins expressed in the vertebrate lens: the second extracellular domain is a determinant of compatibility between connexins. *J. Cell Biol.* 125, 879-892.
106. **White, T. W., Goodenough, D. A. and Paul, D. L.** (1998). Targeted ablation of connexin50 in mice results in microphthalmia and zonular pulverulent cataracts. *J. Cell Biol.* 143, 815-825.
107. **White, T. W. and Paul, D. L.** (1999). Genetic diseases and gene knockouts reveal diverse connexin functions. *Annu. Rev. Physiol* 61, 283-310.

108. **White, T. W., Sellitto, C., Paul, D. L. and Goodenough, D. A.** (2001). Prenatal lens development in connexin43 and connexin50 double knockout mice. *Invest Ophthalmol. Vis. Sci.* 42, 2916-2923.
109. **Willecke, K., Eiberger, J., Degen, J., Eckardt, D., Romualdi, A., Guldenagel, M., Deutsch, U. and Sohl, G.** (2002). Structural and functional diversity of connexin genes in the mouse and human genome. *Biol. Chem.* 383, 725-737.
110. **Willoughby, C. E., Arab, S., Gandhi, R., Zeinali, S., Arab, S., Luk, D., Billingsley, G., Munier, F. L. and Heon, E.** (2003). A novel GJA8 mutation in an Iranian family with progressive autosomal dominant congenital nuclear cataract. *J. Med. Genet.* 40, e124.
111. **Xia, C. H., Cheng, C., Huang, Q., Cheung, D., Li, L., Dunia, I., Benedetti, L. E., Horwitz, J. and Gong, X.** (2006a). Absence of alpha3 (Cx46) and alpha8 (Cx50) connexins leads to cataracts by affecting lens inner fiber cells. *Exp. Eye Res.* 83, 688-696.
112. **Xia, C. H., Cheung, D., DeRosa, A. M., Chang, B., Lo, W. K., White, T. W. and Gong, X.** (2006b). Knock-in of alpha3 connexin prevents severe cataracts caused by an alpha8 point mutation. *J. Cell Sci.* 119, 2138-2144.
113. **Xia, C. H., Liu, H., Cheung, D., Cheng, C., Wang, E., Du, X., Beutler, B., Lo, W. K. and Gong, X.** (2006c). Diverse gap junctions modulate distinct mechanisms for fiber cell formation during lens development and cataractogenesis. *Development* 133, 2033-2040.
114. **Xu, X., Berthoud, V. M., Beyer, E. C. and Ebihara, L.** (2002). Functional role of the carboxyl terminal domain of human Connexin50 in gap junctional channels. *J. Membr. Biol.* 186, 101-112.
115. **Xu, X. and Ebihara, L.** (1999). Characterization of a mouse Cx50 mutation associated with the No2 mouse cataract. *Invest Ophthalmol. Vis. Sci.* 40, 1844-1850.
116. **Yeager, M. and Nicholson, B. J.** (1996). Structure of gap junction intercellular channels. *Curr. Opin. Struct. Biol.* 6, 183-192.

117. **Zampighi, G. A., Simon, S. A. and Hall, J. E.** (1992). The specialized junctions of the lens. *Int. Rev. Cytol.* 136, 185-225.

118. **Zheng, J. Q., Ma, Z. W. and Sun, H. M.** (2005). [A heterozygous transversion of Connexin50 in a family with congenital nuclear cataract in the northeast of China]. *Zhonghua Yi. Xue. Yi. Chuan Xue. Za Zhi.* 22, 76-78.